

Microbial Electrolysis Kinetics and Cell Design

Tom H.J.A. Sleutels

Thesis Committee

Thesis supervisor

Prof. dr. ir. C.J.N. Buisman

Professor of Biological Recycling Technology

Thesis Co-supervisor

Dr. ir. H.V.M. Hamelers

Assistant professor, sub-department of Environmental Technology

Other members

Prof. dr. G. Eggink, Wageningen University

Dr. ir. D.C. Nijmeijer, University of Twente

Prof. dr. U. Schröder, Technical University Braunschweig, Germany

Prof. dr. ir. W. Verstraete, Ghent University, Belgium

This research was conducted under the auspices of the Netherlands Research School for the Socio-Economic and Natural Sciences of the Environment (SENSE)

Microbial Electrolysis Kinetics and Cell Design

Tom H.J.A. Sleutels

Thesis

Submitted in fulfilment of the requirements for the degree of doctor

at Wageningen University

by the authority of the Rector Magnificus

Prof. Dr. M.J. Kropff,

in the presence of the

Thesis Committee appointed by the Academic Board

to be defended in public

on Friday 3 December 2010

at 4 p.m. in de Aula

Tom H.J.A. Sleutels
Microbial Electrolysis, Kinetics and cell design
130 pages

Thesis Wageningen University, Wageningen, NL (2010)
With references, with summaries in Dutch and English

ISBN 978-90-8585-820-1

Table of Contents

1. General Introduction	6
2. Microbial Electrolysis Cells with Anion and Cation Exchange membranes	19
3. Improved performance of porous bio-anodes in Microbial Electrolysis Cells by enhancing mass and charge transport	40
4. Effect of mass and charge transport speed and direction in porous anodes on Microbial Electrolysis Cell performance	55
5. Influencing coulombic efficiency in Bioelectrochemical Systems	67
6. Reduction of Buffer requirement in Bioelectrochemical Systems	80
7. Conclusions and Perspectives	93
References	108
English Summary	117
Nederlandse Samenvatting	121

Chapter 1

General Introduction

Paragraph 1.3 is based on:

Hamelers, H.V.M., Ter Heijne, A., Sleutels, T.H.J.A., Jeremiasse, A.W., Strik, D.P.B.T.B., Buisman, C.J.N., 2010. New applications and performance of bioelectrochemical systems. *Applied Microbiology and Biotechnology*, 85, 1673-1685.

Paragraph 1.3.1 is based on:

Logan, B.E., Call, D., Cheng, S., Hamelers, H.V.M., Sleutels, T.H.J.A., Jeremiasse, A.W., Rozendal, R.A., 2008. Microbial Electrolysis Cells (MECs) for High Yield Hydrogen Gas Production From Organic Matter. *Environmental Science & Technology*, 42, 8630-8640.

1.1. Climate change and fossil fuels

Climate change is considered as a big threat for our planet as it exists now. Climate change is most likely caused by the emission of greenhouse gasses (GHGs). Although the effects of GHG emissions are difficult to determine, the Intergovernmental Panel on Climate Change (IPCC) predicts a temperature increase of 1.1 to 6.4 degrees Celsius worldwide. This temperature increase may lead to a sea level rise of 18-59 cm, depending on the location. The combination of temperature and sea level rises will with almost certainly cause extreme weather conditions like flooding or extreme draught. Furthermore, temperature and sea level rise might also cause a change in ecosystems, which will also affect the agricultural possibilities in those areas, like observed in southern France in 2010 (IPCC, 2007).

The IPCC also predicts an increase in the emission of GHG in the near future and thereby an increase of the effects on our climate. The increase in emission of these GHGs like methane, carbon dioxide, nitrous oxide and halocarbons is most likely caused by human activities. The largest contribution to the increase of the emission of GHGs comes from the increase in energy consumption by the world population. This increase is caused by an increase in the energy use of the domestic sector, transport sector, industry and agricultural activities (IPCC, 2007). Furthermore, the increase in GHG is expected to go even faster in the future by the growing world population and rapid industrialization of the world. The world population is expected to double in 2050 compared to 1980 and the industrialization rate of this growing world population is high. Examples of this industrialization are fast developing countries like China and India which are rapidly increasing their energy consumption.

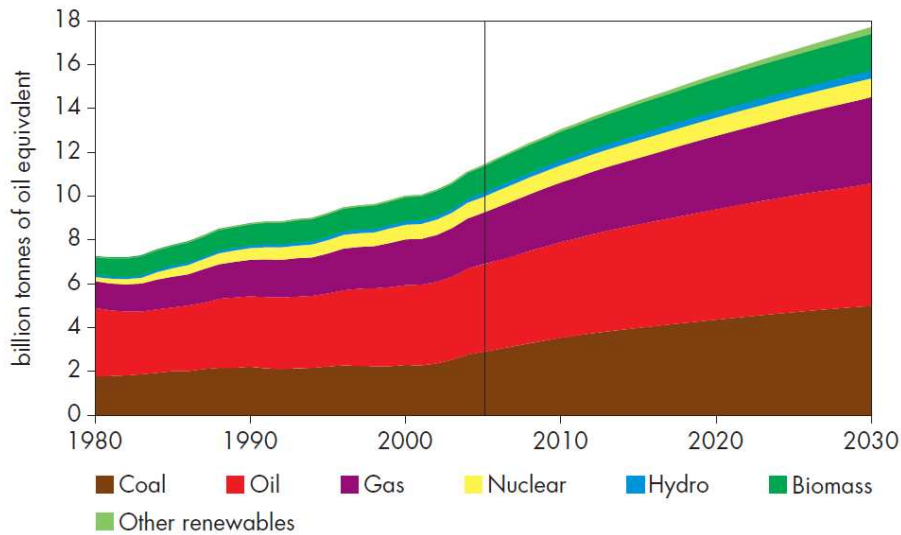


Figure 1 Predicted global energy demand in 2030 (IEA, 2007b).

Besides the high GHG emissions, the use of fossil fuels has some other major drawbacks, like air pollution, uneven distribution and possible scarcity. Besides GHG emissions, combustion of fossil fuels also leads to air pollution with fine particulates. These fine particles can be a big threat to human health as they lead to heart disease, breathing problems and lung cancer. In 2030 still 80% of the total energy production is expected to be from fossil fuels (Figure 1) and the largest contribution to this production comes from oil (IEA, 2009). Most of the world's crude oil supplies are located in the Middle East. This uneven distribution of energy sources may lead to fluctuating market prices and political instability, which were already observed after the war in Iraq in 1990. Furthermore, because of depletion of easily extractable oil reserves the oil production is expected to peak. To prevent this, extra investments in new production capacity are required.

To prevent or slow down climate change, a decrease or stabilization of the emission of GHG is required. To achieve this, the Kyoto protocol was introduced in 1997 (Kyoto-Protocol, 1998). Although major contributors to the emissions of GHG, like the US and Australia did not ratify this protocol, the European Union decided in 2008 to reduce the GHG emissions with 20% in 2020 compared to the 1990 levels.

To achieve this reduction, in 2020, 20% of the produced energy should be from renewable resources and 10% of the fuels used in the EU should be biobased (EU, 2008). Production of energy, fuel and chemicals from biomass instead of fossil fuels is generally known as a biobased economy.

1.2. Biobased economy

As discussed in the previous paragraph climate change is one of the most important drivers for the development of the biobased economy. In the biobased economy, biomass is used as the source for the production of energy, fuel and chemicals. Since CO₂ is captured during the growth of biomass no net CO₂ is emitted when biomass is burned as fuel for example. In this way, transition to a biobased economy can contribute to a reduction in the emission of GHG. Of course care should be taken that all GHG emissions of the total production process are taken into account when comparing the biobased product to products from fossil origin. Extra, indirect, GHG emissions can come from, for example, fertilizer production and transportation of the biomass.

Biomass as a source for the biobased economy is abundantly available; 20 times the amount for energy demand (Greenpeace, 2005). Although other resources like wind and sun are available in even higher quantities they do not offer the advantages of biomass, which can be stored to be used at a desired time. Another advantage of biomass is that technologies are already available to convert biomass into heat, fuels, electricity and chemicals. So far, most biomass is burned for heating purposes but already many other technologies exist to convert biomass into electricity, fuels and chemicals. These technologies include anaerobic digestion for the production of fuel and electricity and fermentation for the production of fuel. Especially the production of chemicals from biomass is interesting since the chemical composition of biomass is often similar to the composition of the desired chemicals and only small changes are required (Cherubini, 2010).

However, before the transition to a biobased economy can become successful some drawbacks have to be overcome. First, care should be taken that the used biomass does not compete with food or feed production. The maximum amount of total

biomass that can be produced worldwide is limited because of reasons like water scarcity. This total amount of biomass has to be sufficient for both food production and the production of energy and chemicals. A solution to avoid competition between different products from the same source is to use waste products from biomass. These waste products can not serve as food or feed and can therefore be use for the production of energy, fuels and chemicals. Second, another important point for the development of the biobased economy is to reach high efficiencies in the conversion of biomass into product. When these conversions occur at low chemical efficiencies (like burning) more biomass is required to produce a certain amount of product while at low energetic efficiency a lot of energy is required to produce a certain amount of product. Finally, some of the available technologies, like for example gasification, require extremely high temperatures (>700°C) which can also reduce the energetic efficiency. Therefore, low temperature conversions are desirable. The development of technologies which are able to produce energy, fuels and chemicals from sustainable sources at high overall efficiency is crucial.

1.2.1. Hydrogen

In 2007 overall 65 million tonnes of hydrogen were produced world wide (IEA, 2007a). Most of this hydrogen is now made from fossil fuels (48% from natural gas, 30% refinery-gas/chemicals, 18% coal (IEA, 2007a) through gasification. Production of this hydrogen from biomass could mean a large step forward in realization of the biobased economy and a reduction of GHG emissions.

A large portion of the produced hydrogen is used in the petrochemical industry for the upgrading of fossil fuels. Also the food industry consumes a large part of the hydrogen for the saturation of unsaturated fats and oils. Finally, hydrogen can be used for the upgrading of biofuels to increase the energy density of these fuels.

The amount of required hydrogen is expected to increase if a hydrogen economy develops. In the hydrogen economy hydrogen is not only used as a chemical but also as a fuel. Hydrogen can be used as a fuel since it is an efficient energy carrier because of a high energy density. Furthermore it can be burned in a fuel cell together with oxygen to produce electricity at a high efficiency and with only pure

water as a waste product. This way energy produced from wind and solar sources can be stored to be used at times when energy demands are high. If hydrogen becomes the fuel of the future depends on a lot of uncertain factors like hydrogen distribution and storage (Mulder et al., 2007; Schlapbach and Zuttel, 2001). However, developments are continuously going forward and hydrogen is now already applied in city buses as a fuel (Christen, 2006). As a chemical there will remain a demand for hydrogen, whether or not the hydrogen economy will develop.

1.2.2. Hydrogen production

There are already several technologies available to produce hydrogen from renewable sources. One method to produce hydrogen in a sustainable way, when electricity is used from wind or solar sources, is through electrolysis. The required energy input for electrolysis however, is high (4.4 - 5.4 kWh/m³ H₂) and typical electrolyzer energy efficiencies are 56–73% (Ivy, 2004). Also biological production methods are available for hydrogen production. Algae and photosynthetic bacteria can use sunlight to make hydrogen gas from water, but efficiencies are currently low and some experts believe the process may never be feasible due the large surface area requirements for the process (Hallenbeck and Benemann, 2002). Fermentation is another way to produce hydrogen; in this case from organic material. Theoretically, one mol of glucose can yield 12 moles of hydrogen. However, because of thermodynamical limitations of the microorganisms the theoretical maximum is only four moles of hydrogen per glucose and two moles of acetate. In practice only yields of 15 % are achieved because of limitations of the involved enzymes (Hawkes et al., 2007). Conversion of the byproducts to useful amounts of hydrogen requires endothermic reactions, which means that these molecules cannot be further converted to hydrogen without an external energy input. Overall, disadvantages of the current renewable production technologies for hydrogen are that they require a high energy input or occur at low efficiency caused by low yields.

1.3. Bioelectrochemical systems

Bioelectrochemical systems (BES) are considered to be a technology that is able to produce renewable energy and chemicals from organic waste materials at high energetic efficiency (Logan et al., 2006; Rabaey and Verstraete, 2005; Rozendal et al., 2008a). BESs are based on the discovery of electrochemically active microorganisms which are able to transfer electrons to a solid surface. This phenomenon was already described by Potter in 1912 but it regained attention of researchers by the discovery of mediator less direct electron transfer (Chaudhuri and Lovley, 2003; Potter, 1912). This discovery provided the basis for multiple applications which are now summarized as BES.

In BESs electrochemically active microorganisms grow on an electrode, which is subsequently called a bioanode and form the basis of all BESs. The bioanode is coupled through an electrical circuit to a (bio)cathode where a reduction reaction takes place. Depending on the reaction at the cathode the system gains energy in a so called fuel cell, or energy input is required in a so called electrolysis cell. Generally the anode and cathode are separated by a membrane but also membraneless designs are being developed. The advantage of BESs when using two compartments is that they not solely convert compounds but also separate oxidation and reduction products, which makes it possible to extract useful products out of wastes.

Nowadays, BESs with bio-anodes use electron donors derived from wastes (e.g. wastewaters) (Logan, 2005), sediments (Reimers et al., 2001), processed energy crops (as cellulose) (Niessen et al., 2005; Ren et al., 2007; Rezaei et al., 2009) photosynthetic microorganisms (Chiao et al., 2006; Fu et al., 2009; Strik et al., 2008b) or in-situ photosynthesized plant rhizodeposits (De Schampelaire et al., 2008; Strik et al., 2008a)

The last years BES research has also moved in the direction from producing electricity in MFCs to MEC applications, using microorganisms as novel biocatalysts that produce all kinds value added products like H₂ (Rozendal et al., 2006b), CH₄ (Cheng et al., 2009), H₂O₂ (Rozendal et al., 2009) or ethanol

(Steinbusch et al., 2009a), while using final electron acceptors like protons, CO₂ and acetate.

1.3.1. Microbial electrolysis cell

It was independently discovered by two different research groups in 2005 that bacteria could be used to make hydrogen gas in an electrolysis-type process based on microbial fuel cells (Liu et al., 2005b; Rozendal and Buisman, 2005; Rozendal et al., 2006b). Different names have been used by the different research groups (BEAMR, biocatalyzed electrolysis) but the process is now generally known as microbial electrolysis and the reactors are called microbial electrolysis cells (MECs) (Call and Logan, 2008; Cheng and Logan, 2007; Rozendal et al., 2008a). MECs theoretically offer the possibility to produce hydrogen gas at high substrate yields (90% of the stoichiometric maximum) and at relatively low energy input (1 kWh/m³H₂) compared to electrolyzers (Rozendal et al., 2008a). The principle of an MEC is shown in Figure 2.

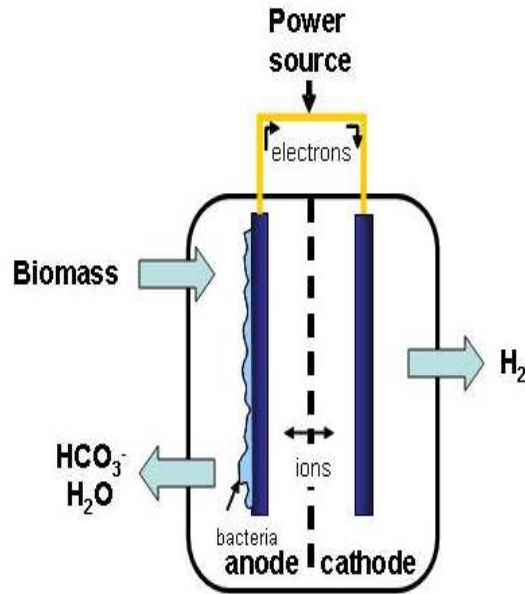


Figure 2 Principle of an MEC; In the anode biomass is oxidized by electrogens to water, bicarbonate and electrons while in the cathode these electrons are reduced to hydrogen. To make this reaction thermodynamically possible a small amount of energy is added to the electrons by means of a power supply. Anode and cathode chamber are separated by a membrane to prevent substrate/product crossover.

1.3.2. Thermodynamics

The theoretical energy in and output of an MEC depends on the reactions occurring at the anode and cathode and is determined by the difference between the potential of both electrodes. To calculate these potentials the Gibbs free energy change of the reactants needs to be calculated. The Gibbs free energy change (ΔG_r ; J) of the reactants determines the energy content of the released electrons. For the reaction $v_A A + v_B B \rightarrow v_C C + v_D D$ in a dilute system the Gibbs free energy change can be calculated with

$$\Delta G_r = \Delta G_r^0 + RT \ln \left(\frac{[C]^{v_C} [D]^{v_D}}{[A]^{v_A} [B]^{v_B}} \right) \quad (1)$$

where ΔG_r^0 is the Gibbs free energy change under standard conditions (298 K, 1 bar and 1M concentration for all species), R is the universal gas constant (8.31 J/mol/K), T the absolute temperature (K), [i] is the concentration of a specific reactant (mol/L) and v_i is the reaction coefficient.

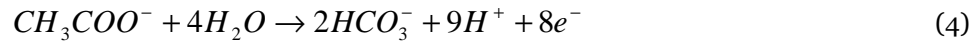
In BESs the energy change (J) is expressed as a standard potential (E^0 ; V) which is related to the Gibbs free energy of a reaction according to

$$E^0 = -\frac{\Delta G_r^0}{nF} \quad (2)$$

Combining of above equations leads to the following equation for the potential of a reaction

$$E = E^0 - \frac{RT}{nF} \ln \left(\frac{[C]^{v_C} [D]^{v_D}}{[A]^{v_A} [B]^{v_B}} \right) \quad (3)$$

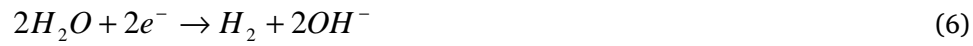
For research purposes mostly acetate is used as substrate which is oxidized in the anode according to



From this reaction equation the theoretical potential can be calculated by combining equation 3 and 4

$$E_{an} = E_{an}^0 - \frac{RT}{8F} \ln \left(\frac{[CH_3COO^-]}{[HCO_3^-]^2 [H^+]^9} \right) \quad (5)$$

For the cathode the theoretical electrode can be calculated at specific conditions according to



$$E_{cat} = E_{cat}^0 - \frac{RT}{2F} \ln \left(\frac{pH_2}{[H^+]^2} \right) \quad (7)$$

From the anode and cathode potential the cell voltage can be calculated using

$$E_{cell} = E_{cat} - E_{an} \quad (8)$$

General introduction

Table 1 gives an overview of the theoretical electrode potentials and cell voltage at typical conditions in an MEC. The cell voltage at these typical conditions is -0.14V (Figure 3A), which means that energy needs to be invested in the overall reaction to drive it. This is because the energy content of the substrate (acetate) is lower than the energy content of hydrogen.

Table 1 Theoretical potentials for typical conditions in an MEC ($[\text{CH}_3\text{COO}^-] = 10$ mM, $[\text{HCO}_3^-] = 10$ mM, pH = 7, $p\text{H}_2=1$). All potentials are reported against Ag/AgCl.

Reaction	E° (V) (from (Bard et al., 1985))	E (V)
$\text{CH}_3\text{COO}^- + 4\text{H}_2\text{O} \rightarrow 2\text{HCO}_3^- + 9\text{H}^+ + 8\text{e}^-$	-0.014	-0.502
$2\text{H}_2\text{O} + 2\text{e}^- \rightarrow \text{H}_2 + 2\text{OH}^-$	-0.201	-0.622
$\text{CH}_3\text{COO}^- + 4\text{H}_2\text{O} \rightarrow 2\text{HCO}_3^- + \text{H}^+ + 4\text{H}_2$	-0.187	-0.119

The practical value however, can be many times higher than the theoretical value because of internal resistances of the system leading to energy losses (Figure 3B). These internal resistances can be caused by for example metabolic energy consumption of the microorganisms and electrode overpotentials. A more detailed overview of these energy losses is given in Chapter 2.

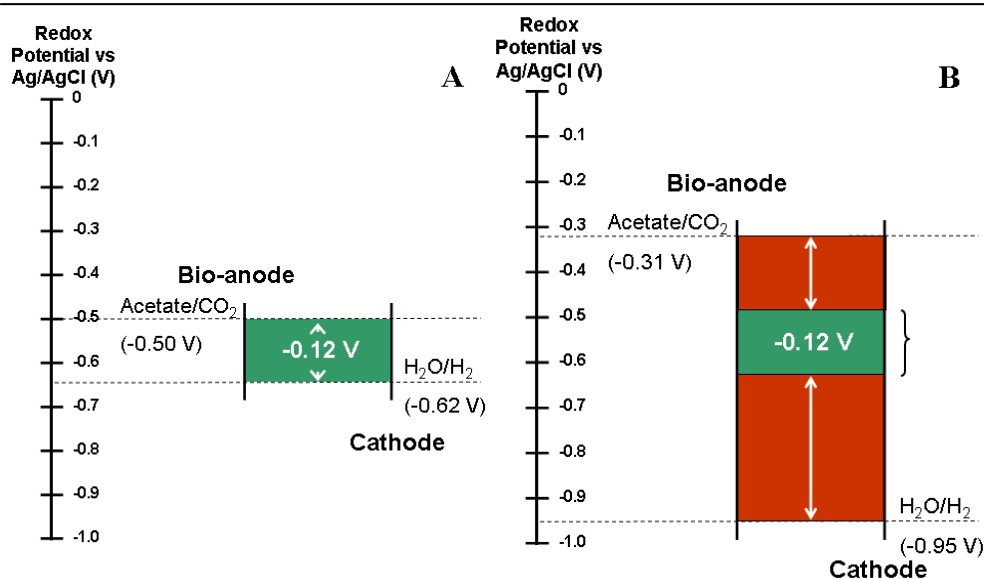


Figure 3 Theoretical (A) and practical (B) energy input for the MEC. The practical energy input is much higher than the theoretical input because of the internal resistance of the different components of the MEC. A more detailed description of these internal resistances is given in chapter 2.

1.3.3. Efficiencies

If MECs, as a hydrogen producing technology from biomass, can compete with other technologies depends on the efficiency of the process. The efficiency of an MEC is generally described by two important parameters: (i) the energetic substrate efficiency and (ii) the specific energy input per amount of product (kWh/m³ H₂).

The energetic efficiency describes how much of the available electrons from the substrate are transferred to the product and what the energy content of these electrons is. Therefore, it is a function of both the voltage efficiency and the coulombic efficiency. The voltage efficiency describes how much of the chemical energy from the substrate eventually ends up in the product while the coulombic efficiency describes the amount of electrons from the substrate that eventually end up in the product. Of course, both efficiencies have to be as high as possible.

The specific energy input for MECs is determined by the total internal resistance of the system and therefore highly depends on design and construction of the system.

1.4. Scope and outline of this thesis

The scope of this thesis is to increase the hydrogen production rate of the microbial electrolysis process and to decrease the specific energy input for this hydrogen. The main focus to achieve this, is on understanding the kinetics of the different processes and use this understanding to make an improved design of the system. The first part of the thesis (chapter 2) gives a model that describes the system in the form of an equivalent circuit. This equivalent circuit represents the internal resistance of the system and forms the basis for possible improvements of the system. Some possible improvements are suggested in the second part of this thesis. Chapters 3 and 4 deal with mass transport processes that led to improvements of the anode performance. This mass transfer also has a strong effect on the coulombic efficiency of the system. Strategies to improve the coulombic efficiency are further investigated in Chapter 5. In chapter 6 a new design is introduced that makes it possible to reuse chemicals that are present in the influent. Reuse of these chemicals reduces operational costs and can take MECs another step closer to practical application. Finally, in chapter 7 a summary of the improvements made to the system is given in terms of production rate and efficiencies and these are compared to a possible technology to produce hydrogen from biomass.

Chapter 2

Microbial Electrolysis Cells with Anion and Cation Exchange membranes

Previous studies have shown that Microbial Electrolysis Cells (MECs) perform better when an anion exchange membrane (AEM) than when a cation exchange membrane (CEM) separates the electrode chambers. Here, we have further studied this phenomenon by comparing two analysis methods for bio-electrochemical systems, based on potential losses and partial system resistances. Our study reconfirmed the large difference in performance between the AEM configuration (2.1 m³/m³/d) and CEM configuration (0.4 m³/m³/d) at 1 Volt. This better performance was caused mainly by the much lower internal resistance of the AEM configuration (192 mΩ m²) compared to the CEM configuration (435 mΩ m²). This lower internal resistance could be attributed to the lower transport resistance of ions through the AEM compared to the CEM caused by the properties of both membranes. By analyzing the changes in resistances the limitations in an MEC can be identified which can lead to improved cell design and higher hydrogen production rates.

This chapter has been published as:

Sleutels, T.H.J.A., Hamelers, H.V.M., Rozendal, R.A., Buisman, C.J.N., 2009. Ion transport resistance in Microbial Electrolysis Cells with anion and cation exchange membranes. *International Journal of Hydrogen Energy*, 34, 3612-3620.

2.1. Introduction

Because of concern of depletion of fossil fuels and the threat of global warming, the search for green energy sources strengthens (Faaij, 2006). A possible green energy source is the chemical energy from organic waste (Angenent et al., 2004). Bioelectrochemical conversion of organic compounds is a novel technology that can efficiently capture this energy and is therefore a topic with increasing research interest (Liu et al., 2005b; Logan and Regan, 2006). One of the most promising emerging bio-electrochemical technologies is hydrogen production in a microbial electrolysis cell (MEC) (Liu et al., 2005b; Logan et al., 2008; Rozendal et al., 2006b). MECs convert the chemical energy of the wastewater into hydrogen gas and at the same time purify the wastewater by degrading the organic compounds (Rozendal et al., 2008a). MECs contain two electrodes: an anode and a cathode. At the anode electrochemically active micro-organisms oxidize the organic compounds to protons, CO₂ and electrons. The electrons are released to the anode and move through an electrical circuit to the cathode (Bond and Lovley, 2003; Lovley, 2006). In the cathode of an MEC the electrons are used to reduce water to hydrogen gas (El-Deab et al., 1996; Rozendal et al., 2007). For this reduction reaction theoretically only a small amount of energy (0.14V) is needed which can be added by means of a power supply (Rozendal et al., 2006b).

To compensate for the negative charge (electrons) moving from anode to cathode, ions move through an ion selective membrane (Kim et al., 2007; Rozendal et al., 2008c; Ter Heijne et al., 2006). Typically cation exchange membranes have been used for this purpose, but several studies have now shown that MEC configuration with an anion exchange membrane (AEM) outperform those with a cation exchange membrane (CEM) (Cheng and Logan, 2007; Rozendal et al., 2007; Rozendal et al., 2008c).

The objective of this study was to further elucidate the reasons for the large difference in performance between MECs with a CEM and an AEM. For this purpose we have developed an analysis method based on partial system resistances. The partial system resistance can be calculated by dividing the potential loss of

every part of the system by the current density ($R=V/j$). At a constant applied voltage the current density that is produced by MECs depends on the internal resistance of the system. Detailed analysis of this internal resistance can give additional information about different systems to the comparison of potential losses. With this analysis method different systems, for example with a CEM and an AEM, can be compared in detail. Furthermore, different experimental conditions, e.g. changes during an experimental run, can be compared. Comparison of these partial resistances can reveal the limitations in the system for optimization. In the future this can lead to improved cell design and higher hydrogen production rates.

2.2. Materials and methods

2.2.1. Electrochemical cell

Experiments were performed in two electrochemical cells similar to the cell used in (Rozendal et al., 2008b), except for the width in the flow channel (1.7 cm) and the channel depth (0.8 cm). The cells consisted of an anode (280 mL) and a cathode chamber (280 mL) separated by a membrane. Two types of ion exchange membranes (surface area 250 cm²) were used: (i) a cation exchange membrane (Fumasep[®] FKE, FuMa-Tech GmbH, Germany) and (ii) an anion exchange membrane (Fumasep[®] FAA, FuMa-Tech GmbH, Germany). In both the anode and cathode the liquid flows parallel to the electrode through the flow channel. This flow channel is used in the anode to press the anode onto the membrane. Both the anode and the cathode chamber were equipped with an Ag/AgCl reference electrode (+0.20 V against NHE - ProSense QiS, Oosterhout, The Netherlands) connected to the cell through a Haber-Luggin capillary. The anode was made of graphite felt (projected surface area 0.025 m², thickness 6.5 mm – National Electrical Carbon BV, Hoorn, The Netherlands). The cathode was made of a platinum coated (50 g/m²) titanium mesh (projected surface area 250 cm², thickness 1 mm, specific surface area 1.7 m²/m² - Magneto Special Anodes BV, Schiedam, The Netherlands). The electrodes were connected to a power supply (ES 03-5, Delta Electronica BV, Zierikzee, The Netherlands).

2.2.2. Experimental procedures

The anode chamber was continuously fed with synthetic wastewater (pH 7) at a rate of 5 mL/min. This synthetic wastewater consisted of 1.36 g/L $\text{NaCH}_3\text{COO}\cdot 3\text{H}_2\text{O}$, 0.74 g/L KCl, 0.58 g/L NaCl, 0.68 g/L KH_2PO_4 , 0.87 g/L K_2HPO_4 , 0.28 g/L NH_4Cl , 0.1 g/L $\text{MgSO}_4\cdot 7\text{H}_2\text{O}$, 0.1 g/L $\text{CaCl}_2\cdot 2\text{H}_2\text{O}$ and 0.1 mL/L of a trace element mixture (Zehnder et al., 1980). To minimize differences in mass transfer losses between the two electrochemical configurations, acetate was always available in excess to ensure no substrate limitations occurred. Each electrochemical cell was started up by inoculating the anode with 100 mL of effluent from an active MEC (Rozendal et al., 2008c). After current production had stabilized, hydrogen production was studied in duplicate runs of 48 hours. Before every run the cathode was flushed with 10 mM of potassium phosphate buffer and subsequently filled with exactly 750 mL of the same buffer solution (pH 7). This flushing of the cathode resulted in a neutral pH in the cathode and limited the pH gradient over the membrane at the start of an experimental run. To remove oxygen the cathode was flushed with N_2 gas (purity >99.9%). The anode was flushed with influent until the pH was 7. A run was started by closing the electrical circuit to apply a voltage of 1V. During a run hydrogen gas accumulated in the headspace of the cathode and gas left the system through a gas flow meter (Milligascounter®, Ritter, Bochum, Germany). The hydrogen fraction in this flow was determined by gas chromatography according to (Rozendal et al., 2007). The anode was sampled every 12 hours and analyzed for acetate content using ion chromatography (Metrohm 761 Compact IC equipped with a conductivity detector and a Metrosep Organic Acids 6.1005.200 ion exclusion column). Ion content of anolyte and catholyte was determined at the start and end of a yield test using a total organic carbon analyzer (Shimadzu TOC-VCPH) for carbonate, an ion chromatograph (Metrohm 761 Compact IC) equipped with a conductivity detector and an anion column (Metrosep A Supp 5 6.1006.520) for other anions (Cl^- , NO_2^- , NO_3^{2-} , PO_4^{3-} , and SO_4^{2-}), a standardized test kit for ammonium (ammonium cuvette test LCK303, XION 500 spectrophotometer, Dr. Lange Nederland B.V., The Netherlands) and inductively coupled plasma-optical emission spectroscopy (ICP-

OES—Perkin Elmer Optima 3000XL) for other cations (Na⁺, K⁺, Ca²⁺, and Mg²⁺). Total charge production in the form of electrons was compared to the transport of charge in the form of these specific ions according to (Rozendal et al., 2007).

A data logger (Memo-graph, Endress + Hauser) continuously logged 8 variables for both cells: anode and cathode potential and cell voltage, current, anode and cathode pH (Liquisys M CPM 253, Endress + Hauser), anode and cathode conductivity (ProSense QiS, Oosterhout, The Netherlands). Conductivity and pH for anode and cathode were measured in a flow cell through which the anolyte/catholyte was continuously pumped at a rate of 340 mL/min. Measured pH values at high salt concentrations can deviate because of liquid junction potentials and were therefore corrected using the measured ion concentrations. The temperature was kept constant at 303K.

2.2.3. Calculations

The applied voltage (E_{cell}) can be divided in two parts: (i) a reversible energy loss and (ii) an irreversible energy loss. The first part of the applied voltage consists of the energy used to overcome the thermodynamical barrier of hydrogen production (equilibrium voltage; E_{eq}). This energy input is recovered in hydrogen gas and is therefore a reversible energy loss. The equilibrium voltage was calculated at pH 7 because this is the pH of the anolyte and catholyte at the start of an experimental run. This way a distinction can be made between the reversible and irreversible energy input. The equilibrium voltage was calculated with the actual concentrations of acetate and bicarbonate using

$$E_{\text{eq}} = E_{\text{cat}} - E_{\text{an}} = \left(E_{\text{cat}}^0 - \frac{RT}{2F} \ln \frac{pH_2}{[10^{-7}]^2} \right) - \left(E_{\text{an}}^0 - \frac{RT}{8F} \ln \frac{[CH_3COO^-]}{[HCO_3^-]^2 [10^{-7}]^9} \right) \quad (1)$$

where E_{cat} is the theoretical cathode potential (V), E_{an} is the theoretical anode potential (V), E_{cat}^0 is the standard cathode potential (V), E_{an}^0 is the standard anode potential (V), R is the universal gas constant (8.3145 J/mol/K), T is the temperature (303 K) and F is the Faraday's constant (96485 C/mol).

The second part of the applied voltage is the irreversible energy loss. This energy is lost as a result of the resistances of different parts of the cell. This voltage loss consists of (i) the pH gradient over the membrane ($E_{\Delta pH}$), (ii) anode overpotential (η_{an}), (iii) cathode overpotential (η_{cat}), (iv) ionic losses (E_{ionic}) and (v) transport losses (E_T) (Fan et al., 2008)

$$E_{cell} = E_{emf} - E_{\Delta pH} - \eta_{an} - \eta_{cat} - E_{ionic} - E_T \quad (2)$$

The Ohmic loss other than the ionic losses of the electrolyte were not measured separately and are included in the overpotential of the anode and cathode (Rozendal et al., 2008c). During an experimental run a pH gradient develops over the membrane which gives an extra amount of potential loss (Rozendal et al., 2006a). This pH gradient loss (V) over the membrane was calculated with

$$E_{\Delta pH} = \frac{RT}{F} \ln(10^{(pH_{cathode} - pH_{anode})}) \quad (3)$$

The anode and cathode overpotential (V) were calculated with

$$\eta_{an} = E_{an,measured} - E_{an}, \quad \eta_{cat} = E_{cat} - E_{cat,measured} \quad (4)$$

where $E_{an, measured}$ is the measured anode potential and $E_{cat, measured}$ is the measured cathode potential. The anode and cathode overpotentials were calculated using the actual concentrations of acetate, bicarbonate and protons at the start and at the end of a run (48 h) (Equation 1). The anode and cathode overpotential include the mass-transfer and charge transfer overpotential and in case of the anode overpotential also the potential that is used by the microorganisms for growth and maintenance. The ionic loss (V) is related to the electrolyte resistance of the anolyte and catholyte and was estimated with (Ter Heijne et al., 2006)

$$E_{ionic} = I_{ions} \left(\frac{1}{2} R_{an} + \frac{1}{2} R_{cat} \right) = I_{ions} \left(\frac{d_{an}}{2A\sigma_{an}} + \frac{d_{cat}}{2A\sigma_{cat}} \right) \quad (5)$$

where I_{ions} is the flow of ions through the electrolyte (A) which is equal to the current, d_{an} is the distance between the anode and the membrane (m), d_{cat} is the distance between the cathode and the membrane (m), A is the surface area (m^2), σ_{an} is the anode conductivity (S/m) and σ_{cat} is the cathode conductivity (S/m).

The transport loss (E_T) was calculated from all other potential losses using equation 2. The transport loss is the potential loss caused by transport of ions through the membrane. The transport loss can also be calculated as the difference between the reference electrode of the anode and the reference electrode of the cathode corrected for the ionic resistance of both anolyte and catholyte and the membrane pH gradient (Ter Heijne et al., 2006). Both methods have been used and the values obtained from both calculation methods correspond.

To calculate the potential losses several parameters should be measured in order to be able to perform the calculations: anode and cathode potential, pH and conductivity, the cell voltage and the produced current density.

2.2.4. MEC performance

The performance of an MEC can be described by the volumetric performance and the energetic performance. The volumetric performance is the amount of hydrogen gas that is produced and the energetic performance is the amount of electrical energy that is required per m³ of hydrogen. Total gas production was measured during a yield test to calculate the volumetric hydrogen production rate. The amount of captured hydrogen can be related to the amount of current produced in the cathodic efficiency. The cathodic efficiency is calculated from the produced current and the measured amount of hydrogen (V_H^m ; L) (Rozendal et al., 2007)

$$\eta_{Cat} = \frac{V_H^m 2F}{V_m \int_{t=0}^t Idt} \quad (6)$$

where V_m is the molar gas volume (22.4 L/mol).

2.3 Results and discussion

2.3.1 MEC performance

In this study we tried to further elucidate the difference in performance of an MEC equipped with an AEM and an MEC equipped with a CEM by looking at changes in

potential losses and internal resistance during an experimental run. The performance of both systems was studied in duplicate runs of 48 hours (Table 1). At the start of an experimental run the pH in both the anode and the cathode was 7. Due to electron transport ions are transported through the membrane. Because ions other than hydroxyl and protons are present in the electrolyte a pH gradient develops over the membrane (Rozendal et al., 2008c). Figure 1A shows the development of this membrane pH gradient and Figure 1B shows the development of the current density for both configurations during an experimental run. The current density shows that the configuration with the AEM outperforms the CEM (CEM 2.3 A/m²; AEM 5.3 A/m²). The higher bioelectrochemical performance of a system equipped with an AEM compared to a system equipped with a CEM is in accordance with results reported in previous research (Cheng and Logan, 2007; Rozendal et al., 2008c). The hydrogen production rate for the AEM configuration (2.1 m³/m³/d) is higher compared to the CEM configuration (0.4 m³/m³/d). This hydrogen production rate for the AEM configuration was high compared to other studies where continuous systems were used (Rozendal et al., 2008c 1.1 m³/m³/d ($V_{\text{cell}} = 1\text{V}$); Tartakovsky et al., 2008 0.92 m³/m³/d ($V_{\text{cell}} = 1.26\text{V}$) and Ditzig et al., 2007 0.01 m³/m³/d ($V_{\text{cell}} = 0.5\text{V}$)). However, hydrogen production rates of these continuous systems are lower than the hydrogen production rates reported for small batch systems (Call and Logan, 2008 3.12 m³/m³/d ($V_{\text{cell}} = 0.8\text{V}$) and Cheng and Logan, 2007 1.23 m³/m³/d ($V_{\text{cell}} = 0.6\text{V}$)).

Anion and cation exchange membranes

Table 1 Comparison of the performance of two MECs equipped with a CEM and an AEM at an applied voltage of 1V.

	Current density (A/m ²)	Cathodic efficiency (%)	Hydrogen production (m ³ H ₂ /m ³ /d)
CEM	2.3 ±0.3	47 ±6	0.4 ±0.1
AEM	5.3 ±0.5	83 ±13	2.1 ±0.5

The cathodic efficiency was higher in the AEM configuration (83%) than in the CEM configuration (47%). Together with the higher current density in the AEM configuration compared to the CEM configuration this higher cathodic efficiency explains the higher hydrogen production rate. The cathodic efficiencies found in this study are low compared to previous studies (101% for both CEM and AEM (Rozendal et al., 2007)). Part of the hydrogen is lost due to diffusion through the membrane. The relative amount of hydrogen lost due to diffusion however is higher at lower hydrogen production rates (Rozendal et al., 2006b). This explains the higher cathodic efficiency in the AEM configuration compared to the CEM configuration which had a lower hydrogen production rate.

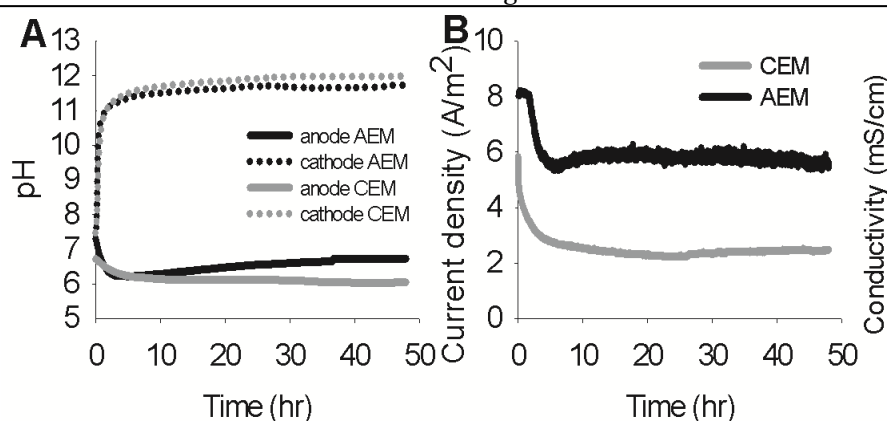


Figure 1 Development of the pH (A) in anode and cathode and current density (B) in MECs equipped with an AEM and a CEM during a 48 h experimental run at an applied voltage of 1V.

2.3.2 Potential losses

An overview of the calculated potential losses (equation 1-5) at the end of a yield test for both membrane configurations is shown in Figure 2A. These potential losses consist of: (i) equilibrium voltage, (ii) pH gradient, (iii) anode overpotential, (iv) cathode overpotential, (v) ionic losses and (vi) transport losses. This figure shows that at the end of a yield test for the CEM configuration (current density 2.3 A/m²) most potential was lost in the pH gradient over the membrane (0.36 V) and the transport loss through the membrane (0.29 V). For the AEM configuration (current density 5.3 A/m²) the anode overpotential (0.33 V) and the pH gradient over the membrane (0.30 V) were the largest losses at the end of a yield test. By comparing the potential losses it does not become clear however why the AEM configuration outperforms the CEM configurations because for both MEC configurations the total potential loss is equal to the applied voltage. This is different from MFCs where the cell voltage is lower when some parts of the system have a higher potential loss (Rabaey and Verstraete, 2005). In MECs it is therefore not possible to compare the performance of different systems by looking at the potential losses. Comparison of potential losses in MECs is only possible at the

same current densities since the total potential loss is current dependent. Within one system on the other hand, it is possible to determine what part within one system is limiting the performance by looking at the potential losses.

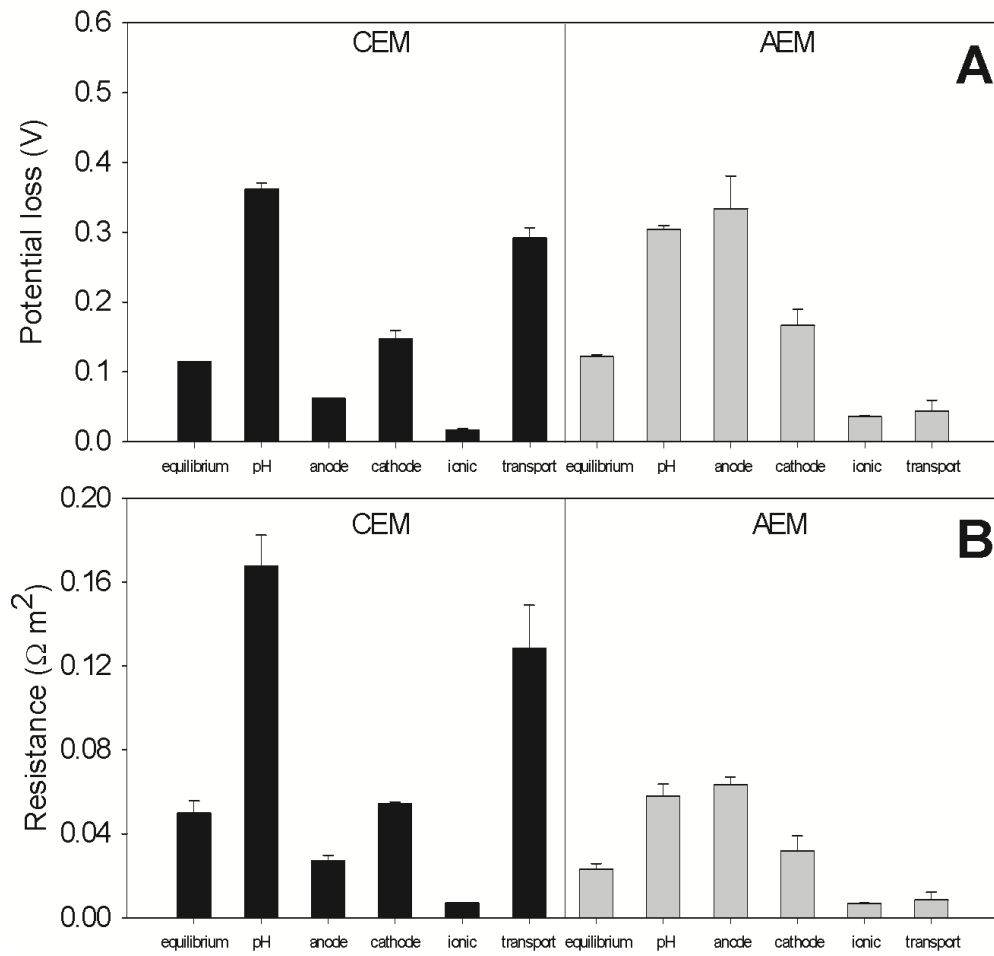


Figure 2 Comparison of potential losses (A) and resistances (B) in MECs equipped with a CEM (2.3 A/m^2) and an AEM (5.3 A/m^2) at the end of a yield test at an applied voltage of 1V.

2.3.3 Resistances

Compared to the potential losses the internal resistance can give additional information about the performance of an MEC, especially when comparing different systems (Bard and Faulkner, 2001; Fan et al., 2008). Since the voltage needed for hydrogen production is constant, the current density depends on the total internal resistance of the system, which in itself is a function of the current density. The total internal resistance is a sum of the partial resistances of the system (Bard and Faulkner, 2001). The partial resistances were calculated by dividing the calculated potential loss by the current density ($R=V/j$). The current density was used here to calculate the resistance instead of the current. This way the resistance is expressed independent of reactor size (Ωm^2) which makes comparison between different reactor systems possible. Some researchers prefer to express resistances and currents as volumetric measures (Clauwaert, 2008). However, the current density depends on the active surface of the electrode material. The projected surface will eventually be the dominant parameter for scaling up of the system (Ramasamy, 2008). For these reasons it is decided here to express the resistance as a measure of the projected surface area.

At the end of a yield test the total resistance of the AEM configuration was $192\text{ m}\Omega\text{ m}^2$ while the total resistance of the CEM configuration was $435\text{ m}\Omega\text{ m}^2$. To explain the differences in performance of the AEM and CEM configuration a more detailed analysis of this internal resistance is necessary. Therefore the partial internal resistances were calculated (Figure 2B). These partial resistances consist of: (i) equilibrium resistance, (ii) pH gradient resistance, (iii) anode resistance, (iv) cathode resistance, (v) ionic resistance and (vi) transport resistance. Figure 3 gives an overview of these partial internal resistances in an MEC, which can be represented by a series of resistances in an equivalent circuit.

When we compare the potential losses in Figure 2A and the internal resistances in Figure 2B it becomes clear that the ratio of potential losses and resistances for one configuration is the same. However, there are also differences between the potential losses and internal resistances between the two configurations. When we

compare the resistances for both systems it immediately becomes clear that the total resistance of the AEM configuration is lower than the total resistance of the CEM configuration.

Furthermore, when we compare the potential losses and partial resistances for the two different membrane configurations some differences in conclusions exist. For example, the cathode potential loss in the CEM configuration (0.15 V) is smaller than the cathode potential loss in the AEM configuration (0.17 V) while the cathode resistance for the CEM configuration is larger (65 mΩm²) than the cathode resistance for the AEM configuration (32 mΩm²).

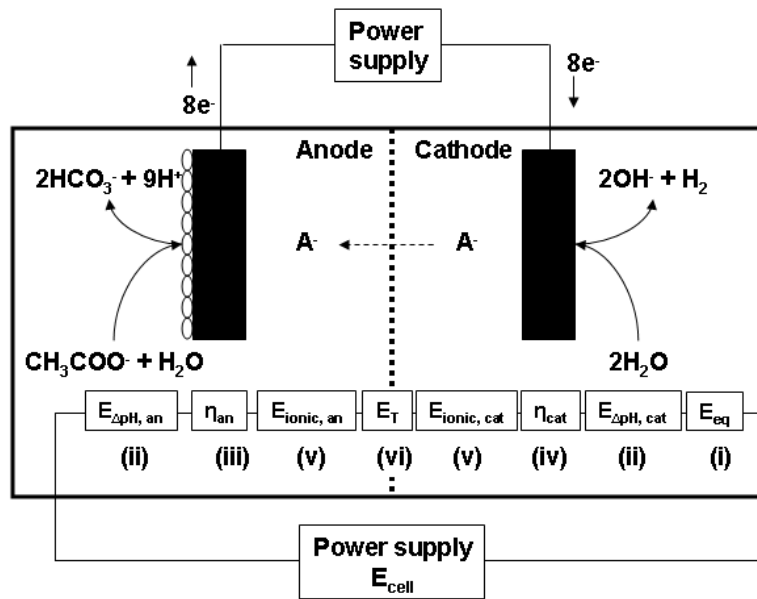


Figure 3 Overview of the potential losses in an MEC equipped with an AEM at an applied voltage of 1V. The potential losses consist of: (i) equilibrium voltage, (ii) pH gradient, (iii) anode overpotential, (iv) cathode overpotential, (v) ionic losses and (vi) transport losses. Both the pH gradient and the ionic losses can be split up in an anodic and a cathodic part. The total internal resistance of an MEC can be represented as a series of resistances in an equivalent circuit. The total potential loss is always equal to the applied voltage (E_{cell}).

The main differences between analysis of internal resistances and analysis of potential losses are: (i) the internal resistances of the different parts of the system can be quantified and compared to the internal resistances of another system e.g. a comparison between a configuration with a CEM and a configuration with an AEM can be made and (ii) it is possible to compare different experimental conditions within one system e.g. it is possible to compare the start of an experimental run with the end of an experimental run. This comparison of resistances is possible because the resistances are independent of the current densities and most potential losses are current dependent. Comparison of potential losses gives more information when current independent parameters like the equilibrium voltage are compared.

2.3.4 Transport resistance

One of the most striking differences between the two membrane configurations is the transport resistance. This transport resistance is the resistance experienced by the ions that are transported through the membrane. The concentration of ions in anolyte and catholyte changes during an experimental run and therefore also the transport resistance changes during an experimental run (Figure 4). Since the comparison of the partial resistances is independent of current density it is also possible to compare different experimental conditions. Therefore it is also possible to compare the transport resistance at the start of an experimental run to the transport resistance at the end of an experimental run. At the start of an experimental run anolyte and catholyte composition for both membrane configurations were comparable. Still the transport resistance of the CEM configuration ($48 \text{ m}\Omega\text{m}^2$) was already much higher than the transport resistance in the AEM configuration ($12 \text{ m}\Omega\text{m}^2$). At the end of an experimental run this difference in transport resistance between CEM ($128 \text{ m}\Omega\text{m}^2$) and AEM configuration ($8 \text{ m}\Omega\text{m}^2$) became only larger.

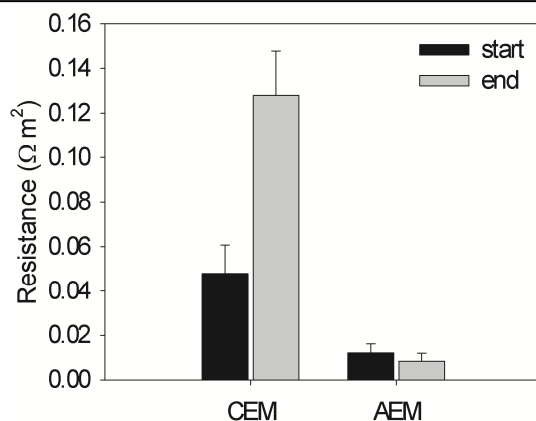


Figure 4 Transport resistance at the start and end of an experimental run in an MEC equipped with an AEM and in an MEC equipped with a CEM

From Figure 2A it seems as if at the end of an experimental run the pH in both the anode and cathode chamber and the current density become constant. This suggests that a significant part of the charge transport was represented by hydroxyl and/or protons. Since hydroxyl and protons are closely linked to buffer components through the water equilibrium it is difficult to distinguish between the transport of hydroxyl, protons and buffer components. Figure 5 shows the conductivity in the cathode as a function of the transported charge through the system during a typical experimental run. This figure confirms that the ion concentration in the cathode of the AEM configuration is already going to equilibrium and the dominant species transported here will be hydroxyl and/or protons and buffer components. The conductivity in the cathode of the CEM configuration, however, still increases linearly. This implies that still other ions than protons and hydroxyl are being transported through the membrane and the pH is not constant. Figure 6 shows an overview of the contribution of ions present in the system to the total charge transport through the membrane during the total experimental runs. This figure confirms that in the AEM configuration hydroxyl and protons represent most charge transport through the membrane. For the CEM

configuration hydroxyl and protons also form the largest fraction of charge transport, but also other, especially cations, take part in charge transport.

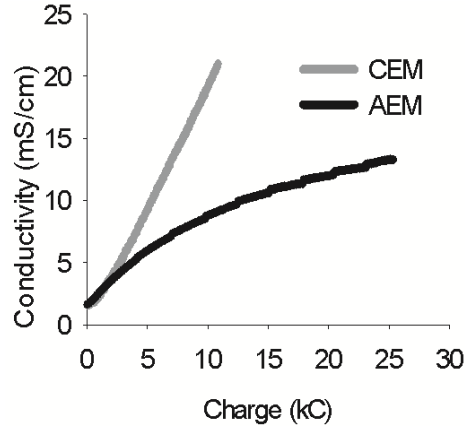


Figure 5 Conductivity of the cathode as a function of the produced charge during an experimental run.

The transport of the type of ion depends on the concentration difference between the anode and cathode compartment for that specific ion. However, because the membrane is charged, counter-ions will move into the membrane to compensate for this charge. As a result, the concentration of ions inside the membrane will be significantly different from the concentration of ions in the solutions and also the actual concentration gradient for those ions will be different. The concentration gradient of ions inside the membrane can be calculated with the Donnan equilibrium (Sata, 2004). This Donnan equilibrium gives the relation between the concentration of ions in the electrolyte (C_{ion} in mol/L) and the concentration of ions in the membrane (\bar{C}_{ion} in mol/L)

$$K_{donnan} = \frac{\bar{C}_{ion}}{C_{ion}} \quad (7)$$

The concentration of ions in the membrane depends on the charge inside the membrane and is represented by the fixed charge density. This fixed charge density (C_{ix} in mol/L) is the amount of charge the membrane contains per liter and can be

calculated from the concentration of ion exchange groups attached to the polymer matrix (IEC; mequiv/g_{dry}) and the swelling degree (SD; g_{H₂O}/g_{dry}) (Dlugolecki et al., 2008). With this Donnan equilibrium the concentration gradient for the most important ions contributing to ion transport were calculated for both membrane configurations at the start and end of an experimental run. Table 2 shows an overview of the estimated concentration gradients inside the CEM and AEM. From this table it becomes clear that at the start of an experimental run the largest concentration gradients are represented by K⁺, Na⁺, NH₄⁺, Mg²⁺ and Ca²⁺ in the CEM. The concentration gradient for K⁺ is -0.60 mol/L. This negative concentration means that the concentration of K⁺ in the cathode is higher than the concentration in the anode. Figure 6 shows that K⁺ contributes to a large part (30%) of the charge transport through the membrane although they are transported against their concentration gradient. Transport of ions against a concentration gradient will give a larger resistance for transport. At the end of the experimental run the concentration gradient for K⁺ and also Na⁺ is even more negative (-4.9 and -2.9 mol/L respectively). The increase in transport resistance at the end of the experimental run compared to the start of the experimental run corresponds to this increase in ion concentration in the membrane. Furthermore the concentration gradient at the end of an experimental run for Ca²⁺ is large (2.8 mol/L) while hardly any Ca²⁺ is transported through the membrane as can be seen from Figure 6. It is likely that Ca²⁺ does contribute to the charge transport but precipitated together with phosphate or carbonate in the cathode compartment.

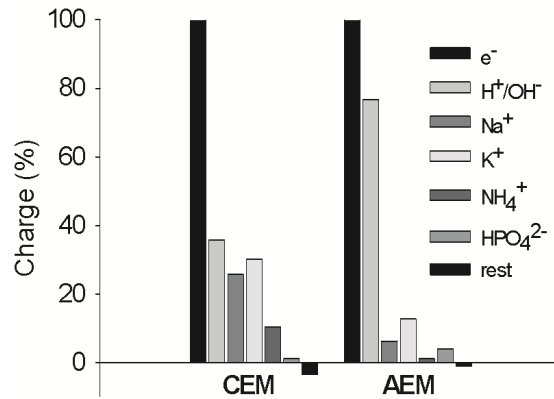


Figure 6 Comparison of the total charge production (e^-) to the transport of specific ions through CEM and AEM in an experimental run at an applied voltage of 1.0 V. Total charge production is set to 100% for relative comparison.

In the AEM configuration especially the concentration gradient for the different phosphate buffer species are important. At the start of an experimental run especially HPO_4^{2-} is transported from the cathode to the anode, while some other species are transported back. At the end of an experimental run the concentration gradient for HPO_4^{2-} is 1.6 mol/L while the concentration gradient for PO_4^{3-} is -1.6 mol/L. This means PO_4^{3-} is transported to the anode while HPO_4^{2-} is transported back to the cathode. This causes shuttling of charge through buffer species that are transported through the membrane. The transport of charge through an AEM through buffer species was also suggested by Cheng and Logan (Cheng and Logan, 2007). From Figure 6 it becomes clear that in the AEM H^+/OH^- contribute to a large extent (77%) to the charge transport through the membrane. However, H^+/OH^- are closely linked to buffer species through the water equilibrium and it is therefore hard to distinguish between these species. So the transport of buffer species through the membrane is actually also transport of H^+/OH^- through the membrane.

For both membranes it is worth mentioning that the concentration gradient for protons is negligible and protons will therefore hardly contribute to charge transport through the membrane. The differences in transport resistance for both

membranes are caused by the properties of the membrane and the concentration gradients these properties cause inside the membrane.

The calculated transport resistance in the AEM configuration ($8 \text{ m}\Omega \text{ m}^2$) is still higher than the membrane resistance alone ($<0.2 \text{ m}\Omega \text{ m}^2$ (GmbH, 2005)). Besides transport losses through the membrane, the transport of ions could also be limited by the anode configuration. In the set-up used, the anode material is pressed against the membrane creating an anolyte layer inside the felt that is not well mixed. Visual inspection of the anode clearly showed that the major part of the biofilm was growing on the anolyte side of the graphite felt. Therefore the charge transport in the AEM configuration has to move from the membrane through the felt towards the biofilm. Ion transport limitations are especially evident in systems with low alkalinity and ionic strength like the system used in this study (Liu et al., 2005a; Rozendal et al., 2008a). These low buffer concentrations were used in this study because eventually the system will be applied in the treatment of wastewater. Wastewater also has a low buffer capacity, so here ion transport will also become a problem.

In this study we presented two methods to analyze MEC systems in detail and to compare different experimental stages. These methods are based on the calculation of the partial internal resistances and potential losses of the system. Comparison of the partial resistances of an MEC equipped with a CEM and with an AEM showed that the AEM configuration outperforms the CEM configuration because of a much lower transport resistance. In the future the calculation of the partial internal resistances can be used to quantify changes in internal resistance and to identify limitations in the system. Because the resistances are expressed as Ωm^2 they are independent of reactor size. In the future this can lead to better cell design and higher hydrogen production rates.

Anion and cation exchange membranes

Table 2 Estimation of most important ion concentration gradients inside cation and anion exchange membranes with the Donnan equilibrium at the start and end of an experimental run. A positive gradient corresponds to a higher anode concentration compared to the cathode concentration.

	CEM		AEM	
IEC (mequiv/g)	1.36 ^a		1.5 ^b	
SD (%)	12 ^a		25 ^b	
C _{fix} (mol/L)	11.3		6.0	
Ion concentration (mol/L)	start	end	start	end
K ⁺	-0.60	-4.9	0	-0.004
Na ⁺	0.23	-2.9	0	-0.002
Ca ²⁺	0.097	2.8	0	0
Mg ²⁺	0.03	0.95	0	0
Cl ⁻	0	0	0.77	0.77
SO ₄ ²⁻	0	0	0.30	0.24
NH ₄ ⁺	0.12	0.26	0	0
Acetate ⁻	0	0	0.16	0.018
HCO ₃ ⁻	0	0	0.046	0.17
H ₂ PO ₄ ⁻	0	0	0.097	0.25
HPO ₄ ²⁻	0	0	-0.84	1.6
PO ₄ ³⁻	0	0	0	-1.6
H ⁺	0	0	0	0
OH ⁻	0	-0.006	0	-0.07

^a data taken from Dlugolecki et al (Dlugolecki et al., 2008)

^b data taken from technical datasheet FuMa-Tech GmbH, Germany (GmbH, 2005)

Acknowledgements

This work was performed in the TTIW-cooperation framework of Wetsus, centre of excellence for sustainable water technology (www.wetsus.nl). Wetsus is funded by the Dutch Ministry of Economic Affairs, the European Union European Regional Development Fund, the Province of Fryslan, the city of Leeuwarden and by the EZ-KOMPAS Program of the “Samenwerkingsverband Noord-Nederland”. The authors like to thank the participants of the research theme “Hydrogen” for the fruitful discussions and their financial support. The authors further thank Annemiek ter Heijne and David Strik for critical reading of the manuscript. René Rozendal is supported by the Australian Research Council (DP 0666927).

Chapter 3

Improved performance of porous bio-anodes in Microbial Electrolysis Cells by enhancing mass and charge transport

To create an efficient MEC high current densities and high coulombic efficiencies are required. The aim of this study was to increase current densities and coulombic efficiencies by influencing mass and charge transport in porous electrodes by: (i) introduction of a forced flow through the anode to see the effect of enhanced mass transport of substrate, buffer and protons inside the porous anode and (ii) the use of different concentrations of buffer solution to study the effect of enhanced proton transport near the biofilm. A combination of both strategies led to a high current density of 16.4 A/m² and a hydrogen production rate of 5.6 m³/m³/d at an applied voltage of 1 V. This current density is 228% higher than the current density without forced flow and high buffer concentration. Furthermore the combination of the anode and transport resistance was reduced from 36 mΩm² to 20 mΩm². Because of this reduced resistance the coulombic efficiency reached values of over 60% in this continuous system.

This chapter has been published as:

Sleutels, T.H.J.A., Lodder, R., Hamelers, H.V.M., Buisman, C.J.N., 2009. Improved performance of porous bio-anodes in microbial electrolysis cells by enhancing mass and charge transport. *International Journal of Hydrogen Energy*, 34, 9655-9661.

3.1. Introduction

A promising alternative energy source is the organic material from wastewaters (Rabaey and Verstraete, 2005). Microbial electrolysis cells (MECs) are devices that are able to convert chemical energy from wastewater directly into hydrogen in one cell (Liu et al., 2005b; Rozendal et al., 2006b). Since these systems produce energy from wastewater their purpose is twofold: efficient purification of wastewater (Ditzig et al., 2007) and high yield hydrogen production (Logan et al., 2008; Rozendal et al., 2008a).

An MEC typically consists of two compartments: an anode and a cathode separated by an ion selective membrane while recently it has also been demonstrated that the membrane can be left out (Call and Logan, 2008). However, leaving the membrane out leads to substrate/product crossover and unwanted side products like methane. In the anode biodegradable material is oxidized by electrochemical active micro-organisms (electrogens) to bicarbonate, protons and electrons. The released electrons are donated to the anode surface and transported through an electrical circuit to the cathode. This flow of electrons can be measured as an electrical current and is a measure for the amount of oxidized biodegradable material by the electrogens. To compensate for this transport of electrons, charged ions are transported through the ion selective membrane that separates both compartments. Typically cation selective membranes are used to separate the compartments but also other membranes have been tested (Kim et al., 2007; Rozendal et al., 2008c; Ter Heijne et al., 2007). At the cathode, electrons are combined with water to form hydrogen gas at neutral and high pH (El-Deab et al., 1996). A small voltage (0.14 V in theory) has to be applied over the cell with a power supply to make this slightly endothermic reaction possible (Logan et al. 2006).

To be efficient as a wastewater treatment system high conversion rates of organic matter are required. Furthermore, to get all the available energy from the substrate high conversion efficiencies are required. The conversion rate of substrate to electrons is expressed as current density while the conversion efficiency is expressed as the coulombic efficiency e.g. the amount of substrate converted to

electrons. So far a current density of 14 A/m² in a batch system has been reported (Hu et al., 2008) and coulombic efficiencies ranging from 23% to over 90% have been reported in continuous systems depending, amongst others, on loading rates and retention times (Clauwaert et al., 2008; Rozendal et al., 2006b; Tartakovsky et al., 2009).

The aim of this study was to increase current densities and coulombic efficiencies in an MEC at a fixed loading rate by influencing the mass and charge transport in the system. A possibility to achieve high volumetric current densities in MEC systems is the use of porous electrodes (Brett and Brett, 1993). Porous electrodes like graphite felt have the advantage of a high specific surface area in a small volume, which potentially lead to high volumetric current densities. An increase of the thickness of these porous electrodes could lead to higher current densities since more surface is available for biofilm attachment. At the same time however, increasing the surface may lead to mass and charge transport limitations inside the porous electrode. Two strategies were tested to study the effect of mass and charge transport in three thicknesses of porous electrodes on current densities and coulombic efficiencies: (i) the introduction of a forced flow through the anode to see the effect of enhanced mass transport of substrate, buffer and protons inside the porous anode and (ii) the use of different concentrations of buffer solution (10 and 50 mM) to study the effect of enhanced proton transport near the biofilm and finally a combination of both strategies.

3.2. Materials and methods

3.2.1. Electrochemical cell

Three electrochemical cells were used in these experiments similar to the cells used by (Rozendal et al., 2008b). Each cell consisted of two parts: an anode and a cathode chamber (280 mL each). Both chambers were equipped with an Ag/AgCl reference electrode (ProSense QiS, Oosterhout, The Netherlands) connected to the cell through a Haber-Luggin capillary. The anode and cathode were separated by an anion exchange membrane (AMX - Neosepta, Tokuyama Corp., Japan). Three

types of porous anode material were used: (i) 6.5mm thick graphite felt (National Electrical Carbon BV, Hoorn, The Netherlands), (ii) 3mm thick graphite felt (FMI Composites Ltd., Galashiels, Scotland) and (iii) 1mm thick carbon felt (Technical Fibre Products Ltd., Kendal, United Kingdom), all with a projected surface area of 0.025 m². In the forced flow experiments, spacer material (64% open; PETEX 07-4000/64, Sefar BV, Goor, The Netherlands) with a total thickness of 4mm was placed between the anode and the membrane. The cathode was made of a platinum coated (50 g m⁻²) titanium mesh (projected surface area 0.025 m², thickness 1mm, specific surface area 1.7 m²/m² - Magneto Special Anodes BV, Schiedam, The Netherlands). The electrodes were connected to an adjustable power supply (ES 03-5, Delta Electronica BV, Zierikzee, The Netherlands). All experiments were performed at an applied voltage of 1V.

3.2.2. Experiments

Our strategy consisted of using three thicknesses of graphite felt (1, 3 and 6.5 mm). All these types of felt were pressed between the flow plate and the membrane causing the anolyte to flow parallel to the felt. When spacer material was placed between the membrane and the felt the anolyte was forced to flow perpendicular through the felt. Both the experiments with and without forced flow through the anode were performed with a 10 and a 50 mM phosphate buffer solution.

3.2.3. Experimental procedures

Each electrochemical cell was inoculated with 100 mL of effluent from an active MEC (Sleutels et al., 2009a). The anode chamber was continuously fed with synthetic wastewater at a rate of 5 mL/min. This synthetic wastewater was prepared in 10 or 50 mM phosphate buffer solution (pH 7) and consisted of 1.36 g/L NaCH₃COO·3H₂O, 0.74 g/L KCl, 0.58 g/L NaCl, 0.28 g/L NH₄Cl, 0.1 g/L MgSO₄·7H₂O, 0.1 g/L CaCl₂·2H₂O and 0.1 mL/L of a trace element mixture (Zehnder et al., 1980). After current production had stabilized, hydrogen production was studied in duplicate runs of 48 hours. Before every run the cathode was flushed with phosphate buffer solution and subsequently filled with exactly 800 mL of the same buffer solution (10 or 50 mM depending on the experiment).

To remove oxygen the cathode was flushed with N₂ gas (purity >99.9%). A run was started by closing the electrical circuit. Hydrogen production during a run was measured using a gas flow meter (Milligascounter®, Ritter, Bochum, Germany). The hydrogen fraction in this flow was determined by gas chromatography (Shimadzu GC-2010 equipped with a thermal conductivity detector and a Varian molsieve 5A column, Shimadzu Benelux, Den Bosch, The Netherlands). The anode was sampled after 0, 24 and 48 hours and analyzed for acetate content using ion chromatography (Metrohm 761 Compact IC equipped with a conductivity detector and a Metrosep Organic Acids 6.1005.200 ion exclusion column). Bicarbonate concentrations were determined using a total organic carbon analyzer (Shimadzu TOC-VCPH) after 0 and 48 hours. A data logger (Memo-graph, Endress + Hauser) continuously logged anode and cathode potential, cell voltage, current, anode and cathode pH (Liquisys M CPM 253, Endress + Hauser) and anode and cathode conductivity (ProSense QiS, Oosterhout, The Netherlands) for each cell. Conductivity and pH for anode and cathode were measured in a flow cell through which the anolyte/catholyte was continuously pumped at a rate of 340 mL/min. The temperature was kept constant at 303K.

3.2.4. Calculations

The total theoretical current (I_{th}) that can be produced from the consumed amount of substrate can be calculated with

$$I_{th} = nFQ(C_{in} - C_{out}) \quad (1)$$

where I is the current in (A), n is the amount of electrons released during the oxidation of substrate, F is Faraday's constant (96458 C/mol), Q is the influent flow rate (L/s) and C_{in} and C_{out} are the in- and outgoing substrate concentrations respectively (mol/L).

Substrate conversion to current can be expressed in the coulombic efficiency. This coulombic efficiency can be calculated from the integrated measured current (I_m) and total theoretical current production using

$$\eta_{CE} = \frac{\int_0^t I_m dt}{I_m t} \quad (2)$$

The changes made to the anode compartment will influence the anode resistance and the resistance for the transport of ions through the membrane (transport resistance). This transport resistance changes because the diffusion layer on the anode side of the membrane is influenced by the design. Since the changes to the design will influence the anode resistance and transport resistance at the same time it is hard to distinguish what the effect will be on the separate resistances. Therefore they are reported together.

Performance of the anode is expressed in the anode overpotential (η_a in V) and can be calculated from the actual concentrations of bicarbonate, acetate and protons using

$$\eta_{an} = E_{measured} - \left(E_{an}^0 - \frac{RT}{8F} \cdot \ln \frac{[CH_3COO^-]}{[HCO_3^-]^2 [H^+]^9} \right) \quad (3)$$

where $E_{measured}$ is the measured anode potential (V), E_{an}^0 is the standard anode potential (V) calculated from the Gibbs free energy, R is the universal gas constant ($J K^{-1} mol^{-1}$) and T is the temperature (K). The anode resistance can be calculated by dividing the anode overpotential by the current density.

The transport resistance (R_t) of ions through the membrane can be calculated from all other resistances as described in (Sleutels et al., 2009a) with

$$R_t = R_{cell} - R_{emf} + R_{an} + R_{cat} + R_{ionic} \quad (4)$$

Where R_{cell} is the applied voltage divided by the current density, R_{emf} is the resistance for hydrogen production at experimental conditions, R_{an} is the anode resistance, R_{cat} is the cathode resistance and R_{ionic} is the total resistance of anolyte and catholyte. All resistances were expressed in Ωm^2 using the projected surface area of the anode ($0.025 m^2$) in the calculations.

3.3. Results and discussion

The aim of this study was to increase current densities and coulombic efficiencies in an MEC at a fixed loading rate by influencing the mass and charge transport in the system. Two strategies were tested to study the effect of mass and charge transport in three thicknesses of porous electrodes: (i) the introduction of a forced flow through the anode to see the effect of enhanced mass transport of substrate, buffer and protons inside the porous anode and (ii) the use of different concentrations of buffer solution (10 and 50 mM) to see the effect of enhanced proton transport near the biofilm and finally a combination of both strategies.

3.3.1. Felt thickness

Figure 1A shows the effect of felt thickness on current densities. When the flow was parallel to the anode (flow past), an increase of the anode thickness resulted in a decrease in current density (6.5 mm 5.1 A/m²; 3 mm 9.2 A/m²; 1 mm 10.0 A/m² or 6.5 mm 227 A/m³; 3 mm 410 A/m³; 1 mm 448 A/m³). However, an increase in current density was expected because in thicker felts more surface is available for biomass growth, potentially leading to higher conversion rates of substrate and higher current densities. Apparently, when the flow was parallel to the anode, the liquid layer inside the felt was not well-mixed because the anode material was pressed against the membrane. Therefore, in thicker types of felt the substrate availability may have been limited in deeper parts of the felt. Besides availability of substrate, diffusion of protons away from the biofilm was also limited (Torres et al., 2008). This causes the biofilm to mainly develop at the anolyte side of the felt leaving a large part of the available surface inside the felt uncovered by the biofilm, which was also shown by visible inspection of the felt. Because the biofilm mainly developed on the anolyte side of the thicker felts, the ions that compensate for the produced electrons had to travel a larger distance, causing a higher ionic resistance and consequently a lower current density.

Enhanced mass and charge transport in porous anodes

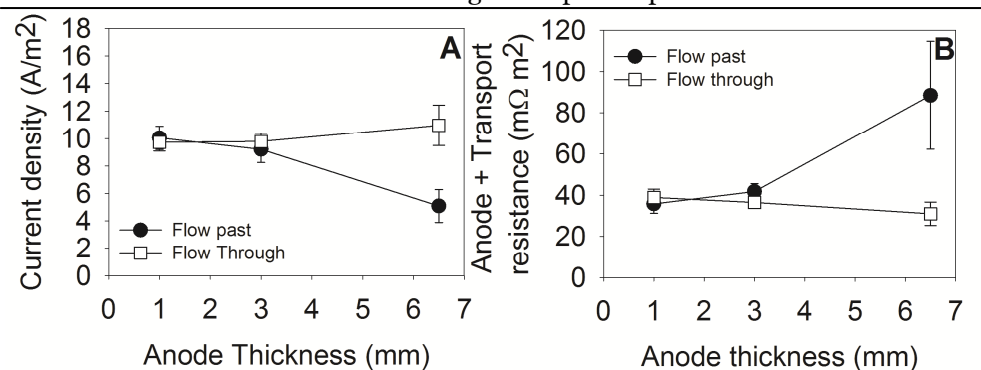


Figure 1 Effect of felt thickness (flow past) and a forced flow through the anode material on (A) current densities (A/m²) and (B) anode + transport resistance (mΩ m²) in an MEC at an applied voltage of 1V.

The resistance as a result of limited transport of protons away from the biofilm and ions through the system is expressed in the anode and transport resistance. Figure 1B shows that this anode and transport resistance increased with increasing felt thickness (1 mm 36 mΩm²; 3 mm 42 mΩm²; 6.5 mm 89 mΩm²). Accumulation of protons near the biofilm leads to a higher overpotential as can be calculated by the Nernst equation (equation 3) resulting in a higher anode resistance. The transport resistance for ions through the membrane is also higher for thicker felt types. This is caused by the bigger liquid layer that is not well mixed inside the felt. This increases the diffusion layer on the membrane surface. A larger diffusion layer on the membrane surface causes a higher the transport resistance for ions through the membrane.

3.3.2. Flow through anode

To increase the availability of substrate inside the felt and to promote the protons to be transported away from the biofilm spacer material was placed between the membrane and the anode felt. When spacer material was placed between the membrane and the felt the anolyte was forced to flow through the felt. This forced flow through the felt enables mixing inside the felt. Because of this mixing, the

substrate is expected to be able to reach every part of the felt increasing the effective surface area of the anode, especially for the thicker felt types. Also the transport of protons away from the biofilm is expected to be better. Figure 1A indeed shows a higher current density for the thicker felts (6.5 mm 11.0 A/m²; 3 mm 9.8 A/m² or 6.5 mm 489 A/m³; 3 mm 437 A/m³) compared to the results without forced flow. However, when 1mm felt was used the current density did not increase compared to the flow past experiment (9.7 A/m² or 434 A/m³). Visual inspection of the 1mm felt after the experiment with anolyte flowing past the anode already showed biomass growth on the membrane side of the felt while with the 3 and 6.5 mm felt no biomass was visible on the membrane side. This indicates that the entire surface of the felt was already used for biomass growth in the 1 mm felt. Since diffusion of substrate was not limiting in the flow past experiment, forced flow of anolyte through the felt was not expected to lead to an increase in current density. For the 3 and 6.5 mm felt the current density did increase compared to the flow past experiment, indicating that substrate availability was limited in the flow past experiments inside these felts. When flowing through the felt the current densities for the 3 mm and 6mm felt were expected to be higher than for the 1mm felt since more surface is available for biomass growth. Unexpectedly, the found current densities were lower. This might be caused by a low flux of ions and substrate inside the electrode due to a slow flow of anolyte through the electrode (1.4 cm/min¹). The time for the anolyte to pass through a thin anode (1 mm) is shorter than the time for the anolyte to pass through a thick anode (6.5 mm). This low flux might still cause accumulation of protons and bicarbonate and a depletion of substrate inside the electrode, causing the overpotential to increase. As this accumulation inside the felt was not measured, it is not expressed in the resistances calculated for the three felt thicknesses (Figure 1B). These values therefore show more or less the same value for all felt types (1 mm 39 mΩm²; 3 mm 37 mΩm²; 6.5 mm 31 mΩm²).

Although the ionic resistance of the system increased (± 1 mΩm²) because of an increase in distance between the electrodes as a result of the spacer material (4 mm), the system performed better because mass and charge transport were

facilitated better in this flow through configuration. In the future this distance between the electrodes can be reduced by choosing a thinner spacer to minimize the ionic resistance of the system.

3.3.3. Buffer concentration

The effect of an increase in buffer concentration in the system is expected to be twofold: (i) an increase in proton transport away from the biofilm (Torres et al., 2008) and (ii) a lower ionic resistance of the system caused by an increased ionic strength of both anolyte and catholyte. The increased proton transport and the lower ionic resistance indeed shows a higher current density for the experiments with 50 mM phosphate buffer in Figure 2A (6.5 mm 10.1 A/m²; 3 mm 9.8 A/m²; 1 mm 13.6 A/m² or 6.5 mm 453 A/m³; 3 mm 438 A/m³; 1 mm 582 A/m³) compared to the experiments with 10 mM phosphate buffer (flow past experiments) as shown in Figure 1A. Since the liquid inside the felt is not well mixed, mass transport is only facilitated by diffusion in this configuration. In the experiments with 10 mM phosphate buffer these mass transport limitations cause substrate limitations in deeper parts of the thicker anodes. Because of these substrate limitations not the entire surface of the electrodes can be utilized for biomass growth. However, because of milder pH conditions inside the felt at 50 mM phosphate buffer the current density did increase compared to the experiments with 10 mM phosphate buffer. An increase in proton transport away from the biofilm leads to a smaller pH drop near the biofilm. Consequently a more neutral pH is created, resulting in a better development and performance of the biofilm. The effect of higher buffer concentrations on current densities for the 3 and 6 mm felt is the same as the effect of forced flow of anolyte through these porous electrodes, as can be seen from Figure 2A. This is confirmed by the values calculated for the anode and transport resistance as shown in Figure 2B, which show more or less the same values for all felt types for both applied strategies. However, the use of high buffer concentrations is undesirable because of increased treatment costs and because discharge of high concentrations of e.g. phosphate is not allowed (Jeremiasse et al., 2009). Therefore the use of a forced flow through porous electrodes as an

alternative for high buffer concentrations is more attractive since the same current densities can be reached.

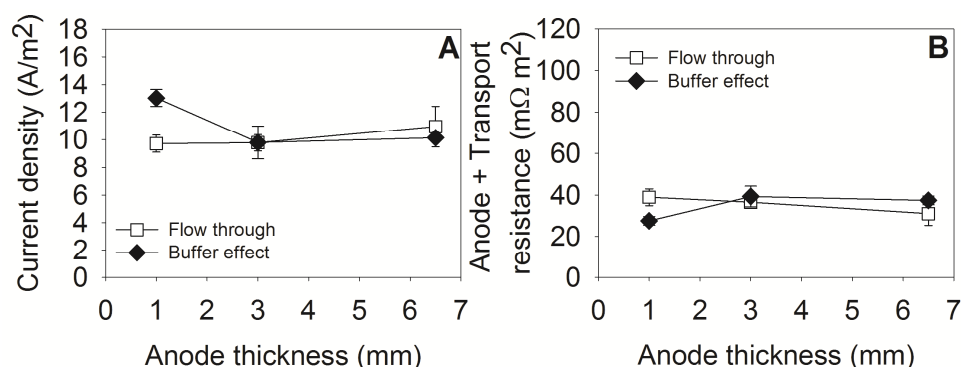


Figure 2 Effect of two methods to increase mass and charge transport in porous electrodes: Forced flow and increased buffer concentrations on (A) current densities (A/m²) and (B) anode + transport resistance (mΩ m²) in an MEC at an applied voltage of 1V.

An increase of ionic strength has a positive effect on current densities since the ionic resistance of the system is smaller. To check whether the buffer concentration indeed had a positive effect on proton transport and on current production an experiment was performed with 10 mM phosphate buffer with an ionic strength (added NaCl) comparable with the ionic strength of 50 mM phosphate buffer (9.8 mS/cm). Figure 3 shows the current densities for 10 mM phosphate buffer (11.0 A/m²), 10 mM phosphate buffer with increased ionic strength (12.5 A/m²) and 50 mM phosphate buffer (13.6 A/m²). This indeed shows that the current density increases at higher ionic strength but increases another 9% when higher phosphate buffer concentrations were used. So the increase in current density could not only be attributed to the lower ionic resistance of the system at 50 mM phosphate buffer but also to a better transport of protons away from the biofilm. An increase in current density with an increase in buffer concentrations is in agreement with results from other researchers (Fan et al., 2007b; Gil et al., 2003).

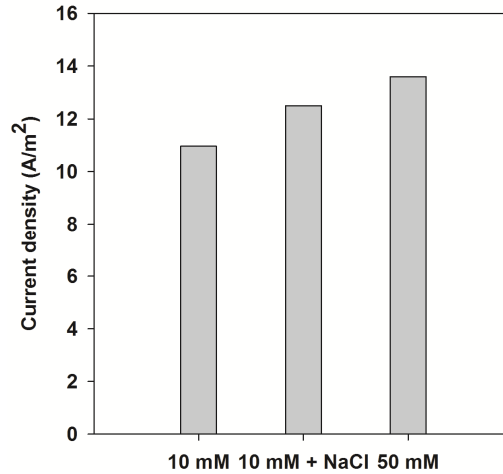


Figure 3 Current density (A/m²) for experiments performed with 10 mM phosphate buffer, 50 mM phosphate buffer and 10 mM phosphate buffer with increased ionic strength comparable with 50 mM phosphate buffer (9.8 mS/cm) in an MEC with 6.5mm felt and forced flow through the felt.

3.3.4. Buffer effect and flow through anode

Combination of a flow through anode and a high buffer concentration (50 mM) increased current densities even further as shown in Figure 4A (6.5 mm 13.6 A/m²; 3 mm 14.4 A/m²; 1 mm 16.4 A/m² or 6.5 mm 607 A/m³; 3 mm 641 A/m³; 1 mm 732 A/m³). The enhanced mass and charge transport can also be seen from the anode and transport resistance in Figure 4B (1 mm 20 mΩm²; 3 mm 23 mΩm²; 6.5 mm 24 mΩm²) which are much lower than the resistances found in the flow past experiments (1 mm 36 mΩm²; 3 mm 42 mΩm²; 1 mm 89 mΩm²). The increase in current densities is the combined result of an increased buffer capacity, an increased ionic strength and increased mass transport through the electrode. The combination of these properties makes this new anode design also suitable for stacking because the total thickness of a cell can be small compared to other anode designs (Logan et al., 2007). The current produced in the 1mm experiment (16.4 A/m² or 732 A/m³) is very high compared to values found by other researchers for both MEC; Hu et al. 14 A/m² (0.6 V applied voltage) (Hu et al., 2008) and

Tartakovsky et al. 6 A/m² (Tartakovsky et al., 2009) (1.0V applied voltage);. and MFC: Fan et al. 6 A/m² (Fan et al., 2007a); Logan et al. 310 A/m³ (Logan et al., 2007). This current density led to a hydrogen production rate of 5.6 m³/m³/d (71% cathodic hydrogen recovery).

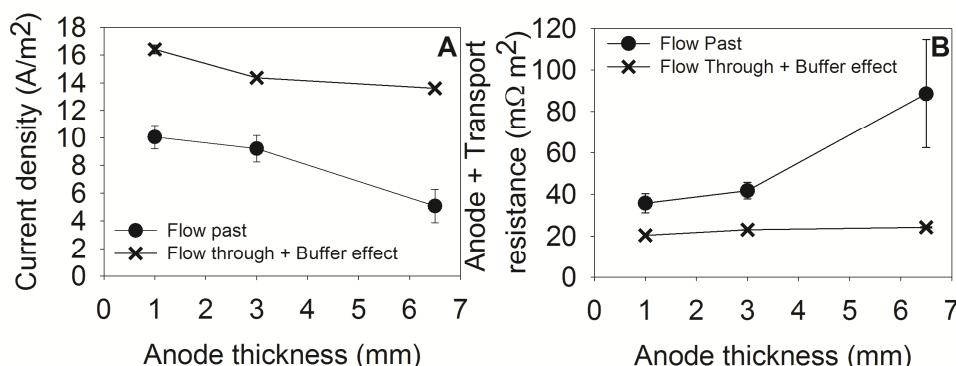


Figure 4 Effect of flow past and flow through of the anode material on (A) current densities (A/m²) and (B) anode + transport resistance (mΩ m²) in an MEC at an applied voltage of 1V.

3.3.5. Coulombic efficiencies

To create an efficient MEC, the system should have a bio-anode that preferably has both a high coulombic efficiency and a low charge transfer resistance. A high coulombic efficiency is required to transfer as much of the available energy from the organic substrate as possible to electrons and eventually to hydrogen and a low transfer resistance is required to minimize the specific energy input of the system (kWh/m³ H₂). The coulombic efficiency is influenced by the presence of methanogenesis. Methanogens convert acetate and thereby negatively influence the coulombic efficiency. For wastewater application the MEC should operate as an open system, which means that methanogenesis will be hard to keep out, as a continuous inoculation takes place. The conditions in an MEC are in general good for the development of methanogens e.g. anaerobic and pH neutral conditions and the presence of a suitable substrate. Since our system made use of a membrane the diffusion of hydrogen into the anode compartment can be considered low

(Rozendal et al., 2006b). Therefore hydrogenotrophic methane production in the anode compartment will also be limited.

It is hypothesized here that under substrate limiting conditions the coulombic efficiency can be improved by a relative improvement of the conditions for the electrogens compared to the conditions for the methanogens. The conditions for the electrogens can be improved by improving the mass transport in the system. Depending on the level of the incoming substrate, it is expected that under substrate limited conditions a large part of the incoming substrate will be consumed. This means that an increase of the coulombic efficiency will be directly associated with a larger produced current which is at the expense of methanogenesis. This means that an increase of the current is directly associated with an increase of the coulombic efficiency.

Figure 5A indeed shows that the coulombic efficiency increased with increasing current density. Figure 5B furthermore shows that the changes made to the system to reduce the anode and transport resistance also had a positive effect on the coulombic efficiency. With this enhanced mass and charge transport the electrogens were able to compete better with methanogens for the available substrate. So the enhanced mass and charge transport in this system not only increased the current output of the system but also increased the efficiency of the system.

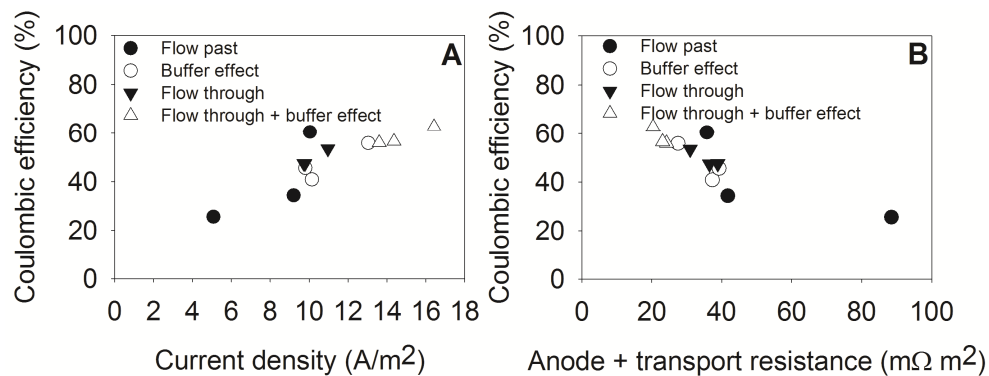


Figure 5 Coulombic efficiency (%) as a function of: (A) current density (A/m^2) and (B) anode + transport resistance ($m\Omega m^2$) for all experiments.

This study showed that current densities and coulombic efficiencies in porous electrodes can be improved by: (i) a forced flow of anolyte through these electrodes and (ii) increased buffer concentrations of the anolyte. A combination of both strategies enhanced mass and charge transport even further and eventually led to a high current density of 16.4 A/m² and a hydrogen production rate of 5.6 m³/m³/d at an applied voltage of 1 V. This current density is 228% higher than the current density without forced flow and high buffer concentration. Furthermore, coulombic efficiencies reached values of over 60% in this continuous system as a result of the applied strategies. Enhancing mass and charge transport in porous anodes through forced flow can be a big step in the development of this technology.

Acknowledgements

This work was performed in the TTIW-cooperation framework of Wetsus, centre of excellence for sustainable water technology (www.wetsus.nl). Wetsus is funded by the Dutch Ministry of Economic Affairs, the European Union European Regional Development Fund, the Province of Fryslan, the city of Leeuwarden and by the EZ-KOMPAS Program of the “Samenwerkingsverband Noord-Nederland”. The authors like to thank the participants of the research theme “Hydrogen” for the fruitful discussions and their financial support. The authors further thank Annemiek ter Heijne for critical reading of the manuscript.

Chapter 4

Effect of mass and charge transport speed and direction in porous anodes on Microbial Electrolysis Cell performance

The use of porous electrodes like graphite felt as anode material has the potential of achieving high volumetric current densities. High volumetric current densities, however, may also lead to mass transport limitations within these porous materials. Therefore, in this study we investigated the mass and charge transport limitations by increasing the speed of the forced flow and changing the flow direction through the porous anode. Increase of the flow speed led to a decrease in current density when the flow was directed towards the membrane caused by an increase in anode resistance. Current density increased at higher flow speed when the flow was directed away from the membrane. This was caused by a decrease in transport resistance of ions through the membrane which increased the buffering effect of the system. Furthermore, the increase in flow speed led to an increase of the coulombic efficiency by 306%.

This chapter has been published as:

Sleutels, T.H.J.A., Hamelers, H.V.M., Buisman, C.J.N. 2011. Effect of mass and charge transport speed and direction on Microbial Electrolysis Cell performance. *Bioresource Technology*, 102(1), 399-403.

4.1. Introduction

The last couple of years research in the field of bioelectrochemical systems (BES) as a renewable energy production technology from organic waste has gained increasing interest (Hamelers et al., 2010a; Logan et al., 2006). A microbial electrolysis cell (MEC) is an example of such a device that converts organic matter to hydrogen gas, hydrogen peroxide, methane or ethanol (Cheng et al., 2009; Logan et al., 2008; Rozendal et al., 2009; Steinbusch et al., 2009b).

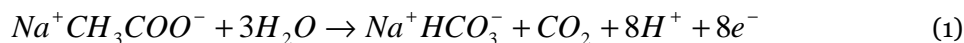
In the anode compartment of an MEC, bioelectrochemical microorganisms oxidize organic matter to carbon dioxide, protons and electrons. These electrons are released to an anode and flow through an electrical circuit to the cathode. In case of a hydrogen producing MEC these electrons are used to reduce water to form hydrogen gas in the cathode (Liu et al., 2005b; Rozendal et al., 2006b). The anode and cathode can be separated by a membrane to produce pure hydrogen gas (Rozendal et al., 2008c) or can be situated in a single compartment to produce a mixture of hydrogen, methane and carbon dioxide (Call and Logan, 2008).

To create an energetic efficient bioelectrochemical system both a high voltage efficiency and a high coulombic efficiency are required (Hamelers et al., 2009). The voltage efficiency is the amount of energy from the substrate that ends up in the product and can be increased by decreasing the internal resistance of the system i.e. by decreasing the electrode overpotentials. The coulombic efficiency is the amount of available electrons from the substrate that end up in the electrical circuit and in the case acetate is used as a substrate is a direct measure for the competition between electrogens and methanogens. It was shown before that this coulombic efficiency can be increased by increasing the mass transport in the system (Sleutels et al., 2009b).

To achieve high hydrogen production rates a high current density is required. The use of porous electrodes like graphite felt and graphite granules as anode material have the potential of achieving high volumetric current densities (Rabaey et al., 2005; Sleutels et al., 2009b). High volumetric current densities, however, may also lead to mass transport limitations within these porous materials. Accumulation of

protons may lead to acidification of the biofilm while substrate depletion may be another factor decreasing biofilm performance.

For every mol of acetate consumed by the biofilm eight moles of protons and one mol of buffer are produced (at pKa 6.37)



At high current densities this will lead to a proton gradient near the biofilm and consequently to a drop in biofilm performance (Torres et al., 2008). To prevent acidification often influent solutions (wastewater) with very high buffer concentrations are used. It has been shown that the performance of the system increases linearly with an increase in buffer concentration (Torres et al., 2008). However, this also increases cost of the system significantly since wastewaters typically do not contain these large amounts of buffer and they would have to be added (Rozendal et al., 2008a). Furthermore, these high concentrations of nutrients can not be disposed and need further cleaning. Therefore, addition of high concentrations of buffer is not desirable in BESs.

Recently it was demonstrated that, instead of using high buffer concentrations, also a forced flow through a porous carbon felt electrode can be applied to give the same performance (Sleutels et al., 2009b). This forced flow enhanced the transport of protons, buffer species and substrate towards and away from the biofilm. However, in case of a forced flow through the anode still mass and charge transport limitations were observed. Therefore, in this study we further investigated these mass and charge transport limitations by: (i) increasing the speed of the forced flow through the porous anode and (ii) changing the flow direction through the porous anode.

4.2. Materials and methods

4.2.1. Bioelectrochemical cell

The three bioelectrochemical cells used were the same as used in (Sleutels et al., 2009b). Each cell consisted of an anode and cathode chamber (280 mL each) separated by an anion exchange membrane (AEM; AMX - Neosepta, Tokuyama

Corp., Japan). For the anode three types of carbon based felts were used: (i) 6.5 mm thick graphite felt (National Electrical Carbon BV, Hoorn, The Netherlands), (ii) 3 mm thick graphite felt (FMI Composites Ltd., Galashiels, Scotland) and (iii) 1 mm thick carbon felt (Technical Fibre Products Ltd., Kendal, United Kingdom). This anode felt was separated from the membrane by a spacer of 4mm (PETEX 07-4000/64, Sefar BV, Goor, The Netherlands). The presence of the spacer forced the anolyte to flow perpendicular through the felt before it left the anodic compartment.

The cathode consisted of a platinum coated (50 g/m^2) titanium mesh (thickness 1mm, specific surface area $1.7 \text{ m}^2/\text{m}^2$ - Magneto Special Anodes BV, Schiedam, The Netherlands). The anode, cathode and membrane all had a projected surface area of 0.025 m^2 . Anode and cathode potentials were measured against Ag/AgCl reference electrodes (+201 mV vs. standard hydrogen electrode) that were connected to the cell through a capillary. Anode and cathode were connected through a power supply (ES 03-5, Delta Electronica BV, Zierikzee, The Netherlands) and the cell voltage was set to 0.8 V for all experiments. Furthermore, all experiments were performed at 303 K.

4.2.2. Experimental procedures

All bioelectrochemical cells were inoculated with 100 mL effluent from a running MEC (Sleutels et al., 2009a). After a stable current was reached, performance was tested in duplicate consecutive 120h runs. Influent, anolyte and catholyte was sampled and analyzed for acetate and bicarbonate content. Acetate concentrations were determined using ion chromatography (Metrohm 761 Compact IC equipped with a conductivity detector and a Metrosep Organic Acids 6.1005.200 ion exclusion column). Bicarbonate concentrations were determined using an total organic carbon analyzer (Shimadzu TOC-VCPH). Furthermore, pH (Liquisys M CPM 253, Endress + Hauser) and conductivity (ProSense QiS, Oosterhout, The Netherlands) were continuously recorded with a data logger (Memo-graph, Endress + Hauser) together with cell voltage, anode and cathode potentials and produced current. The cells were continuously fed with synthetic wastewater at a

rate of 5 mL/min. This synthetic wastewater consisted of 1.36 g/L $\text{NaCH}_3\text{COO}\cdot 3\text{H}_2\text{O}$, 0.68 g/L KH_2PO_4 , 0.87 g/L K_2HPO_4 , 0.74 g/L KCl , 0.58 g/L NaCl , 0.28 g/L NH_4Cl , 0.1 g/L $\text{MgSO}_4\cdot 7\text{H}_2\text{O}$, 0.1 g/L $\text{CaCl}_2\cdot 2\text{H}_2\text{O}$ and 0.1 mL/L of a trace element mixture (Zehnder et al., 1980).

4.2.3. Strategy

The anolyte and catholyte were circulated through a flow cell over the compartment. Depending on the circulation speed this gives different forced flow speeds through the anode electrode. The circulation speed was changed from 340, 680 to 1360 mL/min giving (divided by the projected surface area) a perpendicular flow speed through the felt of 1.4, 2.7 and 5.4 cm/min respectively. Furthermore, by changing the direction of the circulation pump the direction of the flow through the anode was changed, giving a flow directed towards the membrane (A) and a flow directed away from the membrane (B) as indicated in Figure 1.

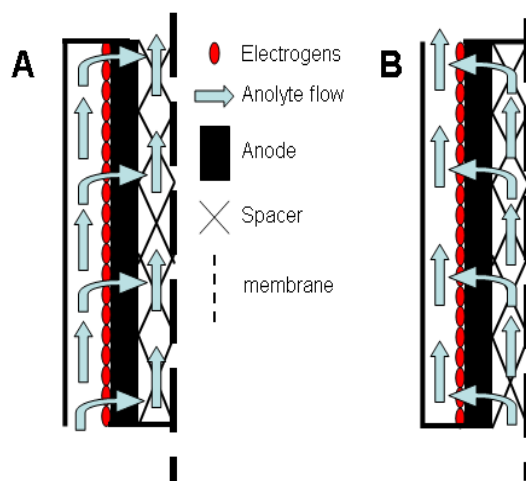


Figure 1 Experimental set-up of the anodic compartment for a forced anolyte flow directed towards the membrane (A) and directed away from the membrane (B)

4.2.4. Calculations

Anode overpotential (η_a ; V) was calculated using the actual concentrations of acetate, bicarbonate and protons with

$$\eta_a = E_{measured} - \left(E_{an}^0 - \frac{RT}{nF} \ln \left(\frac{[Ac^-]}{[HCO_3^-]^2 [H^+]^9} \right) \right) \quad (2)$$

where $E_{measured}$ is the measured anode potential (V), E_{an}^0 is the standard anode potential (V), R is the universal gas constant (8.314 J/K/mol), T is the temperature (K), n is the amount of electrons involved in the reaction (8). Anode resistance (R_a ; Ωm^2) was calculated by dividing the anode overpotential by the produced current density.

Transport resistance for ions (R_T ; Ωm^2) was calculated from the applied voltage and the other resistances as described in (Sleutels et al., 2009a):

$$R_t = R_{cell} - R_{emf} + R_{an} + R_{cat} + R_{ionic} \quad (3)$$

where R_{cell} is the applied voltage divided by the current density, R_{emf} is the thermodynamical resistance for hydrogen production, R_{cat} is the cathode resistance and R_{ionic} is the electrolyte resistance.

Coulombic efficiency (η_{CE} ; %) was calculated by dividing the integrated total amount of produced coulombs (I_m) by the theoretical produced amount of coulombs from the consumed substrate in that same period

$$\eta_{CE} = \frac{\int_0^t I_m dt}{nFQ(C_{in} - C_{out})t} \times 100\% \quad (4)$$

where Q is the influent flow rate (5 mL/min), C_{in} is the influent acetate concentration (mol/L) and C_{out} is the effluent acetate concentration (mol/L).

4.3. Results and discussion

The aim of this study was to investigate the effect of mass and charge transport limitations in porous anodes. Therefore the effect of speed and direction of a forced flow through three thicknesses of porous anodes (1, 3 and 6.5 mm) was investigated.

4.3.1. Current density

Figure 2A shows the current densities for the three types of felt at three different flow speeds directed towards the membrane and Figure 2B shows the current densities for the three types of felt directed away from the membrane. All results were obtained at an applied voltage of 0.8V. At a flow speed of 1.4 cm/min the current densities were more or less the same for all three felt thicknesses (1 mm 3.6 A/m²; 3 mm 3.5 A/m²; 6.5 mm 3.8 A/m²).

The current density for the 1mm felt increases slightly with increasing speed towards the membrane, while for the 3 mm felt speed and the 6.5 mm felt the current density decreases with increasing flow speed.

For the experiments with the flow directed away from the membrane, again, the three felt thicknesses showed the same current densities at the lowest flow speed (1 mm 3.8 A/m²; 3 mm 3.6 A/m²; 6.5 mm 3.8 A/m²). These values correspond with the values found for the flow directed towards the membrane.

Again the current density for the 1mm felt remained constant at increasing flow speed (2.7 cm/min 3.8 A/m²; 5.4 cm/min 3.6 A/m²). Interestingly, for this flow direction the current density increased for the thicker felt types at higher flow speeds. The current density for the 3mm felt increased to 5.3 A/m² while the current density for the 6.5 mm felt even increased to 6.5 A/m².

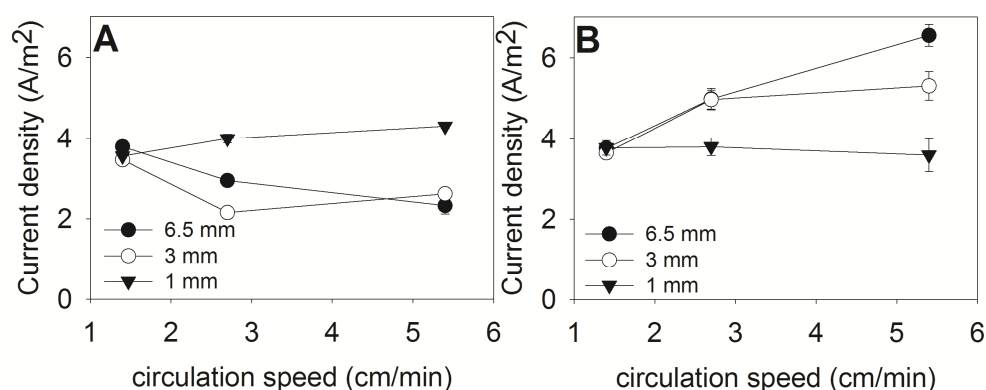


Figure 2 Current density for three thicknesses of felt with different flows directed (A) towards the membrane and (B) away from the membrane in MECs at an applied voltage of 0.8V

4.3.2. Anode and transport resistance

To explain the differences in current densities for the different flow directions, the anode resistance and the transport resistance for ions were calculated for all experiments (equation 2 + 3). The results for the anode resistance are shown in Figure 3 and the results for the transport resistance are shown in Figure 4.

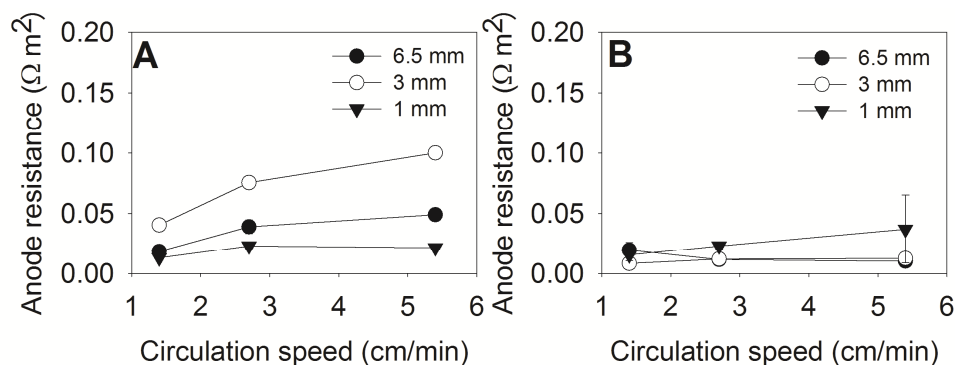


Figure 3 Anode resistance at different flow speeds for a forced anode flow directed (A) towards the membrane and (B) away from the membrane at an applied voltage of 0.8V.

From Figure 3A and Figure 4A it becomes clear that the decrease in current density at higher flow speeds in the experiments with the anolyte flow directed towards the membrane is mainly caused by an increase in anode resistance. The change in transport resistance is relatively much smaller than the change in this anode resistance. From Figure 3B and Figure 4B it becomes clear that the increase in current density at higher flow speeds in the experiments with the anolyte flow directed away from the membrane is mainly caused by a decrease in transport resistance. Here the change in anode resistance is relatively much smaller than the change in transport resistance.

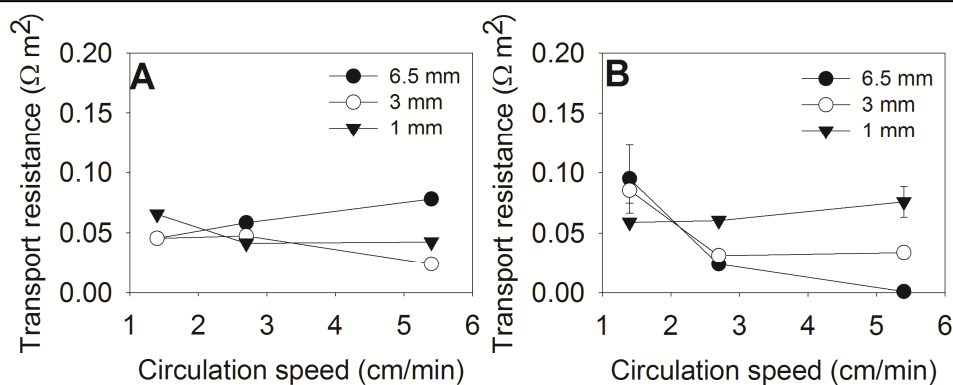


Figure 4 Transport resistance at different flow speeds for a forced anode flow directed (A) towards the membrane and (B) away from the membrane at an applied voltage of 0.8V.

4.3.3. Buffering mechanism

An explanation for the changes in anode and transport resistance, as a function of the flow speed, is the buffering mechanism in an MEC (Figure 5). For a biofilm to produce a high current density a certain amount of buffer is required as can be seen from the anode reaction (equation 1). For every electron produced also one proton is produced. Furthermore, for every mol of acetate oxidized, only 1 mol of buffer ($\text{Na}^+\text{HCO}_3^-$) is produced. So, overall 7 more moles of buffer are required to compensate for the produced protons and maintain a neutral pH and thereby maintain biofilm performance. A buffer species (HPO_4^{2-}) takes up a proton that is produced at the biofilm. With the convective flow this buffer molecule moves towards the membrane where the pH is very high because of the transport of hydroxyl through the membrane. Here the proton from the buffer molecule is combined with the hydroxyl that is transported through the membrane. Because of the internal circulation this buffer molecule is then transported back to the biofilm again to pick up another proton. When the flow speed through the felt is increased, the regeneration is expected to be faster and higher current densities can be expected.

Furthermore, the direction of the flow of anolyte through the anode also affects the diffusion layer on the membrane. Indicated by the lower transport resistance for ions (Figure 4) this boundary layer is much smaller when the flow is directed away from the membrane than when the flow is directed towards the membrane. A smaller diffusion layer makes transport of ions easier and thereby also positively influences buffer regeneration and circulation. Therefore, the increased circulation speed with a flow directed away from the membrane leads to higher current densities.

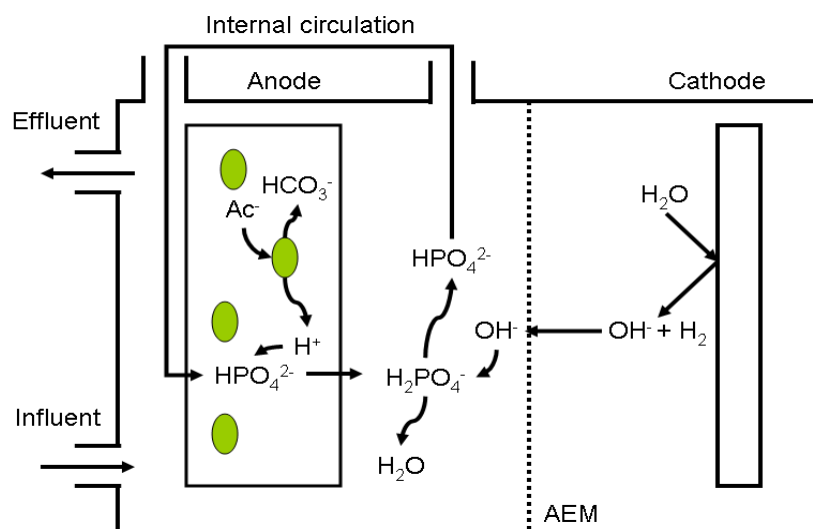


Figure 5 Ion flow in an MEC to illustrate the buffer mechanism in an MEC.

4.3.4. Coulombic efficiencies

When acetate is used as substrate, methanogens and electrogens compete for the available substrate. The electrogens use the substrate to produce electrons while the methanogens use the substrate to produce methane. This competition is expressed in the coulombic efficiency. It was shown before that a change in conditions can help the electrogens to compete with the methanogens for the substrate, resulting in higher coulombic efficiencies (Sleutels et al., 2009b). Figure 6 shows the coulombic efficiencies for the experiments with the flow directed

towards (A) and away from the membrane (B) against a combination of the anode and transport resistance. A combination of the anode and transport resistance was taken here because they both affect anode performance and thereby can have influence on the coulombic efficiency. For the flow directed towards the membrane no effect can be seen on the coulombic efficiency at increasing circulation speed. For the flow directed away from the membrane, however, the coulombic efficiency increases at higher circulation speed. So at higher circulation speed, the electrogens are able to compete better with the methanogens for the available substrate. The electrogens live in the biofilm on the anode surface while the methanogens do not depend on such a surface and can therefore be present everywhere in the anolyte. The protons are produced in the biofilm and will thereby locally affect the pH. Only the electrogens experience this low pH since they are present there. A better buffering mechanism therefore only affects the electrogens leading to higher current densities and coulombic efficiencies. This is another indication that indeed the transport of hydroxyl through the membrane in this configuration is facilitated better and the buffering mechanism works better to provide better conditions for the electrogens.

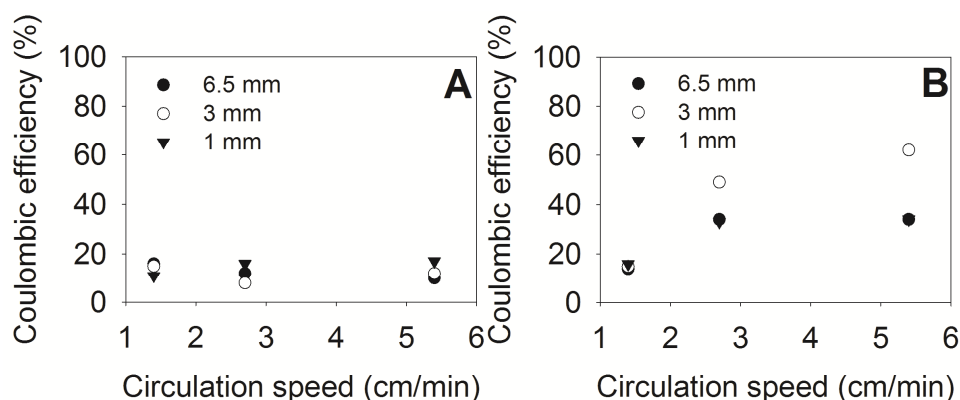


Figure 6 coulombic efficiency vs circulation speed for experiments with a flow directed towards the membrane (A) and a flow directed away from the membrane (B).

4.3.5. Implication

To create an energetically efficient bioelectrochemical system both a high coulombic and voltage efficiency are required (Hamelers et al., 2009). Figure 6 shows that the coulombic efficiency can be influenced by changes in mass transport in the system. When the flow is directed towards the membrane (Figure 6A) the coulombic efficiency is not affected indicating that the mass transport in the system did not change. When the flow was directed away from the membrane however (Figure 6B) the coulombic efficiency increased from 15 to 62% which is an increase of 306%. This shows that the coulombic efficiency can be hugely influenced by changes in the mass transport in the system and that this mass transport has to be taken into consideration when designing an efficient bioelectrochemical system.

4.3.6. Conclusions

This study showed that the speed and direction of mass and charge transport has a big influence on the performance of porous anodes in bioelectrochemical system. An increase of the flow speed directed away from the membrane increased the current density by almost 100%. Furthermore the coulombic efficiency increased by 306% at an increased flow speed. These results show that mass and charge transport in the anode are important parameters that influence the performance of bioelectrochemical systems.

Acknowledgements

This work was performed in the TTIW-cooperation framework of Wetsus, centre of excellence for sustainable water technology (www.wetsus.nl). Wetsus is funded by the Dutch Ministry of Economic Affairs, the European Union European Regional Development Fund, the Province of Fryslan, the city of Leeuwarden and by the EZ-KOMPAS Program of the “Samenwerkingsverband Noord-Nederland”. The authors like to thank the participants of the research theme “Bio-energy” for the fruitful discussions and their financial support. The authors further thank Rob Lodder for help with the experiments and Annemiek ter Heijne for critical reading of the manuscript.

Chapter 5

Influencing coulombic efficiency in Bioelectrochemical Systems

To create an efficient Bioelectrochemical system, as much of the available energy from the substrate as possible needs to be transferred to the eventual product. Therefore a high coulombic efficiency is required. When acetate is used as substrate, it can be converted to either electrons or methane and the coulombic efficiency is a direct measure for the competition between electrogens and methanogens. The aim of this study was to increase the coulombic efficiency by changing the substrate concentration and the anode potential. These parameters were tested under steady state conditions since these are especially of interest when operating a continuous system.

It was shown that a higher anode potential increases the energy available for these electrogens and in that way they could outcompete the methanogens. Furthermore, also a lower substrate concentration made it possible for the electrogens to outcompete the methanogens probably because the electrogens have a higher affinity for the substrate than the methanogens. In both cases the relative amount of substrate available for the methanogens was lower because of a higher consumption rate by the electrogens. Knowledge about the kinetic growth coefficients is required to control and increase the coulombic efficiency. Further research is required to optimize these strategies to find a right balance between the coulombic efficiency, current density and removal rate of organic material. Finally, start-up strategies of Bioelectrochemical systems need to be compared to be able to make a quantitative comparison between the effects of these strategies on coulombic efficiency.

5.1. Introduction

Bioelectrochemical systems (BES) are an emerging technology to convert organic waste to energy or chemicals (Logan et al., 2008; Logan et al., 2006). To transfer as much of the available energy from the substrate to the eventual product, an energetically efficient system is required. For efficient BESs, both a high energetic efficiency and coulombic efficiency are required (Hamelers et al., 2009). The energetic efficiency is determined by the internal losses of the system. A high energetic efficiency can be achieved by minimizing these internal losses by creating a low internal resistance in the system (Sleutels et al., 2009a). In case of the anode for example, this means a low anodic overpotential is required, e.g. the measured anode potential should be close to the thermodynamical potential of the substrate as can be calculated from the Nernst equation. This can be achieved by minimizing the activation and concentration overpotential (Clauwaert, 2008). The concentration overpotential was decreased by increasing the mass transfer in the system in previous work (Sleutels et al., 2009b). Another step forward in creating an efficient BES would be to increase the coulombic efficiency. The coulombic efficiency is a measure for the amount of available electrons in the substrate that end up as electrical current in the system. When acetate is used as substrate, it can be converted to either electrons or methane. Which of these products is formed, depends on the type of microorganisms; current in the form of electrons is produced by electrogenic bacteria (electrogens) while the methane is produced by methanogenic archaea (methanogens). The coulombic efficiency is a direct measure for the competition between electrogens and methanogens. The coulombic efficiency can also increase as a result of hydrogen oxidation in the anode. It was shown before, that hydrogen can be oxidized to electrons at the anode of an MEC leading to increased current densities and relative high coulombic efficiencies (Lee et al., 2009). When a membrane is used however, the amount of hydrogen that diffuses to the anode compartment can be considered constant at saturated hydrogen concentrations in the cathode (Rozendal et al., 2006b). In this case, the contribution of hydrogen oxidation in the anode to current production can be

considered constant and the changes in coulombic efficiency are a direct result of changes in the amount of acetate oxidized to electrons.

So far, a wide range of coulombic efficiencies has been reported ranging from 5% (Min and Logan, 2004) to almost 100% (Aelterman et al., 2008a). The measured coulombic efficiency usually highly depends on the inocula used, the type of wastewater, duration of the experiment, and system design. For example, coulombic efficiencies in continuous systems are mostly lower than the coulombic efficiencies reported for batch systems because of operational and cycle times which are much shorter for batch systems than for continuous systems (Hamelers et al., 2009). The aim of this study was to increase the coulombic efficiency in MECs by changing operational parameters. Possible strategies that are available to influence the competition between electrogens and methanogens and thereby the coulombic efficiency are anode potential, substrate concentration and hydraulic retention time (HRT).

By controlling the anode potential the energy available for the electrogens for growth and maintenance can be controlled. A higher anode potential increases the energy available for these electrogens and in that way they can possibly outcompete the methanogens by increased metabolism. By changing the influent substrate, the acetate concentration in the anolyte can be controlled. A lower substrate concentration makes it possible for the electrogens to outcompete the methanogens if the electrogens have a higher affinity for the substrate than the methanogens.

Since the methanogens do not depend on an electrode surface to grow on like the electrogens it might be possible to wash them out by decreasing the HRT. Because the HRT in previous experiments was already lower than the growth rate of acetotrophic methanogens (HRT: 2.5h (Sleutels et al., 2009b)), this strategy was not further pursued. Therefore, the focus in these experiments was on controlling the anode potential and the substrate concentration and not on changing retention times.

5.2. Materials and methods

5.2.1. Bioelectrochemical cell

The experiments were performed in two identical electrochemical cells previously described by (Sleutels et al., 2009a). The anode consisted of 6.5 mm thick graphite felt (National Electrical Carbon BV, Hoorn, The Netherlands) through which the anolyte was forced to flow perpendicular as previously described in (Sleutels et al., 2009b). The cathode consisted of platinum coated (50 g/m²) titanium mesh (surface areas 0.025 m², thickness 1 mm, specific surface area 1.7 m²/m² – Magneto Special Anodes BV, The Netherlands). The anode and cathode from each other by an anion exchange membrane (AEM) (AMX- Neosepta, Tokuyama Corp., Japan).

Anode and cathode potential were measured using Ag/AgCl reference electrodes (QM710X, ProSense BV, Oosterhout, The Netherlands) which were connected to the cell by a capillary. This capillary was placed just outside the electric field to make sure current lines were not disturbed. The electrochemical cells were connected to a potentiostat (Wenking Potentiostat/Galvanostat KP5V3A, Bank IC, Germany) to control the anode potential (-450, -400, -350, -300 and -250 mV). In this mode of the potentiostat, the cell voltage is adjusted to maintain the desired anode potential. The anolyte and catholyte were continuously recirculated over the compartment via an external loop containing a recirculation bottle (600 ml) at a speed of 340 ml/min. These circulation bottles were equipped with conductivity meters (ProSense QiS, Oosterhout, The Netherlands) and pH meters (Liquisys M CPM 253, Endress + Hauser). A data logger (Memo-graph, Endress + Hauser) was used to record anode and cathode potential, cell voltage, current, anode and cathode pH, and anode and cathode conductivity. All experiments were performed at 303 K.

5.2.2. Experimental procedure

Both cells were started up by inoculating the anode with effluent from an active MEC. The anode chambers of both cells were operated in continuous mode by

supplying influent at a rate of 5 mL/min containing 0.74 g/L KCl, 0.58 g/L NaCl, 0.68 g/L KH_2PO_4 , 0.87 g/L K_2HPO_4 , 0.28 g/L NH_4Cl , 0.1 g/L $\text{MgSO}_4 \cdot 7\text{H}_2\text{O}$, 0.1 g/L $\text{CaCl}_2 \cdot 2\text{H}_2\text{O}$, and 0.1 mL/L of a trace element mixture (Zehnder et al., 1980). As a carbon/electron source $\text{NaCH}_3\text{COO} \cdot 3\text{H}_2\text{O}$ was added in various concentrations depending on the experiment. The cathode chamber of both cells was operated in batch mode.

To study the effect of anode potential and substrate concentration on coulombic efficiencies in one cell the substrate concentration was varied from 35 mM, 20 mM, 10 mM, 5 mM and 1 mM at a controlled anode potential of -350 mV (vs Ag/AgCl electrode). In the second cell the anode potential was controlled at -500 mV, -450 mV, -400mV, -350 mV and -300 mV (vs Ag/AgCl electrode) by a potentiostat. During these experiments the substrate concentration was always 20 mM to ensure current production was not limited by substrate depletion.

5.2.3. Analytical procedures

The substrate concentration in influent and effluent as well as the protein content in anolyte were measured in duplicate once a day. The acetate concentration was determined using Metrohm 761 Compact IC (equipped with a conductivity detector) and the bicarbonate concentration was determined using a total carbon analyzer (Shimadzu TOC-VCPH). The total biomass concentration (electrogens + methanogens) in the anolyte was measured as the total protein content. Protein was measured by firstly breaking the cell wall of bacteria in anolyte samples using an ultrasonic bath (Sonorex digitec DT 512 H, BANDELIN electronic, Berlin, German), then prepared by Bio-Rad Protein Assay method to further be measured by a spectrophotometer (Shimadzu UV-1650PC, UV-Visible spectrophotometer, Japan) (Bradford, 1976).

5.2.4. Calculations

Coulombic Efficiency (CE; %) was calculated using

$$CE = \frac{I_{measured}t}{nFQ(C_{in} - C_{out})} * 100\% \quad (1)$$

$I_{measured}$ is the measured current density (A/m^2), n is the amount of electrons (8 for acetate), F is Faradays constant (96485 C/mol), Q is the influent flow rate (5mL/min), C_{in} and C_{out} are the acetate concentrations in influent and effluent respectively (M).

5.2.5. Steady state

Both the controlled anode potential and substrate concentration experiments were run until steady state conditions were reached. Therefore, to give electrogens and methanogens time to develop, both reactors were run for three months before starting the experiments presented in this paper. After these three months the anode potential was varied in one reactor, while the substrate concentration was varied in the second reactor. Steady state was defined as the situation in which current density, substrate effluent concentration and protein content in the anolyte were constant. A constant current density in combination with a constant substrate concentration in the effluent indicates a stable conversion of acetate to current, as well as a stable conversion of acetate to methane. Furthermore, a constant protein concentration in the anolyte indicates a constant total biomass (electrogens + methanogens) concentration in the anolyte. These steady state conditions were kept for at least 48 hours. The last data point represents steady state and was used in figures 2 and 3.

5.3. Results and discussion

In this paper, the effect of operational parameters on the coulombic efficiency in MECs is investigated. These operational parameters were anode potential and influent acetate concentration. The anode potential regulates the energy that is available for the electrogens and through this might influence competition with methanogens. The influent concentration has effect on the substrate that is available for either electrogens or methanogens and through this is expected to

influence competition between both. The effect of these two parameters on coulombic efficiency is discussed.

5.3.1. Steady state

For a decent comparison between the competition of electrogens and methanogens they should both have sufficient time to grow and develop. Especially acetoclastic methanogens have a low growth rate and therefore a long operation time is required to give these methanogens time to grow (Rajoka et al., 1999; Visser et al., 1996). Here, the operation time before the actual experiments were started was three months. Steady state conditions are especially of interest when operating a continuous system. In the future, a continuous system is the most likable way of operation since batch systems have long down times and therefore require relative high capital costs. Therefore the conditions under which continuous systems operate are of particular interest.

Figure 1 shows an example of an experiment reaching steady state, in this case at 35 mM of acetate and at an applied anode potential of -350 mV. Only the last 14 days of the experiment are pictured. In Figure 1A the concentrations of acetate are shown that end up as current, methane and the acetate that leaves the cell in the effluent. Figure 1B shows the produced current, total protein concentration in the anolyte and the coulombic efficiency for these conditions. When all parameters were stable (day 31), steady state was assumed. The data collected at day 33 was used to construct figures 2 and 3.

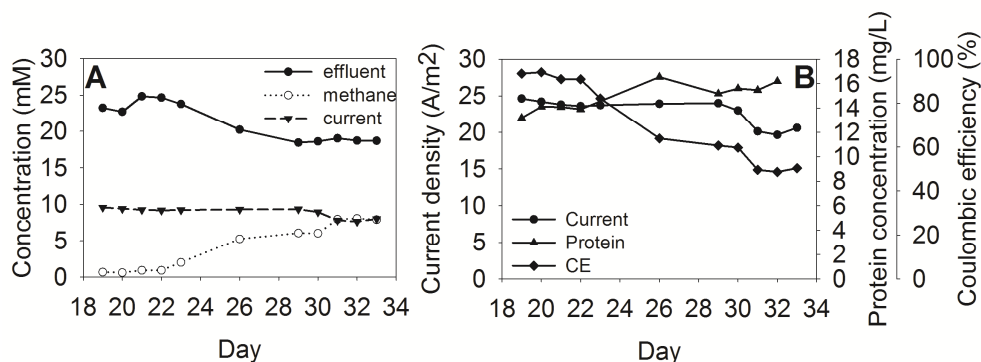


Figure 1 Example of an experiment reaching steady state conditions (from day 31 onwards) in an MEC at 35 mM of acetate in the influent and an applied anode potential of -350 mV. Figure A shows the part of the acetate that is converted to current and methane and the acetate that leaves the system with the effluent. Figure B shows the development of the current, protein concentration and coulombic efficiency in time.

5.3.2. Controlling acetate concentration

To study the effect of acetate concentration on coulombic efficiency, the acetate concentration was decreased from 35, 20, 10, 5 to 1mM. The highest concentration was tested first to make sure the methanogens had a chance to develop at an abundant level of substrate. The anode potential for these experiments was controlled at -350 mV vs Ag/AgCl, because previous experiments, at controlled cell voltage where the anode potential could freely develop, showed that this was a common value for the anode potential (Sleutels et al., 2009b).

Figure 2A shows the coulombic efficiency and current densities at different influent concentrations. This figure shows that the current density increases at higher acetate concentrations, since more substrate is available for current production by the electrogens. However, at these higher acetate concentrations the coulombic efficiency decreases. This means that the relative amount of available substrate going to current generation is smaller than the amount of substrate going towards methane. The electrogens are capable of producing a maximum amount of current

from the available substrate. At higher substrate concentrations this maximum amount of current increases relatively less compared to the available substrate. So, at higher substrate concentrations, the substrate is actually overdosed and is available for methanogens. This implies that at higher substrate concentrations methane will always be produced. This can be explained by the affinity of the electrogens for the substrate compared to the affinity of the methanogens for the substrate. Although not much is known about the kinetic growth coefficients of the electrogens (Hamelers et al. calculated a k_s value of 2.2 mM at high overpotential (Hamelers et al., 2010b)) it seems that the affinity for substrate for the electrogens is higher than for methanogens.. Using the substrate affinity as a parameter to control competition between microorganisms is well known for the competition between acetotrophic methanic bacteria and acetotrophic sulfidogenic bacteria (Visser et al., 1996). The results here show that this strategy is worth investigating further.

At an influent concentration of 10 mM, the coulombic efficiency reached values of almost 80%. However, when an MEC is used as a wastewater treatment system, the effluent acetate concentration is also an important parameter and should be sufficient low according to discharge regulations. The effluent concentration and removal efficiency are shown in Figure 2B. The effluent concentration is lower at lower influent concentrations, but also the current density is lower. This means that, although more of the available energy from the substrate is converted to electrons, the total produced current is lower at lower influent concentration. This is also represented in the removal efficiency, which increases at lower acetate concentrations. At an influent concentration of 10 mM the effluent concentration was 0.2 mM while the removal efficiency was 97%. Therefore, when controlling the influent concentration, a balance should be found between the removal rate of substrate and the production of current and eventually hydrogen gas. In this experiment an influent concentration of 10 mM shows these an ideal combination of these parameters.

Coulombic efficiency

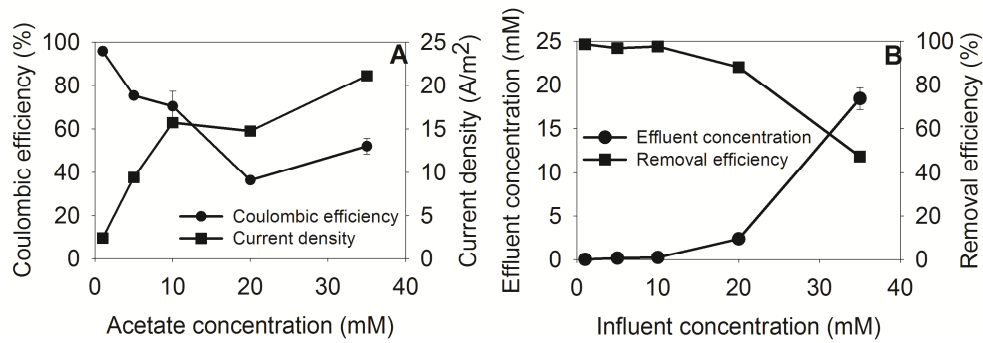


Figure 2 Coulombic efficiency and current density as a function of the acetate concentration (A) and the effluent concentration and removal efficiency as a function of the influent acetate concentration (B).

5.3.3. Controlling anode potential

To study the effect of anode potential on coulombic efficiency, the anode potential was decreased from -250, -300, -350, -400 to -450 mV. The acetate influent concentration was 20 mM for all applied voltages. This range of potentials was chosen for practical and theoretical reasons. At a lower anode potential than -450 mV the potential is too close to the theoretical potential and the energy available for the electrogens for growth and maintenance would have been too low. On the other hand, at a potential higher than -250 mV, the current density would have been higher. However, at higher applied anode potentials the anode overpotential is also higher. These higher overpotentials lead to a higher required applied voltage for the system which directly leads to a higher specific energy input required for the production of hydrogen (Lee et al., 2009).

Figure 3A shows the coulombic efficiency and current density at different anode potentials. Both the current density and the coulombic efficiency increase at higher anode potentials. At higher anode potentials, the anode overpotential is higher and more energy is available for electrogens to develop and to increase their metabolism. At increased metabolism the electrogens produce more current and consume more substrate. When more substrate is consumed by the electrogens,

less substrate is available for the methanogens. This directly leads to a lower methane production rate and an increased coulombic efficiency.

Figure 3B shows the effluent concentration and removal efficiency at different applied anode potentials. The effluent concentration decreases at higher anode potentials and the removal efficiency increases at higher applied potentials. Although this low effluent concentration in combination with a high current density and coulombic efficiency seems to be an ideal situation, the energy input for the produced hydrogen also has to be taken into account.

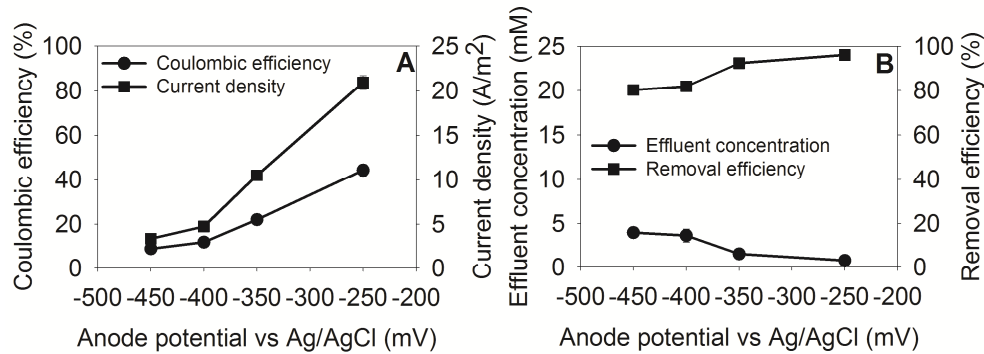


Figure 3 Coulombic efficiency and current density as a function of the applied anode potential (A) and the effluent concentration and removal efficiency as a function of the anode potential (B).

5.3.4. Comparison strategies

Both strategies, increase in the anode potential and decrease of acetate concentration, had a positive effect on the coulombic efficiency. In both cases this was caused by an increased activity of the electrogens which led to a lower substrate concentration available for the methanogens. Two of the experiments were performed under same conditions i.e. an influent concentration of 20 mM and an anode potential of -350 mV but in different set ups. Although the conditions were the same, the results obtained in these experiments were different. In the case of a controlled potential a current density of 10.5 A/m² and a coulombic efficiency of 22% was found while in the experiment with controlled influent concentration a current density of 14.8 A/m² and a coulombic efficiency of 36% was found. These

differences are most likely caused by the different start-up procedure of the two cells. One cell was started with an influent concentration of 35 mM of acetate at an anode potential of -350 mV while the second cell was started with an influent concentration of 20 mM of acetate at an anode potential of -450 m. Therefore, the initial conditions for the competition between electrogens and methanogens were different in both reactors. The difference in start up procedure might explain the differences in eventual performance. It was already shown before that different starting conditions can have influence on the performance of the system. It was shown, for example, that the anode material (ter Heijne et al., 2008), anode potential (Aelterman et al., 2008a; Wang et al., 2009), loading rate (Aelterman et al., 2008b) can have impact on the eventual performance of a bioelectrochemical system. Direct comparison between the two strategies is therefore not possible in this experimental setup, as the starting situation was not the same.

5.3.5. Implications

The results presented here show that both the influent concentration and the anode potential can be used to influence the coulombic efficiency. Further research is required to optimize these strategies to find a right balance between the coulombic efficiency, current density and removal rate of organic material. For the substrate concentrations knowledge from previous research about competing processes with methanogens can be used. Further knowledge about the kinetic growth coefficients (like k_s) is required to control this competition. These coefficients are also interesting for the anode potential control strategy. The growth kinetics are related to the active enzyme complexes for electron transfer. Further knowledge about these processes can make it possible to control the competition. Also a combination of both strategies can be applied to find optimal conditions. Furthermore, also the start-up strategies need to be the same to be able to make a quantitative comparison between both strategies.

The final coulombic efficiencies found here are high (>80%) compared to other studies with continuous system, which often do not exceed 60% (Sleutels et al., 2010; Sleutels et al., 2009b). This coulombic efficiency is especially high when we

consider that these experiments were run for a long period to give the methanogens time to develop. The strategies presented here therefore make it possible to move BES a step forward to practical application.

Acknowledgements

This work was performed in the TTIW-cooperation framework of Wetsus, centre of excellence for sustainable water technology (www.wetsus.nl). Wetsus is funded by the Dutch Ministry of Economic Affairs, the European Union European Regional Development Fund, the Province of Fryslan, the city of Leeuwarden and by the EZ-KOMPAS Program of the “Samenwerkingsverband Noord-Nederland”. The authors like to thank the participants of the research theme “Bio-energy” for the fruitful discussions and their financial support. Libertus Darus is kindly acknowledged for the experimental procedures.

Chapter 6

Reduction of Buffer requirement in Bioelectrochemical Systems

Low pH buffer capacity of waste streams limits further development of bioelectrochemical systems (BES) because accumulation of protons potentially leads to acidification of the anodic biofilm. Here we introduce a system that makes it possible to recover alkalinity in an extra recovery compartment. The extra compartment was located between anode and cathode compartment and was separated from the anode by a cation exchange membrane and from the cathode by an anion exchange membrane, which made clean hydrogen production possible. To compensate for the charge movement as a result of the flow of electrons, both cations and hydroxyl ions moved into the new recovery compartment. When a synthetic waste stream was fed through this recovery compartment, both pH and conductivity increased. When this stream is then fed to the anode of the BES, no additional buffer was required to produce the same current (3.5 A/m^2) at an applied voltage of 1V. Furthermore, this alkaline stream can also be used in other processes.

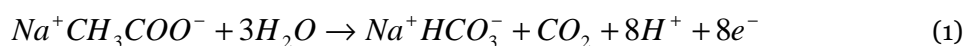
A slightly adapted version of this chapter has been published as:

Sleutels, T.H.J.A., Hamelers, H.V.M., Buisman, C.J.N. 2010. Reduction of pH buffer requirement in Bioelectrochemical systems. *Environmental Science & Technology* **44**(21), 8259-8263.

6.1. Introduction

Production of renewable energy from organic matter in a Bioelectrochemical System (BES) has shown great potential (Logan et al., 2006). In a BES, either electrical energy can be produced from the organic material in a so called microbial fuel cell (MFC) (Logan et al., 2006) or hydrogen in a so called microbial electrolysis cell (MEC) (Logan et al., 2008) by mean of the input of a small amount of electrical energy. Recently, also other products like methane (Cheng et al., 2009), ethanol (Steinbusch et al., 2009b) and peroxide (Rozendal et al., 2009) are being produced in MECs. In a BES, organic matter is oxidized by electrochemical active microorganisms and the electrons are transferred to an anode. The produced electrons move through an electrical circuit to the cathode where they are used, in case of an MEC to reduce water to form hydrogen gas (Rozendal et al., 2006b). To compensate for this movement of negative charge, ions move through the solution, possibly through an ion exchange membrane (Call and Logan, 2008; Rozendal et al., 2006a). The presence of the membrane prevents substrate/product crossover and makes production of a pure product, in the case of an MEC pure hydrogen gas, possible. Unfortunately, the membrane also increases the resistance of the system resulting in an increased energy consumption per m³ of produced hydrogen (Sleutels et al., 2009a). Membranes that have been applied in MECs include cation exchange membranes (CEM), anion exchange membranes (AEM), bipolar membranes and charged mosaic membranes (Rozendal et al., 2008c; Ter Heijne et al., 2006).

Another factor affecting performance of bioelectrochemical systems is the acid producing reaction at the anode. In lab scale BES often acetate is used as substrate which is oxidized according to



From this equation it becomes clear that for every consumed mol of acetate 8 moles of protons are produced while also 1 mole of buffer is produced in the form of bicarbonate. So for every mol of oxidized substrate an additional amount of 7 moles

of buffer is required to maintain a neutral pH and maintain a low anodic overpotential and thereby a high biofilm performance (Torres et al., 2008). Usually, high concentrations of buffer are used to prevent this acidification of the biofilm (Torres et al., 2008). Torres et al. (2008) showed there is a linear increase in current density with increasing phosphate buffer concentration. Unfortunately, addition of these amounts of buffer, sometimes over 300 mM (Tartakovsky et al., 2008), makes the system not practically applicable. Discharge regulations do not allow high concentrations of nutrients, and furthermore adding salts in these concentrations would significantly increase the costs of the system (Sleutels et al., 2009b).

We introduce a system that is able to eliminate the amount of additional buffer needed without reducing the produced current in the system. To meet this objective, an extra ion exchange membrane was placed between the electrodes, creating a three compartment system, where the middle compartment is called recovery compartment. This recovery compartment can be used to produce an alkaline stream. This study shows that when this alkaline stream from the recovery compartment is fed to the anode of the same BES, no buffer needs to be added to waste streams without losing current production in the system.

6.2. Materials and methods

6.2.1. Bioelectrochemical cell

The system consisted of three polycarbonate compartments between which two membranes were placed (Figure 1). The first compartment contained a 6.5mm graphite felt (National Electrical Carbon BV, Hoorn, The Netherlands) through which the anolyte was forced to flow perpendicularly. To achieve this forced flow spacer material (PETEX 07-4000/64, Sefar BV, Goor, The Netherlands) was placed between anode and membrane. As a current collector gold wires were placed between the compartment wall and the felt that were connected to an electrical circuit. The second compartment (thickness 1cm) was used to keep the two membranes separated and to allow liquid to flow in between the two membranes.

The third compartment contained the cathode that consisted of a platinum coated (50 g/m²) titanium mesh (thickness 1mm, specific surface area 1.7 m²/m² - Magneto Special Anodes BV, Schiedam, The Netherlands). All liquid flows were circulated through the three compartments at a flow rate of 340 mL/min. All three compartments (anode, recovery and cathode) had a working volume of 500 mL. On the anode side of the recovery compartment a CEM (Fumasep® FKE, FuMa-Tech GmbH, Germany) was placed and on the cathode side an AEM was placed (AMX - Neosepta, Tokuyama Corp., Japan).

The anode, cathode and membranes all had a projected surface area of 0.025 m². Anode and cathode were connected through a power supply (ES 03-5, Delta Electronica BV, Zierikzee, The Netherlands) and the cell voltage was set to 1V. Potential of anode and cathode were measured separately against Ag/AgCl reference electrodes (+201 mV vs. standard hydrogen electrode). These reference electrodes were connected to the cell through a Haber-Luggin capillary. All experiments were performed at 303 K.

6.2.2. Experimental procedures

The anodic compartment was inoculated with 100 mL effluent from an active MEC (Zehnder et al., 1980) and fed with synthetic wastewater at a rate of 5 mL/min. This synthetic waste water was first pumped through the recovery compartment and then fed to the anode for consumption by electrochemically active microorganisms and left the anode as effluent. The synthetic wastewater contained 1.36 g/L NaCH₃COO·3H₂O, 0.68 g/L KH₂PO₄, 0.87 g/L K₂HPO₄ (10 mM phosphate buffer), 0.74 g/L KCl, 0.58 g/L NaCl, 0.28 g/L NH₄Cl, 0.1 g/L MgSO₄·7H₂O, 0.1 g/L CaCl₂·2H₂O and 0.1 mL/L of a trace element mixture (Sata, 2004) for the start up phase. The pH of the influent was around 7 and the conductivity was 5.86 mS/cm. After two weeks, a steady state had established and measurements were performed for 7 days. This procedure was repeated for buffer concentrations in the influent of 5 mM (0.34 g/L KH₂PO₄, 0.44 g/L K₂HPO₄) and eventually for 0 mM (0 g/L KH₂PO₄, 0 g/L K₂HPO₄). In the final experiment, the other additional salts (KCl, NaCl, NH₄Cl and CaCl₂) were also removed and the influent contained only 10 mM

of acetate and the trace element mixture. Again measurements were performed for 7 days after a steady state had established. Every day, samples were taken from all three compartments and from the influent. From all these samples, pH and conductivity were measured (WTW pH/cond 340i, Weilheim, Germany). All experiments were performed in duplicate.

Anode resistances were calculated from the anode and cathode overpotentials and the current densities.

6.2.3. Ion transport

The concentration of the most dominant cations, being K⁺, Na⁺ and Ca²⁺, in the different compartments was determined using an inductive coupled plasma atom emission spectrometer (ICP, PerkinElmerOptima 5300DV). From these cation concentrations in the anode and recovery compartment, the transport numbers for the various cations (t_{c^+}) through the CEM could be calculated using

$$t_{c^+} = \frac{(C_{recovery} - C_{anode})Q_{in} F}{AI} \quad (2)$$

where $C_{recovery}$ is the ion concentration in the recovery compartment (mol/L), C_{anode} is the ion concentration in the anode (mol/L), Q_{in} is the influent flow rate ($8.3 \cdot 10^{-5}$ L/s), F is Faradays number (96485 C/mol), A is the membrane surface area (0.025 m²) and I is the current density (A/m²).

6.3. Results and discussion

The objective of this research was to create a system that does not require addition of buffer to waste streams by reusing the ions present in these waste streams. This was tested with waste streams with 10, 5 and 0 mM of phosphate buffer.

6.3.1. Steady state

The principle of this system is based on the characteristics of ion exchange membranes (Figure 1): CEMs are negatively charged and allow positively charged species to be transported while AEMs are positively charged and allow negatively charged species to be transported (Rozendal et al., 2006a). Because these

Buffer requirement

membranes do not distinguish between different species of the same charge, they generally transport species that are present in high concentrations, which is in our experiment mostly K^+ and/or Na^+ . It has been shown before that this transport of cations towards the cathode leads to an increase of the pH in the cathode, even when an AEM is used (Rozendal et al., 2007). In the start-up phase (first two weeks) of the experiments presented here, this also occurred and the pH in the cathode reached a value of around 12.8. The hydroxyl concentration was then high enough to be the only species contributing to the charge transport in this case from cathode to the recovery compartment. This steady state situation was indicated by a stable pH and conductivity in all three compartments and a stable current production. The transport from the anode to the recovery compartment however, was still mostly by K^+/Na^+ instead of H^+ , since K^+ and Na^+ are present in the highest concentrations. So, the main overall ion transport in the system in steady state to compensate for the negative flow of electrons from anode to cathode was by K^+/Na^+ from anode to the recovery compartment and by OH^- from cathode to the recovery compartment. This accumulation of ions caused the pH and conductivity of the liquid in the recovery compartment to increase. When the influent is fed through the recovery compartment the pH and conductivity of the influent therefore increased as well.

Buffer requirement

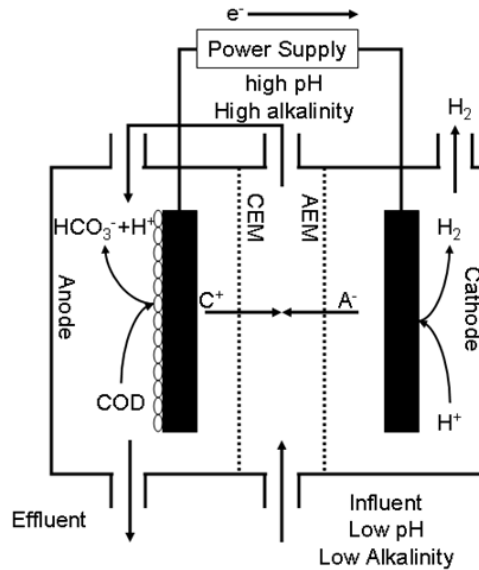


Figure 1 Set-up for reuse of ions present in wastewaters and production of an alkaline stream. The influent is first fed through a recovery compartment before it is fed to the anode of the BES. Because of the produced electrons cations move from the anode to the recovery compartment and anions move from the cathode to the recovery compartment. This transport of ions causes the pH and conductivity of the waste stream to increase.

When the liquid from the recovery compartment is pumped into the anode, the hydroxyl is used to take up a proton from the biofilm. This way, the total buffer capacity of the anolyte is increased and thereby it is possible to produce the same current with lower buffer concentrations than the 8 moles that are required according to the anodic reaction (equation 1).

Figure 2 shows the pH and conductivity for the experiment with 0 mM of phosphate buffer in steady state. Both the pH and conductivity increased in the recovery compartment. In this experiment the pH increased from 6.8 in the influent to 11.4 in the recovery compartment while the conductivity increased from 4.4 mS/cm in the influent to 5.5 mS/cm in the recovery compartment. This picture is representative for the steady state situations for all experiments (10, 5 and 0 mM

phosphate buffer and no additional salts). Both pH and conductivity were stable during operation, and only showed minor variations in time, caused by the sample taking from the set-up, which disturbed the system slightly. The variations in the pH of the influent were caused by the low buffer concentration in this experiment (0 mM phosphate).

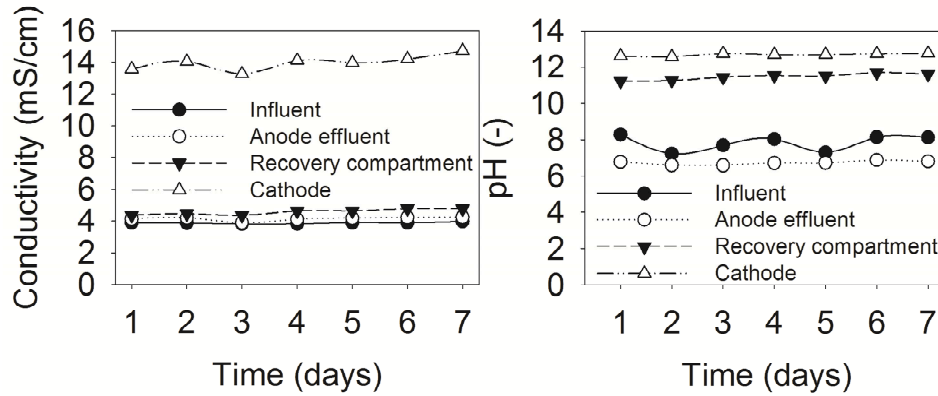


Figure 2 Development of pH and conductivity in time at constant current production at an influent buffer concentration of 0 mM.

6.3.2. Current density

The effect of this three compartment set up on waste streams with different buffer concentrations was tested (10, 5 and 0 mM of phosphate buffer). Figure 3 shows the current densities produced in experiments with 10 (3.46 A/m²), 5 (3.44 A/m²) and 0 mM of phosphate buffer (3.62 A/m²). These results show that it is indeed possible to produce the same current when no buffer is added to waste streams. This is caused by the fact that the higher hydroxyl concentration resulting from the recovery compartment can be used to take up more protons from the biofilm to maintain biofilm performance.

Typical wastewater streams have an even lower conductivity than the influent used in the experiment without phosphate buffer. These lower conductivities usually lead to lower current densities because of a higher internal resistance of the system. To study the effect of lower ion concentrations on current production, the amount of salts present in the influent was decreased even further leaving only acetate and

Buffer requirement

the trace element mixture to be present. This caused the current to drop to 2.32 A/m².

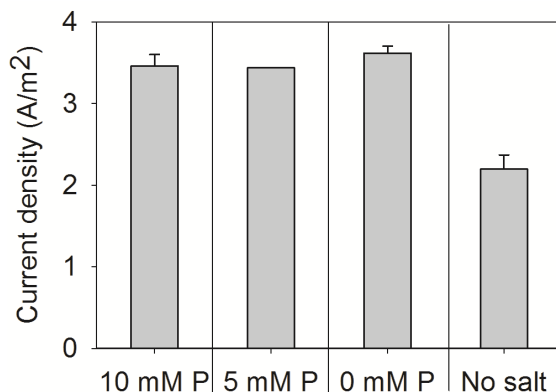


Figure 3 Current densities for experiments with 10, 5 and 0 mM of phosphate buffer and without any additional salts present in the artificial wastewater.

6.3.3. Ion transport

This lower current density without additional salts can be explained by the transport of ions through the membrane. Therefore, the flux of ions (mostly K⁺ and Na⁺) that was responsible for this ion transport through the CEM was calculated. It can be expected that the relative amount of Na⁺ responsible for charge transport increases compared to K⁺ since the concentration of K⁺ decreases at lower buffer concentrations and the concentration of Na⁺ stays the same. Indeed, calculations show (Table 1) that the transport number of Na⁺ increased and the transport number of K⁺ decreased. This relative amount decreases from 2.18 in the experiment with 10 mM of phosphate buffer to almost 0 in the experiment without additional salts. The mobility of Na⁺ (50.1 m²S/mol) is much lower than the mobility of K⁺ (73.5 m²S/mol) (Strathmann, 2004). Since more Na⁺ is transported through the membrane the relative mobility of the transported ions decreases. This lower mobility causes the resistance for transport of ions to increase. Furthermore, low ion concentrations can cause concentration polarization inside the diffusion layer on the anode side of the CEM. This concentration polarization causes limited

Buffer requirement

transport of ions towards the membrane and causes the resistance for ion transport to increase (Sleutels et al., 2009b).

Table 1 Transport numbers for Na⁺ and K⁺ and anode resistances for experiments performed with 10, 5 and 0 mM of phosphate buffer and without additional salts present.

	t_{Na^+}	t_{K^+}	$t_{\text{K}^+}/t_{\text{Na}^+}$	R_{an} (m Ωm^2)
10 mM P	0.27	0.59	2.18	18
5 mM P	0.36	0.53	1.49	17
0 mM P	0.34	0.43	1.25	22
No salt	0.85	0	0	21

The anode overpotential can be another indication that current production was not limited by biofilm performance but by limited ion transport in the concentration polarization layer. The anode overpotential was calculated as resistance for all experiments and is shown in Table 1. This table shows that a decrease in the buffer concentration did not increase the anode resistance, indicating that the biofilm activity was not influenced by the buffer concentration. Furthermore, also removing the other additional salts did not have an effect on the anode resistance.

6.3.4. Increase of pH and conductivity

Figure 4 shows the difference in pH and conductivity between influent and effluent of the recovery compartment for experiments with 10, 5 and 0 mM of phosphate buffer and the experiment without additional salts. The difference in pH between influent and liquid from the recovery compartment increases at lower buffer concentrations. This is caused by the lower buffer capacity of the waste stream. To see the buffering effect of the system, the expected pH in the recovery compartment was calculated if no buffer would have been present. This expected pH can be calculated from the current density and the influent flow rate, according to

$$[OH^-] = \frac{IA}{FF_{in}} \quad (3)$$

where I is the current density in (A/m^2), A is the projected surface area of the membrane ($0.025 m^2$), F is faraday's constant ($96485 C/mol$) and F_{in} is the influent flow rate ($5 mL/min$). The expected pH values for the recovery compartment, when no buffer is present, are also indicated in Figure 4. The actual values indeed approach the expected values when no buffer is present, because no hydroxyl can be taken up by the buffer. At higher buffer concentrations however, the actual values are lower than the expected values, because the hydroxyl is taken up by the buffer.

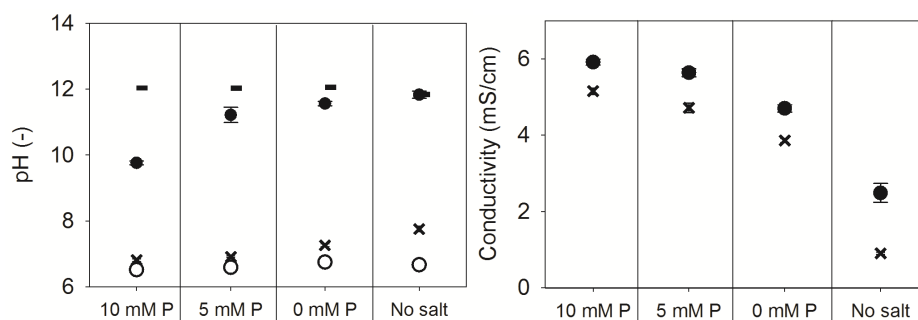


Figure 4 pH (left) and conductivity (right) of influent (x) and liquid in the recovery compartment (●) for experiments with 10, 5 and 0 mM of phosphate buffer and without any additional salts present in the artificial wastewater. For the pH also the calculated value is indicated (-) based on current density and influent flow rate assuming no buffer is present and the anode effluent pH is shown (o).

6.3.5. Internal resistance

The produced current density in this system was lower than the current produced in a comparable MEC (without recovery compartment) for hydrogen production (Call and Logan, 2008). However, for cases where the highest current density is not the main goal, this system does offer benefits. The internal resistance of this system ($289 m\Omega m^2$ with 10 mM of phosphate buffer) was much higher than the internal resistance of another MEC with 10 mM of phosphate buffer ($85 m\Omega m^2$). Reason for

this higher internal resistance can be the extra compartment, creating a distance between the two membranes (1cm) in this setup. Furthermore, the presence of an extra membrane also results in an additional internal resistance. In future, the distance needs to be reduced to decrease the resistance of the system and to increase the current density and hydrogen production.

6.3.6. Alkalinity production.

Alkalinity production was demonstrated here in an MEC. In principle, this is also possible in an MFC as both systems have the same working principle. MFC performance however, could be lower because of thermodynamic constraints caused by the high pH in the cathode. Furthermore, the extra membrane increases the resistance of the system and thereby reduces the current production. However, the extra membrane also has clear advantages. First, compared to a membraneless system (Jeremiase et al., 2010; Rozendal et al., 2008b), the cathode is still separated from the waste stream and in this way a pure product can be produced in the BES. Second, the ions transported away from anode and cathode can be recovered in a new stream that is pumped through the recovery compartment.

This stream can be used in the BES itself as shown in this study, but it can also be used for other applications. In case the stream is used in another application it can not be used to in the BES itself and the anode will acidify. An example of the use of this stream with increased alkalinity in another application is feeding it to another wastewater treatment system like an anaerobic digester to improve performance. In an anaerobic digester, CO₂ is produced that leaves the system with the produced methane. The alkaline waste stream can be used to maintain pH neutrality and thereby maintain performance. Overall the production of an alkaline stream represents great economical and environmental value. So this new system not only produces energy in the form of hydrogen gas but more important, it also produces an alkaline stream.

Acknowledgements

This work was performed in the TTIW-cooperation framework of Wetsus, centre of excellence for sustainable water technology (www.wetsus.nl). Wetsus is funded by

Buffer requirement

the Dutch Ministry of Economic Affairs, the European Union European Regional Development Fund, the Province of Fryslan, the city of Leeuwarden and by the EZ-KOMPAS Program of the “Samenwerkingsverband Noord-Nederland”. The authors like to thank the participants of the research theme “Bio-energy” for the fruitful discussions and their financial support and Annemiek ter Heijne for critical reading of the manuscript.

Chapter 7

Conclusions and Perspectives

7.1. Introduction

This thesis describes the improvements in the hydrogen production rate from biomass in Microbial Electrolysis Cells (MECs). Since the discovery of MECs in 2005 the performance and efficiency of the system was increased considerably. Early systems produced only $0.02 \text{ m}^3 \text{ H}_2/\text{m}^3/\text{day}$ at an applied voltage of 0.5 V (Rozendal et al., 2006b) while in this thesis a production rate of $5.4 \text{ m}^3 \text{ H}_2/\text{m}^3/\text{day}$ at an applied voltage of 1V was found. The hydrogen production rate was increased by a new design of the system. The changes were made based on new insights to the kinetics of the system. In this chapter we will discuss the strategies applied to increase the performance of the system and the effect these changes had on the efficiency of the system. Performance of the system is described by the produced current density and the hydrogen production rate. The efficiency of the system can be described by several parameters. These parameters include anodic and cathodic coulombic efficiency, specific energy input and the chemical input. Finally, a comparison will be made with competing technologies to understand the need for further improvements.

7.2. MEC performance

The hydrogen production rate can be increased by lowering the internal losses of the MEC. It was shown in chapter 2 that these internal cell losses can be represented as an electrical equivalent circuit which consists of several separate resistances in series. These resistances consist of ionic, ion transport through the membrane, anode and cathode resistance and the energy required to overcome the thermodynamical barrier for hydrogen production. Table 2 shows an overview of the applied strategies described in this thesis on the main performance indicators of MECs.

In chapter 2 the internal resistance for MECs equipped with a cation exchange membrane (CEM) and with an anion exchange membrane (AEM) was calculated. It was shown here that the system with an AEM performed better than the system with the CEM because of a lower transport resistance for ions through the AEM

compared to a CEM. Chapter 3 showed that the anode resistance can be decreased by improving the mass transport in the anode compartment. This was achieved by introducing a forced flow through a porous anode. The anode resistance could also be lowered by increasing the buffer concentration. Both an improved mass transport and a higher buffer concentration resulted in a decrease in the ion transport resistance through the membrane. The effect of mass transport in the anode was further investigated in chapter 4. Here it was shown that a higher mass transport rate leads to an increased current production and increased efficiency only if the ion transport through the membrane is stimulated. So, it can be concluded that an improved mass transport rate in the system leads to higher production rates. Mass transport limitations within the system is one of the most important parameters that determines performance of the system.

Table 2 Overview of performance indicators for results obtained in this thesis

Chapter	characteristic	Anodic coulombic efficiency %	Current density A/m ²	Cathodic coulombic efficiency %	Hydrogen production rate m ³ /m ³ /day	Applied cell voltage V	Internal resistance m Ω m ²	Actual specific energy input kWh/m ³ H ₂
2	CEM	13	2.3	47	0.4	1	435	4.53
	AEM	28	5.3	83	2.1	1	189	2.56
3	10 mM P	85	11	42	2.3	1	91	5.08
	50 mM P	93	16.4	71	5.6	1	61	3.01
	1.4 cm/min	14	3.7	89	1.5	0.8	216	1.91
4	2.7 cm/min	34	5.2	60	1.4	0.8	154	2.83
	5.4 cm/min	38	6.3	50	1.6	0.8	127	3.40
5	-350 mV	22	10.5	90 ^a	4.8	0.89	85	2.10
	10 mM Ac	70	15.72	90 ^a	7.1	1.29	82	3.05
	10 mM P	-	3.56	90 ^a	1.6	1	281	2.36
6	0 mM P	-	3.56	90 ^a	1.6	1	281	2.36
	No salt	-	2.32	90 ^a	1.1	1	431	2.36

^a Assumed cathodic coulombic efficiency of 90%

7.2.1. Energy efficiency

The energy efficiency of an MEC is defined by the ratio between energy output and energy input. In an MEC the energy input consists of the organic material in the influent and the electric energy that is needed to overcome the thermodynamical barrier for hydrogen production. The energy output consists of the amount of hydrogen gas produced. The energy efficiency describes how much of the available electrons from the substrate are transferred to the product and what the energy content of these electrons is. Therefore, it is the product of both the coulombic efficiency and the voltage efficiency.

7.2.2. Coulombic efficiency

The coulombic efficiency describes the amount of electrons from the substrate that end up in the product. The coulombic efficiency can be divided in anodic coulombic efficiency (ACE) and cathodic coulombic efficiency (CCE). The ACE describes which part of the electrons from the substrate end up in the electrical circuit and can be calculated with:

$$ACE = \frac{QnF(C_{in} - C_{out})}{\int_0^t I_m dt} \quad (1)$$

where I_m is the measured current density (A/m²), Q is the influent flow rate (m³/s), n is the amount of electrons released from the substrate, F is Faradays constant (96485 C/mol e⁻) and C_{in} and C_{out} are the in and outgoing substrate concentrations (M).

The CCE is a measure for the amount of electrons that come from the electrical circuit and are transferred to the product and can be calculated with:

$$CCE = \frac{\int_0^t I_m dt}{2F} \quad (2)$$

The overall coulombic efficiency, which is a product of anodic and cathodic coulombic efficiency, is lowered by biomass growth and processes that compete for substrate and products in both compartments. In the anode the main competing process is methanogenesis. Acetate can be converted by acetoclastic methanogens into methane. Consequently, the electrons from the substrate do not end up in the electrical circuit which leads to lower coulombic efficiency. Hydrogen gas can also leak from the cathode through the membrane into the anode and is then used by methanogenic bacteria to produce methane from CO₂. Competing processes become more important when the membrane is omitted in a so called membraneless system. In this system both anode and cathode are located in the same compartment. This leads to more mixing of CO₂ and H₂ and consequently to the production of more methane. The formation of methane has a negative effect on the cathode coulombic efficiency since a part of the product (hydrogen) is lost. In some cases also microorganisms are used as a catalyst in the cathode, which is called a biocathode (Liu et al., 2005a; Torres et al., 2008). When such a biocathode is applied in an MEC, other competing processes can occur in the cathode as well. Again the most important competing process is methanogenesis (Jeremiassé et al., 2010; Rozendal et al., 2008b). This is partly caused by CO₂ crossover from the anode, which is converted to methane together with hydrogen. Furthermore, also the organic substrate for the biocathode, when applied, may lead to competition. Table 2 gives an overview of the anodic coulombic efficiencies obtained in several experiments presented in this thesis. In chapter 3 it was shown that an increase in mass transport rate can increase the coulombic efficiency. Furthermore, also an increase in buffer concentration had a positive effect on the coulombic efficiency. Both parameters improved conditions for the electrogens compared to the methanogens. Therefore, the electrogens were able to win the competition for substrate. In chapter 4 the same effect was shown for an increase in mass transport rate in the anode. It was shown that also the buffering mechanism in the anode compartment can be used to influence the coulombic efficiency. Finally, in chapter 5, the effect of the anode potential and the effect of the influent concentration on coulombic efficiency was tested. An increase of anode potential had a positive effect

on the coulombic efficiency, while a decrease in the influent concentration had a positive effect on the coulombic efficiency as well. Further research is required to optimize these strategies to find a right balance between the coulombic efficiency, current density and removal rate of organic material. For the substrate concentrations knowledge from previous research about competing processes with methanogens can be used. Further knowledge about the kinetic growth coefficients is required to control this competition. These coefficients are also interesting for the anode potential control strategy. The growth kinetics are related to the active enzyme complexes for electron transfer. Further knowledge about these processes can make it possible to control the competition. Also a combination of both strategies can be applied to find optimal conditions.

The CCE in MECs is generally considered to be close to 100%, especially when a membrane is applied. When a membrane is applied, most of the hydrogen is kept in the cathode and hardly any substrate/product crossover takes place (Rozendal et al., 2006b). Therefore, the produced hydrogen is not consumed by methanogens. Another advantage of using a membrane is that pure hydrogen is produced in the cathode, since it is not mixed with CO₂ and methane that is produced in the anode. Table 2 also shows lower values than 100% for the CCE. This is assumed to be caused by hydrogen leaking through tubing. Hydrogen is a very small molecule that easily escapes from the system. This does not mean, however, that the actual efficiency of the conversion from electrons to hydrogen is lower. Instead, only the capture efficiency of the produced hydrogen is lower. In future, materials for full scale applications have to be chosen in order to prevent these hydrogen losses from the system. For example, by using the same materials that are used to construct electrolyzers.

7.2.3. Voltage efficiency

The voltage efficiency of an MEC describes which part of the chemical energy from the substrate eventually ends up in the product and how much has to be added in the form of electrical energy and is generally expressed as the specific energy input. In theory, the specific energy input can be close to the thermodynamical energy

level required for hydrogen production, but in practice several internal resistances increase the required specific energy input. Therefore, the required specific energy input strongly depends on the design of the system. There is a difference between the required specific energy input and the actual specific energy input. In an MEC the actual specific energy input is determined by the applied voltage and the CCE. When a membrane is applied in an MEC and when assuming that all hydrogen can be captured, the CCE can be considered to be close to 100%, because substrate/product crossover is prevented. Since a voltage is applied, a certain amount of energy is added per electron that is produced. At a lower internal resistance the amount of produced electrons will be higher and so also the amount of produced H₂ will be higher. However, the energy input per electron and so also for the produced H₂ is determined by the applied voltage. Because the applied voltages used in this thesis are high compared to the thermodynamical minimum (0.14V) the values found in this thesis for the actual specific energy input are high (Table 2). Furthermore, a high CCE is another important criterion for a low specific energy input, as a reduction of the CCE has a direct effect on the specific energy input. At a CCE of 50% the required energy input is twice as high compared to a CCE of 100% because 50% of the produced electrons are not converted to product while the energy has been added to the system. Therefore, the highest specific energy input (5.08 kWh/m³) was found for the lowest CCE (42%). In future, the CCE can be improved by better design of the system and the use of better materials. The required specific energy input of an MEC depends on the internal resistance of the system. As described before, the total internal resistance includes anode and cathode overpotentials, Ohmic resistances of electrolytes and the electrical circuit and the resistance of ion transport through the membrane. In chapter 2 it was shown that the resistance for ion transport through an AEM is lower than the resistance for transport of ions through a CEM. Therefore, the required specific energy input is lower when an AEM is applied in an MEC than when a CEM is applied. In chapter 3 and 4 it was shown that an improved mass transport rate in the system lowers both the anode and the ion transport resistance. Again, this reduction in resistance lowers the required energy input for hydrogen production.

7.3. Chemical efficiency

The efficiency of MECs can be expressed in different ways. Eventually, the aim is to extract as much energy from an organic waste stream as possible and transfer this energy to produce hydrogen gas. To achieve a high energy extraction rate, a high coulombic efficiency in combination with a high current density is required. So far however, not much attention was paid to the addition of chemicals. For example, in many experiments high buffer concentrations are used. The reason to use of buffer is twofold. First, the buffer species take up protons produced by the biofilm and assure neutral conditions. These conditions help in maintaining a high current density. Second, high buffer concentrations lead to high conductivity of the electrolyte. A high conductivity is required to achieve a high ionic current and thus a high current density. At low conductivity the Ohmic resistance of the electrolyte may become a limiting factor in the system. Addition of buffer and/or electrolyte increases the cost of the system. Furthermore, addition of chemicals requires an additional step to remove these chemicals again since disposal of high concentrations of, for example, nutrients, is not allowed.

As a combination of high conversion rate and low chemical input is required, it is interesting to study the contribution of electrolyte and buffer to the performance (current density) of the system. This contribution can be expressed as the relative chemical input (C_{rel}) per mol of produced electrons and can be calculated with

$$C_{rel} = \frac{C_{chem}}{I} Q_{in} F \quad (3)$$

where C_{chem} is the chemical input (mol eq/L), I is the current density (A/m²), Q_{in} is the influent flow rate (L/s) and F is Faradays constant (C/mol e⁻). The contribution of the relative chemical input to current production can be divided over the electrolyte, buffer and substrate in the influent.

It was shown before (chapter 2) that an MEC with an AEM outperforms an MEC with a CEM. This also has a direct influence on the relative chemical input for the system. Figure 1 shows this relative chemical input for both systems and shows that the total chemical input for the AEM is half of the chemical input of the CEM. This

can be explained by the fact that both systems used influent with the same chemical composition while the AEM produced higher current density than the CEM. Therefore, the relative contribution of these chemicals in the best performing system (AEM) was lowest. This shows that, when an AEM is applied not only the performance, considering production rate, of the system is better but also the relative investment to reach this production rate in the form of chemicals is lower.

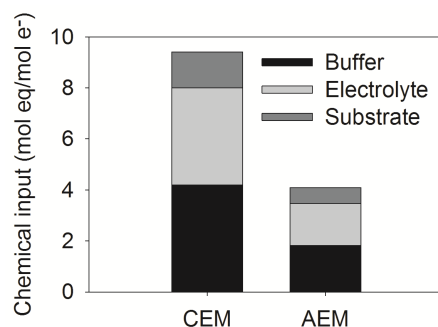


Figure 1 Relative chemical input for an MEC equipped with a CEM compared to a system equipped with an AEM.

It was shown in this thesis (chapter 3) and in previous research (Liu et al., 2005a; Torres et al., 2008) that addition of buffer has a positive effect on the current production of MECs. Also in this case, it is interesting to study the effect of chemical input on productivity. Figure 2 shows the relative chemical input for systems using influent buffer concentrations of 10 mM and 50 mM (chapter 3). The chemical input for the 10 mM system is only 1/3 of the chemical input of the 50 mM system. Although the system with a high buffer concentration (50 mM P) produced considerably more current, the relative contribution to current production is much lower. This shows that a system with lower buffer concentrations produces relatively more current compared to the chemical input. Besides this relative advantage in conversion rate, systems with lower buffer have the additional advantage that they require lower operating costs because of lower chemical requirements and less additional treatments steps to remove chemicals.

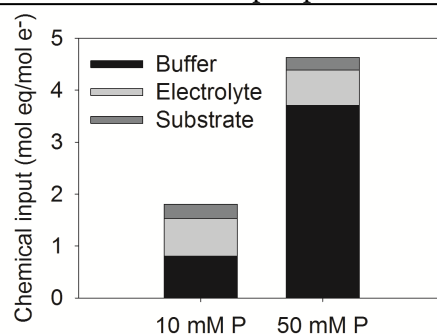


Figure 2 Influence of buffer concentration of relative chemical input for an MEC.

It is generally considered that systems at low conductivity (low ionic strength) perform worse than systems at higher conductivity because of the high Ohmic losses. Figure 3 shows the relative chemical requirement for MECs treating influent with 10 mM of phosphate buffer, 0 mM of phosphate buffer and without addition of electrolyte in the form of buffer. This figure shows that the relative output is higher at low concentrations. Again, the implication is that the system performs better at high buffer and electrolyte concentrations but the relative contribution of these chemicals to current production is smaller, in contrary to what is generally believed. Of course a good mass transport in the system is very important in cases of low ionic strength.

It can therefore be concluded that generally, addition of large amounts of buffer and electrolyte is unnecessary from a chemical efficiency point of view since it only increases costs of the system. This makes the future of MECs promising, as it is believed that the required chemical input hinders practical application.

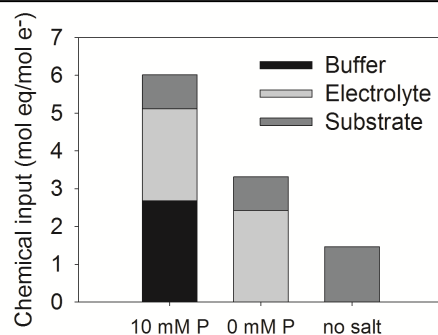


Figure 3 Relative chemical requirement for MECs treating influent with 10 mM of phosphate buffer, 0 mM of phosphate buffer and without addition of additional electrolyte.

7.4. Competing processes and perspective of MECs

Rozendal et al. (2008) predicted that in future hydrogen gas can be produced at a rate of over 10 m³/m³/day at an overall H₂ efficiency of over 90% (Rozendal et al., 2008a). Of course, already mature technologies exist that are able to produce great quantities of hydrogen at high production rates like water electrolysis. When moving towards a biobased economy however, the hydrogen needs to be produced from organic material. The type of technology that is available for the production of hydrogen from biomass highly depends on the type of biomass used. For example, dry biomass (like wood) can be gasified at relatively high rate and efficiency to hydrogen. Wet biomass however, is less suitable for gasification because of the energy requirement for heating. Wet biomass is more suitable to be used in an MEC. Therefore, we will here compare hydrogen production from wet biomass in an MEC to another possible technological route.

An alternative possible technological route to produce hydrogen from biomass is to first digest the wet biomass to methane. This methane gas can then be transformed into a mixture of hydrogen and carbon monoxide by Steam Methane Reforming (SMR). In a second step the carbon monoxide can then be converted together with H₂O into CO₂ and hydrogen (gas shift reaction). The produced gas mixture needs a cleaning step to produce pure hydrogen.

Two parameters are used for comparison of the two production methods for hydrogen from biomass: energy efficiency and conversion efficiency, which are shown in Table 3. The total energetic efficiency for the combination of anaerobic digestion and SMR is around 50% (Rosen and Scott, 1998). This is mainly caused by the number of process steps and the high temperature required (>750 °C) for SMR. In theory, in future the energetic efficiency of MECs can be higher than both suggested routes. Table 3 mentions an efficiency of 67% which would require an energy input of 1 kWh/m³ of produced hydrogen. To achieve such a low specific energy input, the internal resistance of the system needs to be around 30 mΩ m² and the CCE needs to be around 99%. For comparison, the lowest internal resistance found in this thesis was 61 mΩ m². Although this is already a great improvement compared to the first systems (321 mΩ m² by Liu et al 2006 and 1064 mΩ m² by Rozendal et al 2006) still only a factor 2 of improvement is required to make MECs competitive with currently available hydrogen production technologies. Another important parameter is the amount of hydrogen that can be extracted from the biomass. This efficiency is around 50% when a combination of anaerobic digestion (70% efficiency) and SMR (70% efficiency) is applied. Again this efficiency is low because of the number of steps involved in the total route. In theory, the conversion efficiency of MECs is expected to reach values of over 90%. Therefore, both a high ACE ($>90\%$) and a high CCE (99%) are required. As discussed before, the CCE can be close to 100% if a membrane is applied and the right materials are used to construct the system. The ACE however, also needs to reach values that are close to 100%. Although significant steps have been made to increase the ACE, still research is needed to get a better understanding in the competing processes in the anode. Especially when more complex substrates than acetate will be used as electron donor these competing processes will also be more complex. A better understanding and increase of the ACE is therefore of utmost importance to make MECs be able to compete with other processes to produce hydrogen from biomass.

Finally, also the type of biomass used in an MEC is important for the efficiency of the system. For example, solid biomass will not be suitable for hydrogen

Conclusions and perspectives

production in a MEC without pretreatment while it can be gasified. Also other types of biomass that contain a high percentage of lignocelluloses will require pretreatment to make the organic material available for degradation by the electrogenic microorganisms. Most ideal organic waste streams seem to be those that come from biomass processing companies since they mostly contain easy accessible organic material. For food processing industry, another advantage is that these companies are among the largest consumers of hydrogen. Production on site would solve additional problems of storage and transportation of hydrogen gas.

Table 3 Overview of efficiencies for the production of hydrogen from wet biomass.

Process	Energetic efficiency	Conversion efficiency
	(%)	(%)
Anaerobic digestion + SMR	49 ^a	50 ^b
Present MEC ^c	40	66
Future MEC ^d	67	>90

^a Based on 70% efficiency for anaerobic digestion, 78% efficiency for SMR (Rosen and Scott, 1998) and 10% energy loss for gas purification.

^b Based on 70% efficiency for anaerobic digestion and 70% for SMR.

^c (Sleutels et al., 2009b) (ACE: 91%; CCE 71%; specific energy input 3.0 kWh/m³)

^d (Rozendal et al., 2008a) (ACE: >90%; CCE 99%; specific energy input 1.0 kWh/m³)

7.5. Concluding remarks

This chapter describes improvements of the hydrogen production rate in MECs. Crucial parameters, like specific energy input and coulombic efficiencies are presented to be able to compare different MECs. Improvement of these parameters can make MECs a competing technology for the production of hydrogen gas from biomass. Therefore the following three key characteristics of the system have to be optimized: Firstly, the anodic coulombic efficiency needs to be controlled and

Conclusions and perspectives

improved to reach values close to 100% for all possible organic substrates. Secondly, the use of materials and the design should be such that the total internal resistance does not exceed values of 30 m Ω m². Thirdly, the use of added chemicals like buffers should be limited as the relative productivity does not increase with increasing use of chemicals. If we manage to succeed on these issues, production of hydrogen gas from biomass in microbial electrolysis cells will be able to compete with existing technologies.

References

- Aelterman, P., Freguia, S., Keller, J., Verstraete, W., Rabaey, K. 2008a. The anode potential regulates bacterial activity in microbial fuel cells. *Applied Microbiology and Biotechnology*, **78**(3), 409-418.
- Aelterman, P., Versichele, M., Marzorati, M., Boon, N., Verstraete, W. 2008b. Loading rate and external resistance control the electricity generation of microbial fuel cells with different three-dimensional anodes. *Bioresource Technology*, **99**(18), 8895-8902.
- Angenent, L.T., Karim, K., Al-Dahhan, M.H., Wrenn, B.A., Domiguez-Espinosa, R. 2004. Production of bioenergy and biochemicals from industrial and agricultural wastewater. *Trends in Biotechnology*, **22**(9), 477-485.
- Bard, A.J., Faulkner, L.R. 2001. *Electrochemical methods: fundamentals and applications*. 2nd ed. John Wiley & Sons, New York.
- Bard, A.J., Parsons, R., Jordan, J. 1985. Standard potentials in aqueous solution, Marcel Dekker. New York.
- Bond, D.R., Lovley, D.R. 2003. Electricity production by *Geobacter sulfurreducens* attached to electrodes. *Applied and Environmental Microbiology*, **69**(3), 1548-1555.
- Bradford, M. 1976. A rapid and sensitive method for the quantification of microgram quantities of protein utilizing the principle of protein-dye binding. *Anal. Biochem.*, **72**, 248-254.
- Brett, C.M.A., Brett, A.M.O. 1993. *Electrochemistry: Principles, Methods, and applications*. Oxford University Press, Oxford.
- Call, D., Logan, B.E. 2008. Hydrogen production in a single chamber microbial electrolysis cell lacking a membrane. *Environmental Science & Technology*, **42**(9), 3401-3406.
- Chaudhuri, S.K., Lovley, D.R. 2003. Electricity generation by direct oxidation of glucose in mediatorless microbial fuel cells. *Nature Biotechnology*, **21**(10), 1229-1232.
- Cheng, S., Logan, B.E. 2007. Sustainable and efficient biohydrogen production via electrohydrogenesis. *Proceedings of the National Academy of Sciences of the United States of America*, **104**(47), 18871-18873.

References

- Cheng, S., Xing, D., Call, D.F., Logan, B.E. 2009. Direct biological conversion of electrical current into methane by electromethanogenesis. *Environmental Science and Technology*, **43**(10), 3953-3958.
- Cherubini, F. 2010. The biorefinery concept: Using biomass instead of oil for producing energy and chemicals. *Energy Conversion and Management*, **51**(7), 1412-1421.
- Chiao, M., Lam, K.B., Lin, L. 2006. Micromachined microbial and photosynthetic fuel cells. *Journal of Micromechanics and Microengineering*, **16**(12), 2547-2553.
- Christen, K. 2006. Europe's CUTE project for hydrogen-fuel-cell buses deemed a success. *Environmental Science & Technology*, **40**(15), 4541-U1.
- Clauwaert, P. 2008. Minimizing losses in bio-electrochemical systems: The road to applications. *Applied microbiology and biotechnology*, **79**(6), 901-913.
- Clauwaert, P., Toledo, R., van der Ha, D., Crab, R., Verstraete, W., Hu, H., Udert, K.M., Rabaey, K. 2008. Combining biocatalyzed electrolysis with anaerobic digestion. in: *Water Science and Technology*, Vol. 57, pp. 575-579.
- De Schamphelaire, L., Van Den Bossche, L., Hai, S.D., Hofte, M., Boon, N., Rabaey, K., Verstraete, W. 2008. Microbial fuel cells generating electricity from rhizodeposits of rice plants. *Environmental Science and Technology*, **42**(8), 3053-3058.
- Ditzig, J., Liu, H., Logan, B.E. 2007. Production of hydrogen from domestic wastewater using a bioelectrochemically assisted microbial reactor (BEAMR). *International Journal of Hydrogen Energy*, **32**, 2296-2304.
- Dlugolecki, P., Nymeijer, K., Metz, S., Wessling, M. 2008. Current status of ion exchange membranes for power generation from salinity gradients. *Journal of Membrane Science*, **319**(1-2), 214-222.
- El-Deab, M.S., El-Shakre, M.E., El-Anadouli, B.E., Ateya, B.G. 1996. Electrolytic generation of hydrogen on Pt-loaded porous graphite electrodes from flowing alkaline solutions. *Journal of Applied Electrochemistry*, **26**(11), 1133-1137.
- EU. 2008. European Commission's Second Strategic Energy Review.
- Faaij, A.P.C. 2006. Bio-energy in Europe: changing technology choices. *Energy Policy*, **34**(3), 322-342.

References

- Fan, Y., Sharbrough, E., Liu, H. 2008. Quantification of the internal resistance distribution of microbial fuel cells. *Environmental Science & Technology*, **42**(21), 8101-8107.
- Fan, Y.Z., Hu, H.Q., Liu, H. 2007a. Enhanced Coulombic efficiency and power density of air-cathode microbial fuel cells with an improved cell configuration. *Journal of Power Sources*, **171**(2), 348-354.
- Fan, Y.Z., Hu, H.Q., Liu, H. 2007b. Sustainable power generation in microbial fuel cells using bicarbonate buffer and proton transfer mechanisms. *Environmental Science & Technology*, **41**(23), 8154-8158.
- Fu, C.C., Su, C.H., Hung, T.C., Hsieh, C.H., Suryani, D., Wu, W.T. 2009. Effects of biomass weight and light intensity on the performance of photosynthetic microbial fuel cells with *Spirulina platensis*. *Bioresource Technology*, **100**(18), 4183-4186.
- Gil, G.C., Chang, I.S., Kim, B.H., Kim, M., Jang, J.K., Park, H.S., Kim, H.J. 2003. Operational parameters affecting the performance of a mediator-less microbial fuel cell. *Biosensors & Bioelectronics*, **18**(4), 327-334.
- GmbH, F.-T. 2005. Technical datasheet FAA ion exchange membrane.
- Greenpeace. 2005. Energy Revolution: a sustainable pathway to a clean energy future for Europe. www.greenpeace.org.
- Hallenbeck, P.C., Benemann, J.R. 2002. Biological hydrogen production; fundamentals and limiting processes. *International Journal of Hydrogen Energy*, **27**, 1185-1193.
- Hamelers, H.V.M., Sleutels, T.H.J.A., Jeremiasse, A.W., Post, J.W., Strik, D.P.B.T.B., Rozendal, R.A. 2009. Technological factors affecting BES performance and bottlenecks towards scale up. in: *Bio-electrochemical Systems: from extracellular electron transfer to biotechnological application*, (Eds.) K. Rabaey, L.T. Angenent, U. Schroder, J. Keller, IWA Publishing. London.
- Hamelers, H.V.M., Ter Heijne, A., Sleutels, T.H.J.A., Jeremiasse, A.W., Strik, D.P.B.T.B., Buisman, C.J.N. 2010a. New applications and performance of bioelectrochemical systems. *Applied Microbiology and Biotechnology*, **85**(6), 1673-1685.
- Hamelers, H.V.M., ter Heijne, A., Stein, N., Rozendal, R.A., Buisman, C.J.N. 2011. Butler-Volmer-Monod model for describing bio-anode polarization curves. *Bioresource Technology*, **102** (1) 381-387.

References

- Hawkes, F.R., Hussy, I., Kyazze, G., Dinsdale, R., Hawkes, D.L. 2007. Continuous dark fermentative hydrogen production by mesophilic microflora: Principles and progress. *International Journal of Hydrogen Energy*, **32**, 172-184.
- Hu, H., Fan, Y., Liu, H. 2008. Hydrogen production using single-chamber membrane-free microbial electrolysis cells. *Water Research*, **42**(15), 4172-4178.
- IEA. 2007a. Hydrogen production and storage. www.iea.org.
- IEA. 2007b. Key World Energy Statistics. International Energy Agency. www.iea.org.
- IEA. 2009. Key World Energy Statistics. International Energy Agency. www.iea.org.
- IPCC. 2007. Climate change 2007: the physical science basis. Contribution of working group I to the fourth assessment report of the Intergovernmental Panel on Climate Change (IPCC), (Eds.) S. Solomon, D. Qin, M. Manning, Z. Chen, M. Marquis, K.B. Averyt, M. Tignor, H.L. Miller, Cambridge University Press. Cambridge, United Kingdom and New York, NY, USA.
- Ivy, J. 2004. Summary of electrolytic hydrogen production: milestone completion report.
- Jeremiase, A.W., Hamelers, H.V.M., Buisman, C.J.N. 2010. Microbial electrolysis cell with a microbial biocathode. *Bioelectrochemistry*, **78**(1), 39-43.
- Jeremiase, A.W., Hamelers, H.V.M., Kleijn, J.M., Buisman, C.J.N. 2009. Use of biocompatible buffers to reduce the concentration overpotential for hydrogen evolution. *Environmental Science and Technology*, **43**(17), 6882-6887.
- Kim, J.R., Cheng, S., Oh, S.E., Logan, B.E. 2007. Power generation using different cation, anion, and ultrafiltration membranes in microbial fuel cells. *Environmental Science & Technology*, **41**(3), 1004-1009.
- Kyoto-Protocol. 1998. United Nations Framework Convention on Climate Change.
- Lee, H.S., Torres, C.I., Parameswaran, P., Rittmann, B.E. 2009. Fate of H₂ in an upflow single-chamber microbial electrolysis cell using a metal-catalyst-free cathode. *Environmental Science and Technology*, **43**(20), 7971-7976.

References

- Liu, H., Cheng, S.A., Logan, B.E. 2005a. Power generation in fed-batch microbial fuel cells as a function of ionic strength, temperature, and reactor configuration. *Environmental Science & Technology*, **39**(14), 5488-5493.
- Liu, H., Grot, S., Logan, B.E. 2005b. Electrochemically assisted microbial production of hydrogen from acetate. *Environmental Science & Technology*, **39**(11), 4317-4320.
- Logan, B., Cheng, S., Watson, V., Estadt, G. 2007. Graphite fiber brush anodes for increased power production in air-cathode microbial fuel cells. *Environmental Science & Technology*, **41**(9), 3341-3346.
- Logan, B.E. 2005. Simultaneous wastewater treatment and biological electricity generation. in: *Water Science and Technology*, Vol. 52, pp. 31-37.
- Logan, B.E., Call, D., Cheng, S., Hamelers, H.V.M., Sleutels, T.H.J.A., Jeremiasse, A.W., Rozendal, R.A. 2008. Microbial Electrolysis Cells (MECs) for High Yield Hydrogen Gas Production From Organic Matter. *Environmental Science & Technology*, **42**(23), 8630-8640.
- Logan, B.E., Hamelers, B., Rozendal, R., Schröder, U., Keller, J., Freguia, S., Aelterman, P., Verstraete, W., Rabaey, K. 2006. Microbial fuel cells: Methodology and technology. *Environmental Science & Technology*, **40**, 5181-5192.
- Logan, B.E., Regan, J.M. 2006. Microbial fuel cells - challenges and applications. *Environmental Science & Technology*, **40**(17), 5172-5180.
- Lovley, D.R. 2006. Bug juice: harvesting electricity with microorganisms. *Nature Reviews Microbiology*, **4**(7), 497-508.
- Min, B., Logan, B.E. 2004. Continuous electricity generation from domestic wastewater and organic substrates in a flat plate microbial fuel cell. *Environmental Science & Technology*, **38**(21), 5809-5814.
- Mulder, G., Hetland, J., Lenaers, G. 2007. Towards a sustainable hydrogen economy: Hydrogen pathways and infrastructure. *International Journal of Hydrogen Energy*, **32**(10-11), 1324.
- Niessen, J., Schroder, U., Harnisch, F., Scholz, F. 2005. Gaining electricity from in situ oxidation of hydrogen produced by fermentative cellulose degradation. *Letters in Applied Microbiology*, **41**(3), 286-290.
- Potter, M.C. 1912. Electrical effects accompanying the decomposition of organic compounds. *Proc. Roy. Soc. London Ser. B*, **84**, 260-276.

References

- Rabaey, K., Ossieur, W., Verhaege, M., Verstraete, W. 2005. Continuous microbial fuel cells convert carbohydrates to electricity. *Water Science and Technology*, **52**(1-2), 515-523.
- Rabaey, K., Verstraete, W. 2005. Microbial fuel cells: novel biotechnology for energy generation. *Trends in Biotechnology*, **23**(6), 291-298.
- Rajoka, M.I., Tabassum, R., Malik, K.A. 1999. Enhanced rate of methanol and acetate uptake for production of methane in batch cultures using *Methanosarcina mazei*. *Bioresource Technology*, **67**(3), 305-311.
- Ramasamy, R.P. 2008. Impact of initial biofilm growth on the anode impedance of microbial fuel cells. *Biotechnology and bioengineering*, **101**(1), 101-108.
- Reimers, C.E., Tender, L.M., Fertig, S., Wang, W. 2001. Harvesting energy from the marine sediment - Water interface. *Environmental Science and Technology*, **35**(1), 192-195.
- Ren, Z., Ward, T.E., Regan, J.M. 2007. Electricity production from cellulose in a microbial fuel cell using a defined binary culture. *Environmental Science and Technology*, **41**(13), 4781-4786.
- Rezaei, F., Xing, D., Wagner, R., Regan, J.M., Richard, T.L., Logan, B.E. 2009. Simultaneous cellulose degradation and electricity production by *Enterobacter cloacae* in a microbial fuel cell. *Applied and Environmental Microbiology*, **75**(11), 3673-3678.
- Rosen, M.A., Scott, D.S. 1998. Comparative efficiency assessments for a range of hydrogen production processes. *International Journal of Hydrogen Energy*, **23**(8), 653-659.
- Rozendal, R.A., Buisman, C.J.N. 2005. Process for producing hydrogen. Patent WO2005005981. (WO2004NL00499 20040709).
- Rozendal, R.A., Hamelers, H.V.M., Buisman, C.J.N. 2006a. Effects of membrane cation transport on pH and microbial fuel cell performance. *Environmental Science & Technology*, **40**(17), 5206-5211.
- Rozendal, R.A., Hamelers, H.V.M., Euverink, G.J.W., Metz, S.J., Buisman, C.J.N. 2006b. Principle and perspectives of hydrogen production through biocatalyzed electrolysis. *International Journal of Hydrogen Energy*, **31**(12), 1632-1640.
- Rozendal, R.A., Hamelers, H.V.M., Molenkamp, R.J., Buisman, C.J.N. 2007. Performance of single chamber biocatalyzed electrolysis with different types of ion exchange membranes. *Water Research*, **41**, 1984-1994.

- Rozendal, R.A., Hamelers, H.V.M., Rabaey, K., Keller, J., Buisman, C.J.N. 2008a. Towards practical implementation of bioelectrochemical wastewater treatment. *Trends in Biotechnology*, **26**(8), 450-459.
- Rozendal, R.A., Jeremiassé, A.W., Hamelers, H.V.M., Buisman, C.J.N. 2008b. Hydrogen Production with a Microbial Biocathode. *Environmental Science & Technology*, **42**, 629-634.
- Rozendal, R.A., Leone, E., Keller, J., Rabaey, K. 2009. Efficient hydrogen peroxide generation from organic matter in a bioelectrochemical system. *Electrochemistry Communications*, **11**(9), 1752-1755.
- Rozendal, R.A., Sleutels, T.H.J.A., Hamelers, H.V.M., Buisman, C.J.N. 2008c. Effect of the type of ion exchange membrane on performance, ion transport, and pH in biocatalyzed electrolysis of wastewater. *Water Science and Technology*, **57**(11), 1757-1762.
- Sata, T. 2004. *Ion Exchange Membranes: Preparation, Characterization, Modification and Application*. Royal Society of Chemistry, Cambridge.
- Schlapbach, L., Züttel, A. 2001. Hydrogen-storage materials for mobile applications. *Nature*, **414**(6861), 353-358.
- Sleutels, T.H.J.A., Hamelers, H.V.M., Buisman, C.J.N. 2011. Effect of mass transfer direction and speed on Microbial Electrolysis Cell performance. *Bioresource Technology*, **102** (1) 399-403.
- Sleutels, T.H.J.A., Hamelers, H.V.M., Rozendal, R.A., Buisman, C.J.N. 2009a. Ion transport resistance in Microbial Electrolysis Cells with anion and cation exchange membranes. *International Journal of Hydrogen Energy*, **34**(9), 3612-3620.
- Sleutels, T.H.J.A., Lodder, R., Hamelers, H.V.M., Buisman, C.J.N. 2009b. Improved performance of porous bio-anodes in microbial electrolysis cells by enhancing mass and charge transport. *International Journal of Hydrogen Energy*, **34**(24), 9655-9661.
- Steinbusch, K.J.J., Arvaniti, E., Hamelers, H.V.M., Buisman, C.J.N. 2009a. Selective inhibition of methanogenesis to enhance ethanol and n-butyrate production through acetate reduction in mixed culture fermentation. *Bioresource Technology*, **100**(13), 3261-3267.
- Steinbusch, K.J.J., Hamelers, H.V.M., Schaap, J.D., Kampman, C., Buisman, C.J.N. 2009b. Bio-electrochemical ethanol production through mediated acetate reduction by mixed cultures. *Environmental Science & Technology*, **44**(1), 513-517.

- Strathmann, H. 2004. *Ion-exchange membrane separation processes*. Elsevier, Amsterdam.
- Strik, D.P.B.T.B., Hamelers, H.V.M., Snel, J.F.H., Buisman, C.J.N. 2008a. Green electricity production with living plants and bacteria in a fuel cell. *International Journal of Energy Research*, **32**(9), 870-876.
- Strik, D.P.B.T.B., Terlouw, H., Hamelers, H.V.M., Buisman, C.J.N. 2008b. Renewable sustainable biocatalyzed electricity production in a photosynthetic algal microbial fuel cell (PAMFC). *Applied Microbiology and Biotechnology*, **81**(4), 659-668.
- Tartakovsky, B., Manuel, M.F., Neburchilov, V., Wang, H., Guiot, S.R. 2008. Biocatalyzed hydrogen production in a continuous flow microbial fuel cell with a gas phase cathode. *Journal of Power Sources*, **182**(1), 291-297.
- Tartakovsky, B., Manuel, M.F., Wang, H., Guiot, S.R. 2009. High rate membraneless microbial electrolysis cell for continuous hydrogen production. *International Journal of Hydrogen Energy*, **34**(2), 672-677.
- Ter Heijne, A., Hamelers, H.V.M., Buisman, C.J.N. 2007. Microbial fuel cell operation with continuous biological ferrous iron oxidation of the catholyte. *Environmental Science & Technology*, **41**(11), 4130-4134.
- Ter Heijne, A., Hamelers, H.V.M., De Wilde, V., Rozendal, R.A., Buisman, C.J.N. 2006. A bipolar membrane combined with ferric iron reduction as an efficient cathode system in microbial fuel cells. *Environmental Science & Technology*, **40**(17), 5200-5205.
- ter Heijne, A., Hamelers, H.V.M., Saakes, M., Buisman, C.J.N. 2008. Performance of non-porous graphite and titanium-based anodes in microbial fuel cells. *Electrochimica Acta*, **53**(18), 5697-5703.
- Torres, C.I., Marcus, A.K., Rittmann, B.E. 2008. Proton transport inside the biofilm limits electrical current generation by anode-respiring bacteria. *Biotechnology and Bioengineering*, **100**(5), 872-881.
- Visser, A., Hulshoff Pol, L.W., Lettinga, G. 1996. Competition of methanogenic and sulfidogenic bacteria. in: *Water Science and Technology*, Vol. 33, pp. 99-110.
- Wang, X., Feng, Y., Ren, N., Wang, H., Lee, H., Li, N., Zhao, Q. 2009. Accelerated start-up of two-chambered microbial fuel cells: Effect of anodic positive poised potential. *Electrochimica Acta*, **54**(3), 1109-1114.

References

- Zehnder, A.J.B., Huser, B.A., Brock, T.D., Wuhrmann, K. 1980. Characterization of an acetate-decarboxylating, non-hydrogen-oxidizing methane bacterium. *Archives Of Microbiology*, **124**(1), 1-11.

English Summary

This thesis describes the improvements in the hydrogen production rate from biomass in Microbial Electrolysis Cells. This increase was accomplished by changes made to the system and were based on new insights in the kinetics of the system.

In **chapter 1**, the theoretical and societal background of the Microbial Electrolysis Cell is presented. Large amounts of hydrogen are produced worldwide. Nearly all produced hydrogen is from fossil origin, which has serious drawbacks. Besides the emission of greenhouse gasses that can cause climate change and air pollution, the price of fossil fuels is predicted to increase in the future because of scarcity and political instability of production regions. A solution for these problems can be to produce the hydrogen from biomass. Use of biomass instead of fossil fuels to produce electricity, fuel and chemicals in a so called biobased economy can contribute to a reduction of greenhouse gas emissions. To assure that a reduction in greenhouse gas emissions occurs, the hydrogen has to be produced at high yield and efficiency. A Microbial Electrolysis Cell is a new technology that is able to produce hydrogen at high yield and efficiency in one step from biomass. In the anodic compartment the biomass is oxidized to CO_2 , protons and electrons. These electrons flow through an external circuit to the cathodic compartment, where these electrons are reduced to form hydrogen gas. Because this reaction is not spontaneous, energy is added to the electrons by means of a power supply. The energy that needs to be added to produce hydrogen is determined by the internal resistance of the system. In **chapter 2** the internal resistances of the system were divided into the different components of the system and presented as an equivalent circuit. These partial internal resistances were used to explain the difference in performance of Microbial Electrolysis Cells equipped with cation and anion exchange membranes. The better performance was caused mainly by the much lower internal resistance of the anion exchange membrane configuration ($192 \text{ m}\Omega \text{ m}^2$) compared to the cation exchange membrane configuration ($435 \text{ m}\Omega \text{ m}^2$). This lower internal resistance could be attributed to the lower transport resistance for

ions through the anion exchange membrane compared to the cation exchange membrane caused by the properties of both membranes.

The hydrogen production rate is determined by conversion rate of substrate and the coulombic efficiency of this conversion. In **chapter 3** the current density and coulombic efficiency was influenced by increasing the mass and charge transport in porous electrodes. A combination of a forced flow through the electrode and an increased buffer concentration led to a high current density of 16.4 A/m² and a hydrogen production rate of 5.6 m³/m³/d at an applied voltage of 1 V. Furthermore the combination of the anode and transport resistance was reduced from 36 mΩ m² to 20 mΩ m². Because of this reduced resistance the coulombic efficiency reached values of over 60% in this continuous system. The effect of mass and charge transfer in Microbial Electrolysis Cells was further investigated in **chapter 4** by increasing the speed of the forced flow and changing the flow direction through the porous anode. Increase of the flow speed led to a decrease in current density when the flow was directed towards the membrane caused by an increase in anode resistance. However, current density increased at higher flow speed when the flow was directed away from the membrane. This was caused by a decrease in transport resistance of ions through the membrane which increased the buffering effect in the system. Furthermore, the increase in flow speed led to an increase of the coulombic efficiency from 15 to over 60%.

To create an efficient Microbial Electrolysis Cell, as much of the available energy from the substrate as possible needs to be transferred to hydrogen. Therefore a high coulombic efficiency is required. The aim of **chapter 5** was to increase the coulombic efficiency by changing the substrate concentration and the anode potential. It was shown that a higher anode potential increased the energy available for these electrogens and in that way they could outcompete the methanogens. Furthermore, also a lower substrate concentration made it possible for the electrogens to outcompete the methanogens. In both cases the relative amount of substrate available for the methanogens was lower because of a higher consumption rate by the electrogens. Further research is required to optimize these

strategies to find a right balance between the coulombic efficiency, current density and removal rate of organic material.

It is claimed that low pH buffer capacity of waste streams limits further development of Microbial Electrolysis Cells because accumulation of protons potentially leads to acidification of the anodic biofilm. Furthermore, a low ionic strength increases the internal resistance of the system. In **chapter 6** a system was introduced that makes it possible to recover alkalinity in an extra recovery compartment. The extra compartment was located between anode and cathode compartment. The compartment was separated from the anode by a cation exchange membrane and from the cathode by an anion exchange membrane. Application of two membranes made it possible to produce clean hydrogen. To compensate for the charge movement as a result of the flow of electrons, both cations and hydroxyl ions moved into the new recovery compartment. When a synthetic waste stream was fed through this recovery compartment, both pH and conductivity increased. When this stream was then fed to the anode of the Microbial Electrolysis Cell, no additional buffer was required to produce the same current (3.5 A/m²). Furthermore, this alkaline stream can also be used in other processes. This chapter showed that it is possible to produce the same current from waste streams with a low buffer capacity or that it is possible to produce a highly alkaline stream with additional economic value.

Chapter 7 describes the improvements of the hydrogen production rate in Microbial Electrolysis Cells. Crucial parameters, like specific energy input and coulombic efficiencies were presented to be able to compare different Microbial Electrolysis Cells. Improvement of the following three key characteristics can make Microbial Electrolysis Cells a competing technology for the production of hydrogen gas from biomass. Firstly, the coulombic efficiency needs to be controlled and improved to reach values close to 100% for all possible organic substrates. Secondly, the use of materials and the design should be such that the total internal resistance does not exceed values of 30 mΩ m². Thirdly, the use of added chemicals like buffers should be limited, as the relative productivity does not increase with

English summary

increasing use of chemicals. Then, production of hydrogen gas from biomass in Microbial Electrolysis Cells will be able to compete with existing technologies.

Nederlandse Samenvatting

Dit proefschrift beschrijft de verbeteringen in de productiesnelheid van waterstof uit biomassa in een Microbiële Elektrolyse Cel. Deze toename is bewerkstelligd door veranderingen in het systeem die gebaseerd zijn op nieuwe inzichten in de kinetiek van het proces.

In **hoofdstuk 1** worden de theoretische en maatschappelijke achtergrond van de Microbiële Elektrolyse Cel gepresenteerd. Wereldwijd worden grote hoeveelheden waterstof geproduceerd. Bijna al deze waterstof is van fossiele herkomst, hetgeen serieuze nadelen heeft. Naast de uitstoot van broeikasgassen die klimaatverandering kunnen veroorzaken, wordt verwacht dat de prijs van fossiele brandstoffen in de toekomst zal stijgen door schaarste en politieke instabiliteit van de productieregio's. Een mogelijke oplossing kan zijn om waterstof uit biomassa te produceren. Gebruik van biomassa in plaats van fossiele brandstoffen om elektriciteit, brandstof en chemicaliën te produceren in een zogenaamde "biobased economy" kan bijdragen aan een vermindering in uitstoot van broeikasgassen. Om te garanderen dat een vermindering in uitstoot van broeikasgassen plaatsvindt, moet de waterstof met hoog rendement en efficiëntie geproduceerd worden. Een Microbiële Elektrolyse Cel is een nieuwe technologie die in staat is om waterstof, in een stap, te produceren uit biomassa met hoog rendement en efficiëntie.

In het anodecompartiment wordt de biomassa geoxideerd naar CO_2 , protonen en elektronen. Deze elektronen stromen via een extern circuit naar het kathodecompartiment waar deze elektronen worden gereduceerd om waterstof te vormen. Omdat deze reactie niet spontaan is, wordt energie aan de elektronen toegevoegd door middel van een voedingsbron. De energie die noodzakelijk is om waterstof te produceren wordt bepaald door de interne weerstand van het systeem. In **hoofdstuk 2** is deze interne weerstand opgedeeld in de verschillende componenten van het systeem en gepresenteerd als een equivalent elektrisch circuit. Deze partiële interne weerstanden zijn gebruikt om de verschillen in waterstofproductiesnelheid in een Microbiële Elektrolyse Cel met een kation en met een anion wisselend membraan te verklaren. De hogere productie werd

hoofdzakelijk veroorzaakt door een veel lagere interne weerstand van de configuratie met het anion wisselend membraan ($192 \text{ m}\Omega \text{ m}^2$) in vergelijking met de configuratie met het kation wisselende membraan ($435 \text{ m}\Omega \text{ m}^2$). Deze lagere interne weerstand kon worden toegeschreven aan de lagere transport weerstand voor ionen door het anion wisselend membraan vergeleken met het kation wisselend membraan, veroorzaakt door de eigenschappen van beide membranen.

De waterstof productiesnelheid wordt bepaald door de omzettingssnelheid van het substraat en de coulombische efficiëntie van deze omzetting. In **hoofdstuk 3** worden de stroomdichtheid en de coulombische efficiëntie beïnvloed door het verhogen van het massa- en ladingstransport in poreuze elektroden. Een combinatie van een geforceerde doorstroming van de elektrode en een verhoogde buffer concentratie leidde tot een hoge stroomdichtheid van 16.4 A/m^2 en een waterstofproductiesnelheid van $5.6 \text{ m}^3/\text{m}^3/\text{d}$ bij een aangebracht voltage van 1V . Verder werd de combinatie van anode en transportweerstand verlaagd van $36 \text{ m}\Omega \text{ m}^2$ naar $20 \text{ m}\Omega \text{ m}^2$. Door de verlaagde weerstand bereikte de coulombische efficiëntie een waarde van meer dan 60% in dit continue systeem.

Het effect van massa- en ladingstransport in een Microbiële Elektrolyse Cel is verder onderzocht in **hoofdstuk 4** door het opvoeren van de snelheid van de geforceerde doorstroming en het veranderen van de doorstroomrichting door de poreuze elektrode. Een toename van de doorstroomsnelheid leidde tot een afname in stroomdichtheid als de stroming naar het membraan toe was gericht. Dit werd veroorzaakt door een toename van de anode weerstand. Echter, de stroomdichtheid nam bij hogere doorstroomsnelheden als de doorstroming van het membraan af gericht was. Dit werd veroorzaakt door een afname van de weerstand voor iontransport door het membraan, hetgeen het buffereffect in het systeem deed toenemen. Verder leidde een toename van de doorstroomsnelheid tot een toename van de coulombische efficiëntie van 15% tot meer dan 60%.

Om een efficiënte Microbiële Elektrolyse Cel te creëren moet zoveel mogelijk van de beschikbare energie van het substraat overgedragen worden naar waterstof. Hiervoor is een hoge coulombische efficiëntie noodzakelijk. Het doel van **hoofdstuk 5** is om deze coulombische efficiëntie te verhogen door het veranderen

van de substraatconcentratie en het veranderen van de anodepotentiaal. Hier werd aangetoond dat een hogere anodepotentiaal de beschikbare energie voor de electrogenen verhoogde waardoor de electrogenen in staat waren om de competitie met de methanogenen te winnen. Verder maakte ook een lagere substraatconcentratie het mogelijk voor de electrogenen om de competitie met methanogenen te winnen. In beide gevallen was de relatieve hoeveelheid substraat die beschikbaar was voor de methanogenen lager door een hogere consumptiesnelheid door de electrogenen. Verder onderzoek is noodzakelijk om deze strategieën te optimaliseren om een goede balans te vinden tussen coulombische efficiëntie, stroomdichtheid en verwijderingsnelheid van organisch materiaal.

Algemeen wordt aangenomen dat de lage pH buffercapaciteit van afvalstromen verdere ontwikkeling van Microbiële Elektrolyse Cellen limiteert omdat ophoping van protonen potentieel leidt tot verzuring van de anodische biofilm. Verder verhoogt een lage ionsterkte de interne weerstand van het systeem. In **hoofdstuk 6** wordt een systeem geïntroduceerd dat het mogelijk maakt om alkaliteit terug te winnen in een extra terugwincompartiment. Dit extra compartiment bevindt zich tussen het anode- en kathodecompartiment. Het compartiment was gescheiden van de anode door een kation wisselend membraan en van de kathode door een anion wisselend membraan. Toepassing van twee membranen maakte het mogelijk om pure waterstof te produceren. Ter compensatie van het ladingstransport ten gevolge van de elektronenstroom, bewegen zowel kationen als hydroxyl naar het nieuwe terugwincompartiment. Als een synthetische afvalstroom door dit terugwincompartiment wordt gevoerd nemen zowel de pH als de geleidbaarheid toe. Wanneer deze stroom vervolgens aan de anode van een Microbiële Elektrolyse cel wordt gevoed, is geen aanvullende hoeveelheid buffer noodzakelijk om dezelfde stroomdichtheid te produceren (3.5A/m^2). Verder kan deze alkaline stroom ook gebruikt worden in andere processen. Dit hoofdstuk laat zien dat het mogelijk is om dezelfde stroomdichtheid uit afvalstromen met lage buffercapaciteit te produceren of dat het mogelijk is om een stroom met hoge alkaliteit te produceren met toegevoegde economische waarde.

Hoofdstuk 7 beschrijft de verbeteringen in de waterstofproductiesnelheid in Microbiële Elektrolyse Cellen. Bepalende parameters, zoals specifieke energievereiste en coulombische efficiëntie worden gepresenteerd om vergelijking van verschillende Microbiële Elektrolyse Cellen mogelijk te maken. De Microbiële Elektrolyse Cel kan in de toekomst een competitieve technologie voor de productie van waterstof uit biomassa worden als de volgende drie hoofdkenmerken verbeterd worden. Ten eerste moet de coulombische efficiëntie gecontroleerd en verbeterd worden om waarden dicht bij 100% te bereiken voor alle mogelijke substraattypen. Ten tweede moeten materialen zo gekozen worden en moet het ontwerp zo zijn dat de totale interne weerstand niet boven de $30 \text{ m}\Omega \text{ m}^2$ uitkomt. Ten derde moet het toevoegen van chemicaliën zoals buffer beperkt worden omdat de relatieve productiviteit niet toeneemt bij het gebruik van meer chemicaliën. Alleen dan zal de productie van waterstofgas uit biomassa in een Microbiële Elektrolyse Cel competitief worden met bestaande technologieën.

Acknowledgements/dankwoord

Na vier jaar ligt hier dan het resultaat: mijn proefschrift. Hoewel alleen mijn naam op de voorkant staat ben ik een oneindig aantal mensen dank verschuldigd die direct of indirect hebben bijgedragen aan het tot stand komen van dit boekje.

Allereerst wil ik mijn begeleiding vanuit Wageningen bedanken. Cees, bedankt dat je me de mogelijkheid en het vertrouwen hebt gegeven om aan dit mooie project te werken. Ook voor je kritische blik en aanwijzingen vanaf de zijlijn ben ik je dankbaar. Bert, zonder jou was dit proefschrift nooit mogelijk geweest. Je kritische blik en unieke inventieve manier om naar onderwerpen te kijken zijn van onschatbare waarde geweest. Daarnaast zal ik je enthousiasme over nieuwe data, maar zeker ook in het algemeen, herinneren. Maar vooral je uiterst prettige manier van samenwerken en het plezier dat we gehad hebben de afgelopen vier jaar zullen me altijd bij blijven. Ook mijn begeleider vanuit Wetsus wil ik hartelijk danken. Michel, naast je nooit aflatende stortvloed aan woorden, ideeën en suggesties heb ik je enthousiasme voor ongeveer alles wat het leven te bieden heeft altijd erg gewaardeerd. René, zonder jou zou was het überhaupt niet mogelijk geweest om dit project (in Nederland) te beginnen. Dank voor het bijbrengen van de basisprincipes van Biocatalyzed Electrolysis en je bevlogen manier om over het proces te praten. Samen met Adriaan en Elsemieke heb ik dit onderzoek de afgelopen vier jaar voortgezet. Naast de prettige manier van samenwerken in ons waterstof thema heb ik ook erg genoten van de beruchte H₂ etentjes. Ik ben dan ook erg blij dat jullie me op dit laatste moment willen bijstaan als paranimf.

Onhandig als ik ben is dit werk uiteraard niet alleen door mij uitgevoerd. Daarom ben ik alle handige mensen in het lab, die mijn gepruts hebben moeten aanzien, erg dankbaar (Wim, Harrie, Harm en Jan). Ook de mensen van het labteam die mijn monsters omtoverden in getalletjes wil ik erg bedanken (Janneke, Jelmer, Pieter, Petra en Mieke). Verder wil ik ook alle andere mensen bij Wetsus bedanken voor de ondersteuning die heeft bijgedragen aan dit proefschrift.

In de afgelopen vier jaar hebben een drietal studenten me aardig wat werk uit handen genomen. Thomas, Rob en Libertus, thank you very much for taking care of

Acknowledgements

our cells, floodings and all the samples and calculations, but also for your enthusiasm about the project and the many laughs we had in the lab.

Uiteindelijk is het leven veel meer dan het schrijven van een proefschrift. Daarom ben ik erg blij dat ik de afgelopen vier jaar simpelweg erg veel plezier heb gehad. In de eerste plaats komt dat door de unieke plek die Wetsus is. Cees en Johannes, bedankt voor het bij elkaar brengen van een unieke groep mensen in een unieke omgeving. This unique group of people made Wetsus, besides an inspiring place to work, above all, a fun place to work. Therefore, I would like to thank all my colleagues at Wetsus and especially all the people who were willing to spend time with me outside working hours for a pint at the Irish pub, answering questions at the pub quiz, playing squash, one of the many housewarming and birthday parties or offering me a place to sleep. I could put an endless list of names here that joined in these activities, but besides forgetting some, it wouldn't do justice to the grateful individual memories I have with so many of you. Thank you all so much for all the laughs and friendship!

Verder wil ik ook iedereen van de vakgroep in Wageningen bedanken. Hoewel ik ver weggestopt zat in Fryslân, heb ik altijd het gevoel gehad dat ik onderdeel was van de vakgroep. In het bijzonder wil ik iedereen van de bio-energiegroep bedanken voor de inspirerende meetings en het creëren van een unieke onderzoeksgroep. Annemiek, je wordt al na ieder hoofdstuk bedankt, maar ik ben ook erg blij dat we dit hele traject in exact dezelfde tijd hebben doorlopen (ik zonder het krijgen van een kind). Je kritische en nuchtere kijk op zaken hebben mij bijzonder geholpen.

Uiteindelijk wil ik mijn familie en vrienden bedanken die me hebben afgeleid van het soms solistische bestaan van een Aio.

Het is gedaan. Op naar de volgende uitdaging.

Mol, België, november 2010

About the author



Tom Sleutels was born on the 23rd of August 1979 in Deurne, the Netherlands. After his secondary education at College Asten Someren in Asten, he started studying Bioprocess Engineering at Wageningen University in 1997 from which he received his master's degree in 2004. During this period he did a thesis at the Process Engineering group and a thesis at the Systems and Control group, both at Wageningen University. Finally, he did a research internship at the Chemical and Process Engineering group at the University of Canterbury, New Zealand.

In 2006 he started his PhD research at the sub-department of Environmental Technology at Wageningen University, stationed at Wetsus, centre of excellence for sustainable water technology in Leeuwarden. The results from this research are presented in this thesis.



Netherlands Research School for the
Socio-Economic and Natural Sciences of the Environment

C E R T I F I C A T E

The Netherlands Research School for the
Socio-Economic and Natural Sciences of the Environment (SENSE),
declares that

Tomas Hubertus Johannes Antonius Sleutels

born on 23 August 1979 in Deurne, The Netherlands

has successfully fulfilled all requirements of the
Educational Programme of SENSE.

Wageningen, 3 December 2010

the Chairman of the SENSE board

Prof. dr. Rik Leemans

the SENSE Director of Education

Dr. Ad van Dommelen

The SENSE Research School has been accredited by the Royal Netherlands Academy of Arts and Sciences (KNAW)



K O N I N K L I J K E N E D E R L A N D S E
A K A D E M I E V A N W E T E N S C H A P P E N



The SENSE Research School declares that **Mr. Tomas Hubertus Johannes Antonius Sleutels** has successfully fulfilled all requirements of the Educational PhD Programme of SENSE with a work load of 34 ECTS, including the following activities:

SENSE PhD courses

- o Environmental Research in Context
- o Research Context Activity: Co-organizing and communicating a Biocatalyzed Electrolysis meeting (24 October 2007 at Wetsus, Leeuwarden)
- o Sustainable bio-energy and innovation

Other PhD and MSc courses

- o Scientific Writing
- o Electrochemistry Summer School
- o Renewable Energy: Sources, Technology and Applications

Research Skills

- o Inventing and writing a patent application (NL2003812)

Oral Presentations

- o Microbial Fuel Cells Meeting; Workshop, 19 November 2007, Lyon, France
- o 1st international conference on Microbial Fuel Cells; Symposium, 29 May 2008, State College, USA
- o Innovative techniques for a sustainable environment; Sense symposium, 20 February 2009, Wageningen, The Netherlands

SENSE Coordinator PhD Education and Research

Mr. Johan Feenstra

This work was performed in the TTIW-cooperation framework of Wetsus, centre of excellence for sustainable water technology (www.wetsus.nl). Wetsus is funded by the Dutch Ministry of Economic Affairs, the European Union European Regional Development Fund, the Province of Fryslan, the city of Leeuwarden and by the EZ-KOMPAS Program of the “Samenwerkingsverband Noord-Nederland”. Funding was also provided by the participants of the research theme “Bio-energy”.

Cover design by Ivonne Sleutels

Printed by drukkerij Macula bv